Department für Experimentelle und Klinische Pharmakologie
und Pharmakogenomik der Universität Tübingen

Abteilung Pharmakologie, Experimentelle Therapie und Toxikologie

# Analysis of p53-mediated dysfunction of SLy1-deficient NK cells

**Inaugural-Dissertation**
**zur Erlangung des Doktorgrades**
**der Medizin**

**der Medizinischen Fakultät**
**der Eberhard Karls Universität**
**zu Tübingen**

**vorgelegt von**

**Blumendeller, Carolin**

**2022**

| | |
|---|---|
| Dekan: | Professor Dr. B. Pichler |
| 1. Berichterstatter: | Professorin Dr. S. Beer-Hammer |
| 2. Berichterstatter: | Professor Dr. J. Leibold |
| Tag der Disputation: | 23.08.2022 |

# TABLE OF CONTENTS

# LIST OF TABLES

# LIST OF FIGURES

# LIST OF ABBREVIATIONS

| | |
|---|---|
| **ADCC** | Antibody-dependent cell-mediated cytotoxicity |
| **BAL** | Bronchoalveolar lavage |
| **BiKEs** | Bispecific killer enhancers |
| **bp** | basepairs |
| **CAR-NK cell** | Chimeric antigen receptor-expressing NK cell |
| **CD** | Cluster of differentiation |
| **CDK** | Cyclin dependent kinase |
| **Cre** | Cre recombinase |
| **Da** | Dalton |
| **DAMP** | Damage-associated molecular pattern |
| **DC** | Dendritic cell |
| **DDR** | DNA damage response |
| **DNA** | Desoxyribonucleic acid |
| **EOMES** | Eomesodermin |
| **GM-CSF** | Granulocyte macrophage colony-stimulating factor |
| **gMFI** | geometric mean fluorescence intensity |
| **ILC** | Innate lymphoid cell |
| **IFN** | Interferon |
| **KIR** | Killer immunoglobulin-like receptor |
| **KO** | Knock-out |
| **LLC** | Lewis Lung Carcinoma |
| **mAB** | monoclonal antibody |
| **MCMV** | Mouse cytomegalovirus |
| **Mdm2** | Mouse double minute 2 homolog |
| **Met** | Methionin |
| **MHC** | Major histocompatibility complex |
| **mRNA** | messenger ribonucleic acid |
| **MTOC** | Microtubuli organizing centre |
| **NCR1** | Natural cytotoxicity triggering receptor 1 |
| **NK cell** | Natural killer cell |
| **NKAR** | Natural killer cell activating receptor |

| | |
|---|---|
| **NKD** | Natural killer cell deficiency |
| **NKIR** | Natural killer cell inhibitory receptor |
| **NLS** | Nuclear localization signal |
| **PAMP** | Pathogen-associated molecular pattern |
| **RNA** | Ribonucleic acid |
| **rpm** | rounds per minute |
| **RPS3** | Ribosomal protein S3 |
| **RPL5** | Ribosomal protein L5 |
| **rRNA** | ribosomal RNA |
| **SAM** | Sterile alpha motif |
| **SEM** | Standard error of the mean |
| **Ser** | Serin |
| **SH3** | Src homolgy 3 domain |
| **SLy** | SH3 Lymphocyte protein |
| **SPF** | Specific pathogen-free |
| **TG** | Transgenic |
| **TLR** | Toll-like receptor |
| **TNF** | Tumor necrosis factor |
| **TRAIL** | Tumor necrosis factor related apoptosis inducing ligand |
| **TRAIL-R** | Tumor necrosis factor related apoptosis inducing ligand receptor |
| **TriKEs** | Trispecific killer enhacers |
| **WT** | Wildtype |

# 1 Introduction

## 1.1 The immune system

Because of constant exposure to infectious agents and their toxins, the human body has evolved an effective defense system to protect itself. This system consists of a variety of effector cells and molecules that together make up the immune system. It can be divided up into two parts: The innate and the adaptive immunity (Murphy and Weaver, 2016).

Innate immunity serves as a first line of defense but can recognize only certain pathogens, and recognition occurs only in an unspecific manner. Therefore, it cannot provide the protective immunity that prevents reinfection (Murphy and Weaver, 2016). The most primitive form of immunological protection are anatomic barriers and various chemical barriers such as complement and antimicrobial proteins. They form the first line of defense against the entry of commensal organisms as well as pathogens into the host tissue (Murphy and Weaver, 2016). Innate immune sensor cells, such as macrophages or dendritic cells, express specific receptors on their surface that react with inflammatory inducers. These inducers may be either chemical structures unique to microbes (Pathogen-Associated Molecular Patterns, PAMPs) or the chemical signals of tissue damage (Damage-Associated Molecular Patterns, DAMPs). Upon stimulation, the sensor cells can either directly execute their effector activity, for example phagocytosis, or they respond with the production of inflammatory mediators (Murphy and Weaver, 2016). These mediators are typically cytokines or chemokines that inform the immune system about the infection and recruit other immune cells, such as natural killer (NK) cells and other Innate Lymphoid Cells (ILCs). Specific types of immune-response effector activities, such as cell killing or production of cytokines with direct antiviral activity, will then be provided by the recruited cells. All these processes aim to reduce or eliminate infection by pathogens. Different mediators can lead to the activation of several types of inflammatory cells that are spezialised in eliminating viruses, intracellular bacteria, extracellular pathogens, or parasites (Murphy and Weaver, 2016).

In contrast to the innate immune system, the adaptive immune system contains a repertoire of antigen receptors and can therefore recognize structures that are specific to individual pathogens (Murphy and Weaver, 2016). This leads to a higher sensitivity and specificity of the adaptive immune system. Furthermore, the adaptive immunity has the feature of immunological memory that is provided by the clonal expansion of antigen-reactive lymphocytes and ensures protection against reinfection by the same pathogen (Murphy and Weaver, 2016).

Adaptive immunity relies on two major types of lymphocytes: B cells, that mature in the bone marrow and produce circulating antibodies, and T cells, that develop in the thymus and recognize peptides from pathogens. These peptides can be presented to the T cells by infected cells or specific Antigen-Presenting Cells (APCs) *via* Major Histocompatibility Complex (MHC) molecules. There are two main types of T cells: $CD8^+$ T-killer cells and $CD4^+$ T-helper cells. $CD8^+$ T-killer cells recognize antigens which are located on MHC class I molecules of infected cells. If T-killer cells are activated, they cause direct killing of the affected cell by inducing cell lysis. By contrast, $CD4^+$ T-helper cells recognize antigens that are presented to them by specialized APCs *via* MHC class II molecules. T-helper cells are classified into different subtypes, such as $T_H1$-, $T_H2$-, $T_H17$-, $T_{FH}$- and $T_{reg}$ cells, each fulfilling a specific effector function in the immune system (Murphy and Weaver, 2016). **Figure 1** summarizes the phases of the immune response.

| Phases of the immune response | |
|---|---|
| **Innate immune response** | Inflammation, complement activation, phagocytosis and destruction of pathogen. |
| **Adaptive immune response** | Interaction between antigen-presenting dendritic cells and antigen-specific T cells: recognition of antigen, adhesion, co-stimulation, T-cell proliferation and differentiation. |
| | Activation of antigen-specific B cells. |
| | Formation of effector and memory T cells. |
| | Interaction of T cells with B cells, formation of germinal centers. Formation of effector B cells (plasma cells) and memory B cells. Production of antibodies. |
| | Emigration of effector lymphocytes from peripheral lymphoid organs. |
| | Effector cells and antibodies eliminate the pathogen. |
| **Immunological memory** | Maintenance of memory B cells and T cells and high serum or mucosal antibody levels. Protection against reinfection. |

**Figure 1: Phases of the immune response**

Figure adapted and modified from Janeway's immunobiology, 9th edition, page 6.

## 1.2 Natural killer cells and their function

In addition to B and T cells, NK cells represent one of the three main types of lymphocytes in humans. Although allegations differ between different sources, in humans, they make up approximately 5 - 15 % of the peripheral blood lymphocytes (Langers *et al.*, 2012; Mahapatra *et al.*, 2017; Angelo *et al.*, 2015). Generally, NK cells can be found in lymphatic as well as non-lymphatic tissues (Cudkowicz and Stimpfling, 1964). These include, for example, spleen, thymus, lymph nodes, bone marrow, lung, skin and gut (Carrega and Ferlazzo, 2012; Trinchieri, 1989). The existence of NK cells was first described in the 1960s by several groups (Rosenau and Moon, 1961; Smith, 1966; Cudkowicz and Stimpfling, 1964), but it was not until 1975 that they were further characterized as large granules-containing lymphocytes and were eventually named “natural killer cells” (Kiessling *et al.*, 1975; Herberman *et al.*, 1975; Kiessling, Klein and Wigzell, 1975). This name was chosen because of their cytotoxic activity. Historically, a rather simple classification of human NK cells was used which depended on their expression of CD56 and CD16: IFN-$\gamma$ producing NK cells were classified as $CD56^{high}CD16^{+}$, whereas cytotoxic NK cells were classified as $CD56^{low}CD16^{high}$ (Freud *et al.*, 2017). In mice, NK cells were classified according to their expression of CD27 and CD11b (Chiossone *et al.*, 2009). Today, it is clear that NK cell classification is much more complex, and many distinct NK cell subsets exist that each fulfill different functions, as reviewed by Stabile *et al.* (Stabile *et al.*, 2017). Furthermore, due to the fact that they do not require prior binding of any antigen for their activation, NK cells were assigned to the innate immune system (Kiessling *et al.*, 1975; Kiessling, Klein and Wigzell, 1975). However, more recently, NK cells were described to also possess features of adaptive immunity, including antigen specifity, clonal proliferation, and long-lived memory similar to T and B cells (Sun, Beilke and Lanier, 2009; Vivier *et al.*, 2011). Because of the combinatory presence of innate as well as adaptive characteristics, NK cells are considered to be located at the boundary between these two immune compartments (Sun, 2015). NK cells were therefore newly classified to the group of ILCs, immune cells that have lymphoid characteristics

but lack specific antigen receptors. ILCs exist in humans as well as in mice, and three significant subgroups are defined, mainly based on the types of cytokines that each produces (Scoville, Freud and Caligiuri, 2017; Spits *et al.*, 2013). NK cells show most similarities with group 1 ILCs (Spits *et al.*, 2013; Vivier *et al.*, 2018). When activated, both cell types release IFN-γ and TNF-α (Zhang and Huang, 2017). However, the function of NK cells is more similar to $CD8^+$ cytotoxic T cells, whereas group 1 ILCs resemble more closely to the $T_H1$ subset of $CD4^+$ T-helper cells (Zhang and Huang, 2017).

NK cells fulfill two main functions (**Figure 2**). On the one hand, they can produce different soluble factors, such as inflammatory cytokines (**Figure 2A**), and on the other hand, they are also able to directly attack and kill target cells (**Figure 2B**).

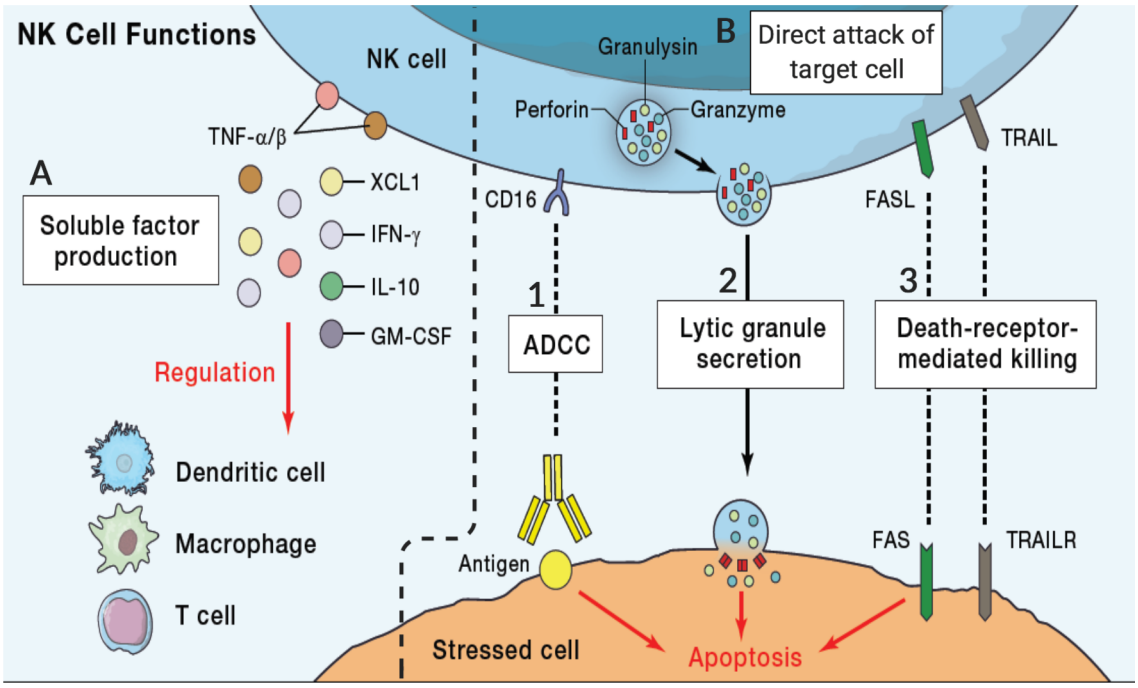


**Figure 2: NK cell functions**

NK cells fulfill two main functions. On the one hand **(A)**, they can produce an array of proinflammatory cytokines (e.g. IFN-γ, TNF-α/β, GM-CSF) to regulate other immune cells, such as dendritic cells, macrophages and T cells. On the other hand **(B)**, they can also directly attack and kill target cells. Death of the target cell can be mediated by three different mechanisms: **1)** Antibody-dependent cell-mediated cytotoxicity (ADCC), **2)** Lytic granule secretion and **3)** Death-receptor-mediated killing. Figure adapted and modified from Crinier *et al.*, 2020.

Target cells that can be attacked by NK cells comprise for example tumor cells or virally-infected cells (Zhang and Huang, 2017; Parham, 2006). If an NK cell

recognizes such a cell, formation of an immunological synapse occurs (Krzewski and Strominger, 2008; Mace *et al.*, 2014). This leads to death of the target cell through three mechanisms (**Figure 2B**): 1) Antibody-dependent cell-mediated cytotoxicity (ADCC), 2) degranulation of cytolytic granules and 3) death receptor ligation (Stabile *et al.*, 2017; Smyth *et al.*, 2005; Crinier *et al.*, 2020).

Upon NK cell binding, certain death receptors on the surface of the target cell are activated and as a result, several pro-apoptotic signal pathways will be executed in the target cell (Nagata and Golstein, 1995; Degli-Esposti, 1999; Khosravi-Far and Esposti, 2004; Smyth *et al.*, 2005). Examples for such death receptors are TRAIL-R and Fas (CD95). Their according ligands, TRAIL and FasL, are located on the NK cell surface. Furthermore, the lytic granules that are released by NK cells upon stimulation can induce direct killing of cells (Bhat and Watzl, 2007). These granules consist of many different molecules, but granzyme B (Smyth *et al.*, 2005) and perforin (Osinska, Popko and Demkow, 2014) are the ones mainly responsible for their lytic activity. Granzyme B, for example, can induce apoptosis of the target cell in a caspase-dependent manner by directly cleaving caspase-8 and caspase-3 (Atkinson *et al.*, 1998; Barry *et al.*, 2000). Additionally, release of granzyme B can cause liberation of cytochrome-c from the mitochondria which causes induction of apoptosis in the target cell without involvement of caspases (Pinkoski *et al.*, 2001). Under normal conditions, granzyme B and perforin are stored in vacuoles in the NK cells. Upon activation, they are then released into the target cell at the immunological synapse (Krzewski and Strominger, 2008) which leads to apoptosis of that cell (Krzewski and Strominger, 2008; Stinchcombe *et al.*, 2006). In order to mediate fusion of the granules with the target cell, reorganization of the cytoskeleton of the NK cell is required. Processes involved in this reorganization are, for example, polymerization of actin filaments at the immunological synapse (Mace *et al.*, 2012; Mizesko *et al.*, 2013) and polarization of the Microtubuli Organizing Centre (MTOC) towards the target cell (Chen *et al.*, 2007b; James *et al.*, 2013; Mentlik *et al.*, 2010).

The second critical effector function of NK cells is the production of different inflammatory cytokines in response to stimulation of their activation receptors or cytokine-induced activation signaling (Fauriat *et al.*, 2010; Freeman *et al.*, 2015)

(**Figure 2A**). It is important to know that this constitutes an independent process which has to be delimited from the secretion of cytolytic granules (Reefman *et al.*, 2010). The produced cytokines are mainly IFN-γ, TNF-α and GM-CSF (Vitale *et al.*, 2004; Biron *et al.*, 1999). These all belong to the group of $T_H1$-type cytokines (Vivier *et al.*, 2011; Cook, Waggoner and Whitmire, 2014). $T_H1$-type cytokines fulfill stimulatory effects on other immune cells, such as T cells, macrophages, neutrophils, and dendritic cells (Blanchard, Michelini-Norris and Djeu, 1991; van den Bosch *et al.*, 1995). Nevertheless NK cells are not restricted to the production of these types of cytokines (Kiniwa *et al.*, 2016; Vivier and Ugolini, 2009). Furthermore, upon stimulation, NK cells also secrete so called chemokines. These are molecules that can lead to the recruitment of other effector immune cells to the site of inflammation (Walzer *et al.*, 2005).
These two NK cell effector functions (direct lysis of target cells and production of pro-inflammatory cytokines) are essential components of the immune response and are the primary mechanisms through which NK cells mediate protective immunity (Abel *et al.*, 2018).

### 1.2.1 Natural killer cell receptors

A critical feature of NK cells in order to defend the host against tumor cells or viruses is their ability to distinguish between diseased cells and uninfected healthy cells. In contrast to B and T lymphocytes, NK cells do not express a specific antigen receptor, such as the BCR or TCR, emerged from RAG-dependent VDJ-rearrangement (Mombaerts *et al.*, 1992; Shinkai *et al.*, 1992). However, the general belief is that an individual NK cell expresses various combinations of germline-encoded activating receptors (NKARs) and inhibitory receptors (NKIRs) on its surface. In addition to the NKARs and NKIRs, NK cells also express chemotactic, cytokine, and adhesion receptors, and some of these receptors differ between humans and mice (Vivier *et al.*, 2011) (**Figure 3**). Even though not all details of this process are fully understood yet, it seems that the overall balance of signaling by these activating and inhibitory receptors

determines whether an NK cell will be activated and attacks a target cell or not (Lanier, 2008).

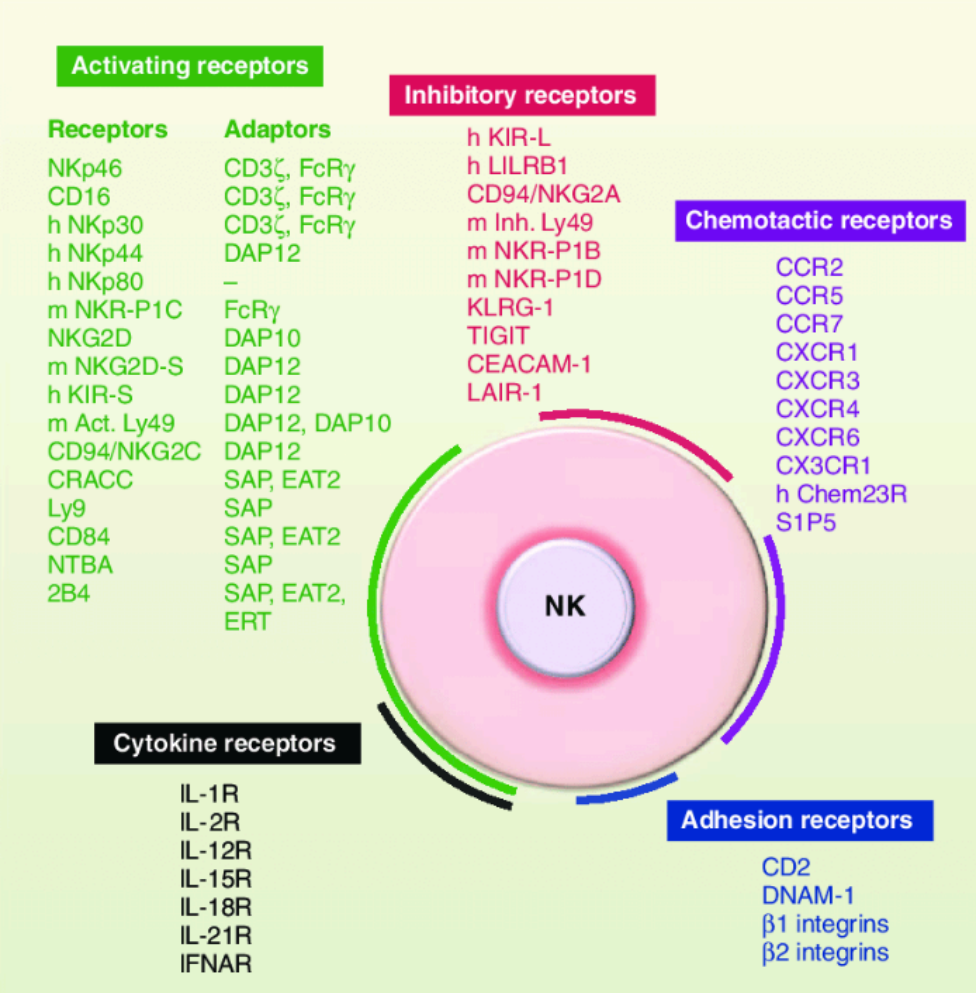


**Figure 3: NK cell receptors**

NK cells express many cell surface receptors that can be grouped into activating (green), inhibitory (red), adhesion (blue), cytokine (black) and chemotactic receptors (purple). Adaptor molecules involved in the signaling cascade downstream of the engagement of activating receptors (green) are also indicated. The list of cell surface molecules involved in the regulation of mouse and human NK cell function is not exhaustive. Unless indicated (h, human; m, mouse), receptors are conserved in both species. Figure and legend from Vivier *et al*., 2011.

With the help of their activating receptors, NK cells can mediate anti-tumor cytotoxicity and produce significant amounts of pro-inflammatory cytokines, although they do not express any clonotypic receptors (Rajasekaran *et al.*, 2016). The NKARs can detect expressional changes of various surface proteins on a target cell. This process is referred to as ‘dysregulated self’. More precisely, if a

target cell experiences metabolic stress, such as malignant transformation or microbial infection, the expression of specific cell-surface proteins will be induced. These changes of protein expression, referred to as ‘stress-induced self’, can be recognized by the activating receptors. Examples of NKARS are NKG2D, NK1.1 and NKp46 (CD161). For the transduction of their signal, NKARs need to recruite specific receptor-associated adaptor molecules, such as FcεRIγ, CD3ζ, and DAP12 (Lanier, 2008). For example, the activating receptors CD16, NKp46, Ly49D, Ly49H, and NKG2D make use of these signaling adaptors (Arase *et al.*, 2001; Augugliaro *et al.*, 2003; May *et al.*, 2013; Rosen *et al.*, 2004; Smith *et al.*, 1998). If one or several NKARs are stimulated, it becomes more likely that the NK cells will attack the target cell.

One important activating receptor that is highly conserved from mice to humans is NKG2D, a homodimer forming C-type lectin-like type II transmembrane glycoprotein (Lopez-Soto *et al.*, 2015). It is constitutively expressed on NK cells (Spear *et al.*, 2013) and recognizes stress-inducible ligands that are structurally related to MHC class I (Lopez-Soto *et al.*, 2015). Upon NK cell activation through NKG2D, lytic granules are mobilized and activation of transcription factors (including activator protein-1 and NF-κB) leads to the production of cytokines (Kwon *et al.*, 2016; Rajasekaran *et al.*, 2013; Abel *et al.*, 2018).

By contrast, inhibitory receptors on NK cells interact with surface molecules that are constitutively expressed at high levels by most cells, e.g. MHC class I. The loss of these molecules is referred to as ‘missing self’ (Karre *et al.*, 1986; Ljunggren and Karre, 1990). If an inhibitory receptor recognizes MHC class I molecules on the surface of a target cell, it becomes less likely that the NK cell will be activated and attacks the target cell. This prevents NK cells from killing uninfected host cells. The higher the number of MHC class I molecules on a surface, the better protected the cell is against attack by NK cells (Murphy and Weaver, 2016). An important inhibitory receptor is KLRG-1 which was lately also characterized as an NK cell exhaustion marker (Alvarez *et al.*, 2019).

Interferons, that are produced by different immune cells as a response to infection, cause an increased expression of MHC class I molecules and thereby protect healthy host cells from being killed by NK cells, while also activating NK

cells to kill virus-infected or tumor cells (Murphy and Weaver, 2016). Initially, researchers believed that the only mechanism for self-tolerance was the inhibitory receptor signaling upon MHC class I engagement when interacting with normal host cells (Valiante *et al.*, 1997). However, in 2005 Fernandez *et al.* discovered a small subset of NK cells that achieves self-tolerance without expressing inhibitory receptors specific for self-MHC molecules (Fernandez *et al.*, 2005; Abel *et al.*, 2018).

It is thought that the balance of signals from 'stress-induced self' and 'missing self' determines whether an individual NK cell will be triggered to kill a particular target cell (Vivier *et al.*, 2011) (**Figure 4**). Thus, receptors expressed on NK cells integrate the signals from two types of surface receptors, which together control the NK cell's cytotoxic activity and cytokine production (Murphy and Weaver, 2016).

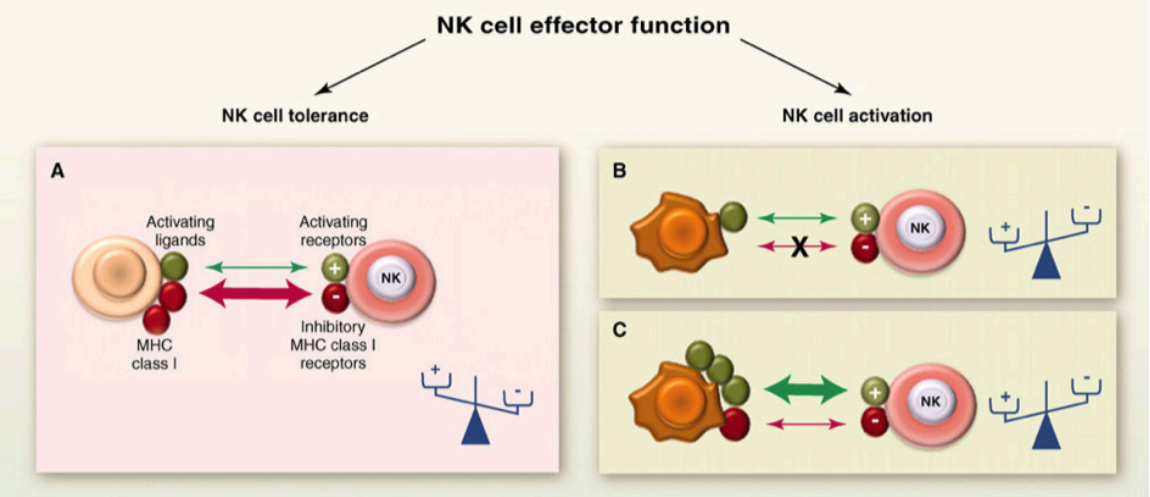


**Figure 4: The dynamic regulation of NK cell effector function**

NK cells sense the density of various cell surface molecules expressed at the surface of interacting cells. The integration of these distinct signals dictates the quality and the intensity of the NK cell response. NK cells spare healthy cells that express self-MHC class I molecules and low amounts of stress-induced self molecules **(A)**, whereas they selectively kill target cells "in distress" that down-regulate MHC class I molecules **(B)** or up-regulate stress-induced self molecules **(C)**. +, activating receptors; -, inhibitory receptors. Figure and legend from Vivier *et a*l., 2011.

### 1.2.2 Natural killer cells in health and disease

Until today, the diverse functions of NK cells in mammalian immunity are not fully understood (Abel *et al.*, 2018), but analyses of clinical phenotypes of patients suffering from rare monogenetic NK cell deficiencies (NKDs) can give insights into the importance of NK cells for maintaining human health. The clinical presentation of NKDs can be very variable, depending on the underlying gene mutation, but one common mutuality seems to be the increased susceptibility of patients towards herpesviral infections. These viruses are reported to be present in almost 60 % of NKD cases (Orange, 2013). In 2019, Mace and Orange reviewed the insights about NK cell biology gained through the study of NKDs and concluded that "the severe clinical phenotype of patients with NKD *(…)* reinforces the conclusion that NK cells play at least some non-redundant role in human health" (Mace and Orange, 2019).

NK cells are commonly known for their ability to kill virally infected cells as well as tumor cells. Furthermore, altered NK cell function was observed in several autoimmune disorders, such as type 1 diabetes (Negishi *et al.*, 1986; Akesson *et al.*, 2010), rheumatoid arthritis (Dalbeth and Callan, 2002; de Matos *et al.*, 2007), systemic lupus erythematodes (Green *et al.*, 2005; Park *et al.*, 2009), systemic sclerosis (Horikawa *et al.*, 2005) and others. Interestingly, Perricone *et al.* found that NK cell function can either promote or even protect against the onset of an autoimmune condition (Perricone *et al.*, 2008). Emerging evidence also demonstrates regulation of anti-inflammatory programs, such as tissue repair, by NK cells (Jewett, Man and Tseng, 2013; Kumar *et al.*, 2013).

Because of their ability to attack and lyse malignantly transformed cells, increasing interest has risen concerning the use of NK cells in new anti-tumor immunotherapies. In 2019, the different types of NK cell therapies that are currently being developed were extensively reviewed (Hodgins *et al.*, 2019). Besides adoptive NK cell transfer, which, in combination with oncolytic virotherapy, might be a promising treatment for e.g. pediatric sarcomas (Klose *et al.*, 2019), potential new therapies include the use of chimeric antigen receptor-expressing (CAR-) NK cells (Tang *et al.*, 2018), bispecific/ trispecific killer cell

engagers (BiKEs/ TriKEs) (Felices *et al.*, 2016; Gleason *et al.*, 2012; Vallera *et al.*, 2016) and checkpoint blockade. Concerning the latter, the clinical use of the checkpoint inhibitor Monalizumab, a newly generated anti-NKG2A monoclonal antibody (mAB), is currently explored in several clinical trials, including a phase III clinical trial investigating the combined use of Monalizumab and Cetuximab in the treatment of advanced head and neck cancer (van Hall *et al.*, 2019; Andre *et al.*, 2018; Cohen and Fayette, 2020).
Nevertheless, these new NK cell therapies still have to overcome several burdens in order to display successful treatment options. For example, recent findings show that the tumor microenvironment can mediate NK cell suppression through several mechanisms, such as expression of immunosuppressive cytokines (mainly TGF- $\beta$) (Lee *et al.*, 2004; Viel *et al.*, 2016). This could have a negative effect on the efficacy of NK cell-based anti-tumor therapies.

## 1.3 The SLy-family of adaptor proteins

Adaptor proteins belong to a class of proteins that are involved in regulatory cell mechanisms by mediating protein-protein-interactions *via* specific protein domains. In contrast to enzymes, they do not contain a catalytic centre and therefore, they cannot activate or inactivate other proteins or accelerate chemical reactions. However, through the mediation of protein-protein-interactions, they are able to stabilize protein complexes and indirectly regulate signaling cascades. Because of this feature, they are referred to as ‘scaffold proteins’ (Peterson *et al.*, 1998). In 2009, Shaw and Filbert extensively reviewed the importance of scaffold proteins in immune cells. They reported about their critical functions during T cell activation, $Ca^{2+}$-signaling, activation of the inflammasome, Toll-like receptor (TLR) signaling, as well as formation of the immunological synapse (Shaw and Filbert, 2009).

An emerging family of adaptor proteins is the SH3 Lymphocyte protein (SLy) family which was recently reviewed by our group (Jaufmann *et al.*, 2021). It includes SLy1, SLy2, and the sterile alpha motif (SAM) and SH3 domain-

containing protein 1 (SASH1) (**Figure 5**). In 2001, SLy1 was discovered as the first member of this family by Beer *et al.* (Beer *et al.*, 2001) and SLy2 (also termed HACS1, NASH1, SAMSN1) was also described in the same year (Claudio *et al.*, 2001; Uchida *et al.*, 2001). Two years later, the candidate tumor suppressor in breast cancer, SASH1, was published as the third member of the family (Zeller *et al.*, 2003). As SLy1, SLy2, and SASH1 all express an SH3- and a SAM-domain with substantial sequence similarity, they were grouped into one family of adaptor proteins, called the SLy family (Claudio *et al.*, 2001) (Zhu *et al.*, 2004), eventhough they are not functionally related to each other.

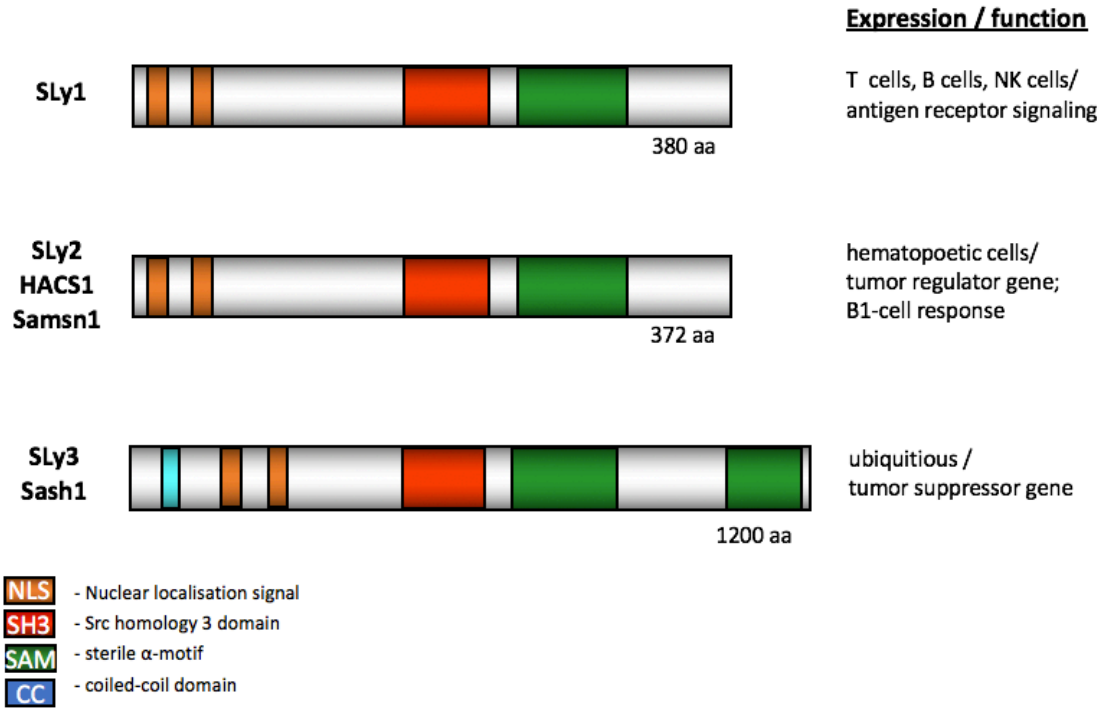


**Figure 5: The SLy-family of adaptor proteins**

SLy1, SLy2 (HACS1/ Samsn1) and SLy3 (Sash1) belong to the family of SLy-proteins. They are each expressed in different cell types and fulfill distinct functions, but because of their structural similarity, they are all assigned to the same protein family; aa = amino acid.

### 1.3.1 SLy1 protein

The first member of the SLy-family of adaptor proteins is the SH3 Lymphocyte protein 1, shortly termed SLy1, which is exclusively expressed in lymphocytes (B cells, T cells and NK cells) and was first described by Beer *et al.* in 2001.
In order to be able to fully investigate and understand the function of SLy1 in lymphocytes, it is critical to have knowledge about the protein's biochemical features, such as cellular localization, intracellular shuttling, phosphorylation status and its interaction with other proteins.
The human and the murine SLy1 gene are both located on the X-chromosome (Xq25-Xq26.3 and XA5 48,146,436-48,161,565, respectively). Interestingly, other genes that are encoded in the same region of the chromosome are linked to lymphoid disorders, for example CD40L and SH2D1A. Mutations in these genes lead to Hyper-IgM-Syndrome and X-linked lymphoproliferative disease, respectively (Coffey *et al.*, 1998; Ramesh *et al.*, 1995).
The full-length cDNA of the SLy1 protein compromises 2600 bp with an open reading frame of 1143 bp. The protein itself consists of 381 amino acids and has a size of 55 kDa. There is an 89 % nucleotide sequence identity and a 94 % amino acid sequence identity between the human and murine SLy1 (Beer *et al.*, 2001). SLy1 contains a SH3-domain, which is located within the amino acids 176–233, and a Sterile Alpha Motif (SAM), which is located at the C-terminus of the protein (amino acids 249 – 316) (Beer *et al.*, 2001). The SH3 domain is essential for protein-protein-interactions and the formation of signal complexes. It contains 50 amino acids that bind to proline-rich sequences of other proteins with the consensus PXXP. The SAM-domain, by contrast, mediates cell-cell initiated signal transduction by connecting downstream signaling components to surface receptors. Furthermore, SLy1 contains a bipartite Nuclear Localization Signal (NLS) (Beer *et al.*, 2005) and at position 27, SLy1 comprises the amino acid serine, which is a physiological substrate for antigen receptor-activated serine kinases (Astoul *et al.*, 2003). **Figure 6** illustrates the structure of SLy1.

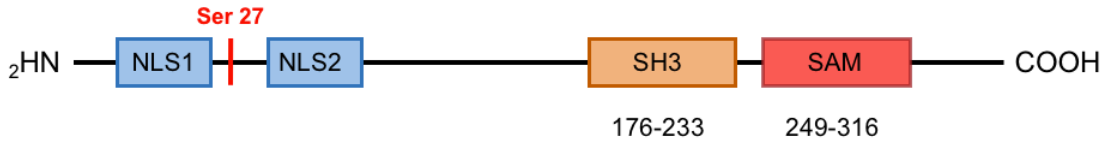


**Figure 6: Structure of SLy1**

The SLy1-protein contains a bipartite nuclear localization signal (NLS), a Src homology 3 (SH3) domain and a sterile alpha motif (SAM). At position 27, SLy1 contains the amino acid serine which is a substrate for antigen receptor-activated serine kinases. Numbers indicate the according amino acid positions.

Concerning the tissue distribution of the protein, SLy1 messenger RNA (mRNA) was detected in the bone marrow, in the lung, in the medulla and cortex of the thymus, in the spleen, in both T- and B-cell areas of the lymph nodes and Peyer's patches (Beer *et al.*, 2001). Nevertheless, a strong expression of the SLy1 mRNA was only detected in the spleen and lung. In the spleen, SLy1 can be specifically detected in the white pulp with both T- and B-cell areas, but not in the red pulp (Beer *et al.*, 2001). The expression was detected exclusively in lymphocytes (T, B and NK cells). Within the cell, SLy1 was found to be located in the cytoplasm as well as in the nucleus, which is likely regulated by the NLS and the phosphorylation of Ser-27 (Beer *et al.*, 2005).

In 2005, Beer et al. generated SLy1 mutant ($SLy1^{d/d}$) mice that harbor a deletion within the protein from Leu-20 to Met-100. These mice express a truncated form of SLy1 that lacks the Ser-27 phosphorylation site and the C-terminal part of the bipartite NLS. In contrast to the wildtype SLy1 protein, the mutant SLy1 protein is only located in the cytoplasm and is not found in the nucleus (Beer *et al.*, 2005). $SLy1^{d/d}$ mice as well as later generated $SLy1^{KO}$ mice show significantly reduced cell numbers in thymus, spleen, peripheral lymph nodes, and Peyer's patches. Furthermore, the amount of macroscopically visible Peyer's patches is significantly lower in $SLy1^{d/d}$ mice compared to wildtype littermates. This impaired lymphoid organ development in SLy1 mutant mice occurs due to an impaired ability of hematopoietic cells to reconstitute T- and B-cell compartments (Beer *et al.*, 2005; Reis, Pfeffer and Beer-Hammer, 2009).

As mentioned before, the SLy1 protein fulfills a specific function in each of the different cell types in which it is expressed (T cells, B cells and NK cells). In T cells, SLy1 indirectly regulates proliferation upon infection. It stabilizes the complex of the transcription factor Foxo1 and 14-3-3 protein in the cytoplasm which causes a decreased transcription of the cell-cyle inhibiting genes *p130* and *p27* and hence leads to proliferation of the T cells (Schäll *et al.*, 2015). The function of SLy1 in B cells is yet to be fully investigated, but Beer *et al.* could already show that in splenic marginal-zone B cells, the mutation of SLy1 causes an impaired development and proliferation after stimulation with anti-IgM and anti-CD40 (Beer *et al.*, 2005). The function of SLy1 in NK cells will be described in detail in the following chapter.

### 1.3.2 SLy1 in natural killer cells

Natural Killer cells are known for their exclusive cytolytic activity against virally infected and malignantly transformed cells. In order to investigate the role of SLy1 on NK cell function, the previously generated SLy1 knockout mice ($SLy1^{KO}$) (Reis, Pfeffer and Beer-Hammer, 2009) were used in the Lewis Lung Carcinoma (LLC) model, which is known to be controlled by NK cells. It was demonstrated that $SLy1^{KO}$ NK cells lyse LLC cells with less efficiency *in vitro*. As a consequence of the reduced efficiency, LLC growth in $SLy1^{KO}$ mice is enhanced compared to $SLy1^{WT}$ mice. Consistent with this, $SLy1^{KO}$ NK cells produce less IFN-$\gamma$ and degranulate less efficiently in plate-bound antibody stimulation assays. These findings demonstrate that SLy1 deficiency leads to impaired NK cell function and therefore to decreased tumor cell clearance (Arefanian *et al.*, 2016).

Interestingly, $SLy1^{KO}$ mice have fewer NK cells in spleen and lung, but neither is there a difference in the maturation between $SLy1^{WT}$ and $SLy1^{KO}$ splenic or lung-resident NK cells, nor does SLy1 affect NK cell development in the bone marrow. These findings suggest that – in contrast to the function of SLy1 in T cells – in NK cells, SLy1 exerts its function only in mature cells (Arefanian *et al.*, 2016).

Furthermore, SLy1$^{KO}$ NK cells exhibit an altered activation status as they show a decreased expression of the activating receptors NK1.1, NKp46, Ly49H, and NKG2D compared to SLy1$^{WT}$ controls (Arefanian *et al.*, 2016). Under cytokine stimulation, which leads to NK cell maturation and activation, these differences in the expression levels disappear (Arefanian *et al.*, 2016). Also, SLy1$^{KO}$ NK cells show lower mRNA levels as well as protein expression levels as determined by flow cytometry for multiple NK cell-activating receptors compared to wildtype littermates, and there is evidence for a decreased viability of splenic SLy1$^{KO}$ NK cells in comparison to wildtype controls (Arefanian *et al.*, 2016).
In summary, these findings suggest that the adaptor protein SLy1 contributes to the viability and activation of mature, peripheral NK cells but is unlikely to control their development in the bone marrow (Arefanian *et al.*, 2016).

Astonishingly, in contrast to T lymphocytes, where SLy1 shuttles between the cytoplasm and the nucleus to facilitate signal transduction (Schäll *et al.*, 2015), Arefanian *et al.* discovered a different, unique function of SLy1 in NK cells.
In resting NK cells, SLy1 contributes to ribosomal stability and maintenance and is solely located in the cytoplasm without any nuclear or nucleolar localization (Arefanian *et al.*, 2016). In SLy1$^{KO}$ NK cells, there is an increase in various free ribosomal proteins, such as RPS3 and RPL5, compared to SLy1 wildtype controls. Nevertheless, despite ribosomal instability, SLy1$^{KO}$ NK cells seem to have an equivalent amount of mature assembled ribosomes as SLy1$^{WT}$ NK cells (Arefanian *et al.*, 2016).
Interestingly, the overabundance of free ribosomal proteins in SLy1$^{KO}$ NK cells has been demonstrated to interfere with the function of Mdm2, an E3 ubiquitin ligase that, under normal conditions, sequesters p53 and therefore targets it for proteasomal destruction (Arefanian *et al.*, 2016). In other words, in the absence of SLy1, free ribosomal protein obstructs the Mdm2-mediated clearance of p53, which leads to an accumulation of p53 in SLy1$^{KO}$ NK cells. Since p53 is known for its ability to induce apoptosis or senescence, it is thus no more surprising that SLy1$^{KO}$ NK cells have a lower viability compared to wildtype controls (Arefanian *et al.*, 2016). Furthermore, the accumulation of p53 in SLy1$^{KO}$ NK cells leads to a

downregulation of the transcription factor Eomesodermin (EOMES), which causes lower levels of NK cell activating receptors and thus results in NK cell dysfunction and increased cancer susceptibility (Arefanian *et al.*, 2016). **Figure 7** summarizes the probable role of SLy1 in NK cells.

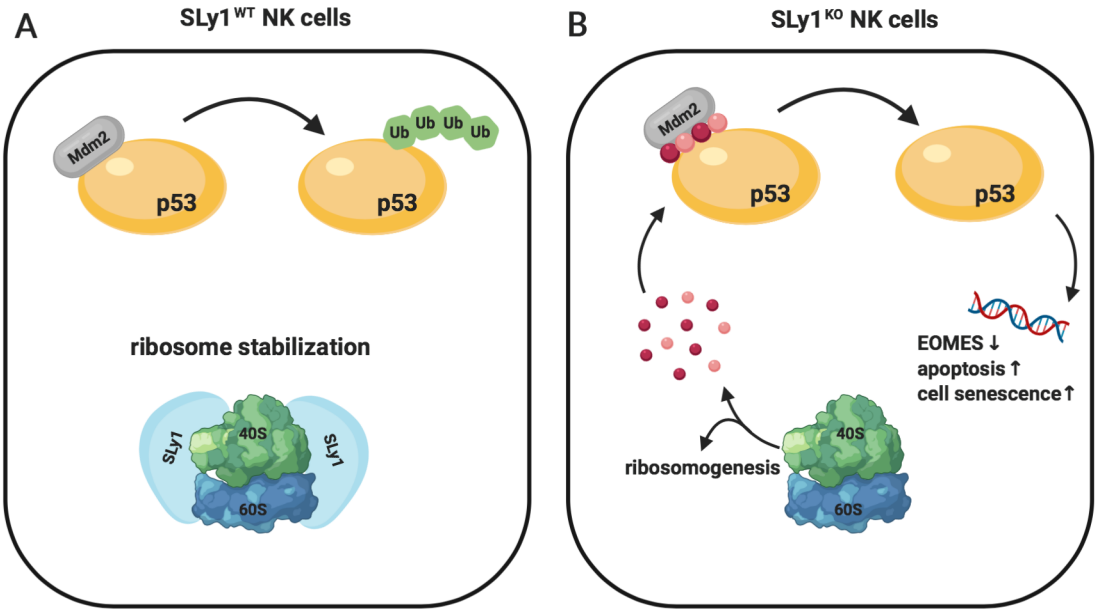


**Figure 7: Graphic representation of SLy1 function in NK cells**

**(A)** In SLy1$^{WT}$ NK cells, SLy1 contributes to ribosomal stability. If SLy1 is missing **(B)**, increased amounts of free ribosomal proteins (RPL5, RPS3; red and pink dots) obstruct the Mdm2-mediated clearance of p53. Accumulation of p53 leads to a downregulation of the transcription factor EOMES, increased apoptosis and cell senescence. Figure adapted and modified from Arefanian *et al.*, 2016, created with BioRender.com.

As NK cells have not only an essential role in eliminating malignantly transformed but also virally infected cells, Arefanian *et al.* furthermore evaluated the role of SLy1 in a mouse cytomegalovirus (MCMV) viral infection model. Interestingly, the functional and phenotypic defects of SLy1$^{KO}$ NK cells are reversible under inflammatory conditions that are caused by the viral infection *via* spillage of pro-inflammatory cytokines, such as IL-2. Thus, MCMV viral clearance is comparable between SLy1$^{WT}$ and SLy1$^{KO}$ littermate mice (Arefanian *et al.*, 2016).

## 1.4 The tumor suppressor p53

The tumor suppressor p53 plays a central role in the response to cellular stress. After its initial identification in complex with the simian virus 40T antigen in transformed rodent cells (Lane and Crawford, 1979; Linzer and Levine, 1979), its function as a tumor suppressor protein was first discovered in 1989 (Baker *et al.*, 1989; Hollstein *et al.*, 1991). Today, p53, also referred to 'the guardian of the genome', is known to be the most frequently mutated gene in cancer (Kandoth *et al.*, 2013; Lawrence *et al.*, 2014).
*TP53*, the gene encoding p53, is the best studied human gene of all time (Dolgin, 2017), yet many open questions remain concerning the regulation of p53 activity by cellular stress (Hafner *et al.*, 2019).

### 1.4.1 The ribosomal protein – Mdm2 – p53 pathway

The two critical mechanisms that are essentiell for cell viability and progeny are cell growth, driven by protein synthesis, and cell division, governed by regulation of the cell cycle. There is emerging evidence of signaling pathways that converge on p53 to connect these two processes with each other (Deisenroth, Franklin and Zhang, 2016), and one of them is the ribosomal protein – Mdm2 – p53 pathway.
Ribosomes play a crucial role in protein synthesis by mediating translation of mRNA into amino acids. In mammalian cells, they consist of two subunits (60S and 40S) that together make up the 80S ribosome. Apart from the ribosomal proteins, they also contain certain auxiliary factors and ribosomal RNA (rRNA). The process of ribosome formation, also called ribosome biogenesis, takes place in the nucleolus, and it is thought that 30% of nucleolar proteins are involved in this process (Boisvert *et al.*, 2007). Different structures of the ribosome fulfill distinct functions. The main function of ribosomal proteins, for example, is the stabilization of the ribosome. Nevertheless, emerging evidence shows that they are also part of other processes, such as rRNA folding, processing, and transport (Tschochner and Hurt, 2003). Furthermore, ribosomal proteins have also been reported to play part in a number of extraribosomal processes, including cell growth and division, as well as cell death (Lindstrom, 2009; Deisenroth, Franklin

and Zhang, 2016). For example, free ribosomal proteins, such as RPL5 (Dai and Lu, 2004), RPL11 (Lohrum *et al.*, 2003; Zhang *et al.*, 2003; Dai *et al.*, 2006), RPL23 (Dai and Lu, 2004; Jin *et al.*, 2004), and RPS7 (Chen *et al.*, 2007a), have been shown to bind to and thereby inhibit Mdm2 which leads to an activation of the p53 signaling pathway. They are therefore emerging as critical regulators of p53 activity (Deisenroth, Franklin and Zhang, 2016). Together with other processes, the existence of free ribosomal proteins in the cell, caused by perturbations of ribosome biogenesis or stabilization, can be considered as 'nucleolar stress'. Nucleolar stress is the key event capable of inducing the ribosomal protein – Mdm2 – p53 stress response and therefore, today, the nucleolus is hypothesized to be a central stress response regulator for activation of p53 (Rubbi and Milner, 2003; Deisenroth, Franklin and Zhang, 2016).

### 1.4.2 Activation of p53

Different types of cellular stress including DNA damage, hypoxia, oncogene activation, and ribosomal stress can cause activation of p53. The activation of p53 then leads to promotion of cell cycle arrest, DNA damage repair, activation of various pathways of cell death and metabolic changes (Hager and Gu, 2014; Kang, Kroemer and Tang, 2019; Kruiswijk, Labuschagne and Vousden, 2015). This happens through protein stabilization and rapid increase of the total p53 protein abundance in the cell, which then initiates the p53 transcriptional response. In non-stressed conditions, the E3 ubiquitin ligase Mdm2 keeps the p53 protein level low (Haupt *et al.*, 1997; Honda, Tanaka and Yasuda, 1997; Kubbutat, Jones and Vousden, 1997). In contrast to that, in a situation of cellular stress, phosphorylation of p53 occurs. This phosphorylation causes an insensitivity of p53 towards Mdm2 (Shieh *et al.*, 1997), which leads to its accumulation in the cell. Furthermore, a regulatory feedback loop is formed, as Mdm2 itself is a transcriptional target of p53 (Barak *et al.*, 1993; Liu, Tavana and Gu, 2019). Although Mdm2 is an important transcriptional target of p53, the tumor suppressor additionally regulates the transcription of many other genes that play a role in a multitude of cell processes, such as DNA damage repair (DDR), cell

cycle arrest, apoptosis and senescence (Aylon and Oren, 2016; Hafner *et al.*, 2019). However, it is still largely unknown how p53 integrates different signals to choose between the competing cell survival and cell death outcomes. To gain further knowledge about these processes has been of great interest and is under current investigation (Hafner *et al.*, 2019).

## 1.5 Aim of the present work

Over the past years, SLy1 was characterized as a novel contributor to ribosomal stability in NK cells. Its deficiency causes a previously unappreciated X-linked ribosomopathy that results in a specific and subtle NK cell dysfunction leading to immunologic susceptibilty to cancer (Arefanian *et al.*, 2016). Evolving evidence shows an involvement of p53-upregulation that is caused by free ribosomal proteins in this process, yet, the exact mechanism of the NK cell dysfunction remains unclear. The present work has two major aims:

1) Provide further evidence for the crucial role of p53 in the dysfunction of $SLy1^{KO}$ NK cells.
2) Analysis of the p53 signaling pathway in $SLy1^{KO}$ NK cells and potential identification of other dysregulated genes in this pathway.

To achieve the first aim, experiments with a newly generated $SLy1^{WT/\ KO}$ NCR-$Cre^{WT/\ TG}$ $p53^{flox/flox}$ mouse model will be performed. Through the NK cell specific expression of the NCR-Cre recombinase, an enzyme that cleaves DNA at specific LoxP sites, p53 can be specifically deleted in NK cells of this mouse model. In a first step, the previous results by Arefanian *et al.* concerning the effects of the absence of SLy1 on NK cells will be verified in order to validate this new mouse model. In order to do so, $SLy1^{WT}$ and $SLy1^{KO}$ NK cells are going to be examined with regards to their numbers, viability, expression of certain activating and inhibitory receptors and their functional capability to kill tumor cells. Afterwards, analyses with $SLy1^{WT}$ and $SLy1^{KO}$ NK cells that lack p53 are going to be conducted to provide further evidence for the crucial role of p53 in the dysfunction of $SLy1^{KO}$ NK cells.

To address the second aim, the p53 signaling pathway is going to be extensively analyzed in $SLy1^{KO}$ NK cells compared to wildtype controls in order to potentially reveal other dysregulated genes in these cells. In a first step, a p53 signaling pathway array analyzing 84 genes that are involved in the pathway is going to be conducted in order to screen for potentially dysregulated up- or downstream located genes. Genes that are detected as dysregulated in $SLy1^{KO}$ NK cells by the array will then be further examined *via* qPCR to validate the array results.

# 2 Materials and Methods

## 2.1 Laboratory equipment

**Table 1: Laboratory equipment**

| Name | Manufacturer | Location |
|---|---|---|
| BD FACSCanto II | BD Biosciences | Heidelberg, Germany |
| CASY cell counter | Roche Diagnostics | Mannheim, Germany |
| Centrifuge 5810 R | Eppendorf | Hamburg, Germany |
| Centrifuge 5430 | Eppendorf | Hamburg, Germany |
| HERAcell incubator | Thermo Scientific | Schwerte, Germany |
| HERAsafe clean bench | Thermo Scientific | Schwerte, Germany |
| LightCycler® 480° | Roche Diagnostics | Mannheim, Germany |
| MACS Multi Stand | Miltenyi Biotec | Bergisch-Gladbach, Germany |
| MidiMACS™ Separator | Miltenyi Biotec | Bergisch-Gladbach, Germany |
| Microscope PrimoVert | Zeiss | Oberkochen, Germany |
| NanoDrop Lite | Peqlab | Erlangen, Germany |
| Neubauer counting chamber | Hecht Assistent | Sonderheim von der Rhoen, Germany |
| Pipetting aid | Integra Biosciences | Zizers, Switzerland |
| QIAxcel | Qiagen | Hilden, Germany |
| peqSTAR 2x Gradient Thermocycler | Peqlab | Erlangen, Germany |
| Waterbath DB15103 | Fisher Scientific | Schwerte, Germany |

## 2.2 Disposable materials

Disposable materials that are not listed in **Table 2** were ordered from Sarstedt, Greiner, BD Biosciences, or Eppendorf.

**Table 2: Disposable materials**

| Name | Manufacturer | Location |
|---|---|---|
| 24/ 48/ 96 well plate | Greiner | Frickenhausen, Germany |
| Cell Strainer, 70 μm | BD Biosciences | Heidelberg, Germany |
| FACS tubes | BD Biosciences | Heidelberg, Germany |
| Falcon tubes, 15 ml/ 50 ml | BD Biosciences | Heidelberg, Germany |
| MACS® Separation Columns, LS | Miltenyi Biotec | Bergisch-Gladbach, Germany |
| Micropipettes, 10/ 100/ 1000 μl | Brand | Wertheim, Germany |
| PCR 8er-SoftStrips | Biozym Biotech Trading | Vienna, Austria |
| Pipettes, 5 ml/ 10 ml/ 25 ml | Greiner | Frickenhausen, Germany |
| Reaction tubes, 1.5 ml/ 2 ml | Eppendorf | Hamburg, Germany |
| Syringe, 5 ml | B. Braun | Melsungen, Germany |
| T75 cell culture flask | Greiner | Frickenhausen, Germany |

## 2.3 Buffers, solutions, and media

All solutions were prepared in water (Millipore quality), and pH was adjusted using NaOH or HCl.

| | |
|---|---|
| Erythrocyte lysis buffer | 0.155 M $NH_4Cl$ |
| | 0.01 M $KHCO_3$ |
| | 0.1 mM EDTA |
| Tissue lysis buffer | 500 mM KCl |
| | 100 mM Tris mit pH 8,3 |
| | 0,1 mg/ml Gelatine |
| | 1 % NP-40 (v/v) |
| | 1 % Tween20 (v/v) |
| | 500 μg/ml Proteinase K |

| | |
|---|---|
| MACS buffer | 500 ml PBS<br>0.5 % BSA (w/v)<br>2.5 mM EDTA |
| Cell culture medium | 500 ml RPMI 1640<br>10 % FCS<br>1 % L-Glutamine<br>1 % Penicillin / Streptomycin<br>0.1 % β-Mercaptoethanol |
| LLC cell culture medium | 500 ml DMEM High Glucose<br>10 % FCS<br>1 % L-Glutamine<br>1 % Penicillin/ Streptomycin<br>0.05 mM β-Mercaptoethanol |

## 2.4 Chemicals and biological kits

Chemicals that are not listed in **Table 3** were ordered in pro analysis quality from Merck, Roth, Serva or Sigma-Aldrich.

**Table 3: General chemicals**

| Name | Manufacturer | Location |
|---|---|---|
| 7-AAD | BD Biosciences | Heidelberg, Germany |
| Annexin-V | BD Biosciences | Heidelberg, Germany |
| β-Mercaptoethanol, 50mM | Gibco® Life Technologies | Darmstadt, Germany |
| Collagenase | Gibco® Life Technologies | Darmstadt, Germany |
| Dispase | Corning | Corning, NY, USA |
| DMEM High Glucose | Sigma-Aldrich | St. Louis, MO, USA |
| DNase | Roche | Mannheim, Germany |
| FCS | GE Healthcare | Munich, Germany |
| Isoflurane | CP Pharma | Burgdorf, Germany |
| L-Glutamine, 200 mM | GE Healthcare | Munich, Germany |

| | | |
|---|---|---|
| Nuclease-free water | Qiagen | Hilden, Germany |
| PBS | Gibco Life Technologies | Darmstadt, Germany |
| Penicillin/ Streptomycin | GE Healthcare | Munich, Germany |
| RPMI | GE Healthcare | Munich, Germany |
| Trypsin-EDTA | Gibco Life Technologies | Darmstadt, Germany |

**Table 4: Commercially available biological kits**

| Kit | Purpose | Manufacturer |
|---|---|---|
| BD™ CompBeads | Compensation particles set | BD Biosciences |
| BIOTAQ™ DNA Polymerase | Amplification of DNA in PCR | Bioline |
| NK Cell Isolation Kit II | NK cell isolation | Miltenyi Biotec |
| NK Cell Isolation Kit mouse | NK cell isolation | Miltenyi Biotec |
| p53 Signaling Pathway RT² Profiler PCR Array | p53 signaling pathway analysis | Qiagen |
| RNeasy Plus Mini Kit | RNA isolation | Qiagen |
| RT² First Strand Kit | cDNA synthesis | Qiagen |
| RT² PreAMP PCR Mastermix | Preamplification of cDNA | Qiagen |
| RT² PreAMP Pathway Primer Mix | Preamplification of cDNA | Qiagen |
| RT² SYBR Green Mastermix | qPCR reaction Mastermix | Qiagen |
| Transcription Factor Buffer Set | Lysis of LLC cells | BD Biosciences |

## 2.5 Oligonucleotides

All primers that are listed in **Table 5** were purchased from biomers.net, Ulm, Germany. ($T_m$ = melting temperature)

**Table 5: PCR primers**

| Target | Length [nu] | Sequence 5' – 3' | $T_m$ [°C] |
|---|---|---|---|
| Screening Primer 3 (for) | 21 | tgacggcagtagggatggtag | 54 |
| Screening Primer 4 (neo-rev) | 22 | cgccttcttgacgagttcttct | 52 |
| Screening Primer 6 (rev-wt) | 19 | agtggcctgggggagatgt | 55 |
| Atm fwd | 24 | tgcagatttatatccatcatccac | 60 |
| Atm rev | 23 | tttcatggattcataagcacctt | 59 |

| | | | |
|---|---|---|---|
| Atr fwd | 20 | tggagagtcacgacttgctg | 60 |
| Atr rev | 20 | aacaataagcgcctggtgaa | 60 |
| Chek1 fwd | 20 | gagggaaggccatatccagt | 60 |
| Chek1 rev | 21 | ttgttcaggcatccctatgtc | 59 |
| Chek2 fwd | 24 | ttattcctgaagtctggacagatg | 59 |
| Chek2 rev | 24 | ctaacagtttcttgacaaggtcca | 59 |
| IPC fwd | 20 | caaatgttgcttgtctggtg | 52 |
| IPC rev | 20 | gtcagtcgagtgcacagttt | 52 |
| NCR-Cre fwd | 28 | gaccatgatgctgggtttggcccagatg | 71 |
| NCR-Cre rev | 24 | atgcggtgggctctatggcttctg | 64 |
| p53flox fwd | 20 | ggttaaacccagcttgacca | 52 |
| p53flox rev | 20 | ggaggcagagacagttggag | 51 |
| Sirt1 fwd | 21 | cagtgagaaaatgctggccta | 60 |
| Sirt1 rev | 23 | ttggtggtacaaacaggtattga | 59 |
| Xrcc4 fwd | 20 | aaatggctccacaggagttg | 60 |
| Xrcc4 rev | 20 | ggtgctctcctctttcaagg | 59 |
| Zmat3 fwd | 18 | cacacccctcgttcctgt | 59 |
| Zmat3 rev | 23 | tcattctctgtagccaggatcac | 60 |

## 2.6 Antibodies

### 2.6.1 Purified antibodies

**Table 6: Purified antibodies**

| Antigen | Species | Clone | Manufacturer |
|---|---|---|---|
| CD16/CD32 | rat | 93 | BioLegend |

### 2.6.2 Fluorescently labeled antibodies

**Table 7: Fluorescently labeled antibodies**

| Antigen | Fluorochrome | Species | Clone | Manufacturer |
|---|---|---|---|---|
| CD3e | Pacific Blue | hamster | 500A2 | BD Biosciences |
| CD45.2 | FITC | mouse | 104 | BD Biosciences |
| CD49b | APC | hamster | HMa2 | BD Biosciences |

| | | | | |
|---|---|---|---|---|
| NK1.1 (PK136) | PE | mouse | | BD Biosciences |
| NKG2D (CD314) | PE | rat | | BD Biosciences |
| NKp46 (CD335) | PE | rat | 29A1.4 | BD Biosciences |
| KLRG1 | PE | hamster | 2F1 | BD Biosciences |
| Sca-1 (Ly-6 A/E) | PE | rat | D7 | BD Biosciences |
| IgG1, κ Isotype Control | PE | hamster | | BD Biosciences |

## 2.7 Animal experiments

### 2.7.1 Breeding of gene targeted mice

For this work, experiments with two different mouse strains (strain 3 and strain 76) of a C57BL/6N background were performed. Strain 3 comprises mice of two different genotypes: SLy1$^{WT}$ and SLy1$^{KO}$ mice (Reis, Pfeffer and Beer-Hammer, 2009). Strain 76, by contrast, was generated by crossing strain 3 with p53 floxed mice (Jax strain 008462) and subsequently with NCR-Cre mice (kindly provided by Veronika Sexl, (Eckelhart *et al.*, 2011)). This strain comprises mice of four different genotypes:

1) SLy1$^{WT}$ NCR-Cre$^{WT}$ p53$^{flox/flox}$
2) SLy1$^{KO}$ NCR-Cre$^{WT}$ p53$^{flox/flox}$
3) SLy1$^{WT}$ NCR-Cre$^{TG}$ p53$^{flox/flox}$
4) SLy1$^{KO}$ NCR-Cre$^{TG}$ p53$^{flox/flox}$

Mice of all four genotypes contain specific *LoxP* sites flanking exons 2-10 of the *Tp53* gene on both alleles. SLy1$^{WT}$ NCR-Cre$^{WT}$ p53$^{flox/flox}$ mice resemble the SLy1$^{WT}$ mice of strain 3, whereas SLy1$^{KO}$ NCR-Cre$^{WT}$ p53$^{flox/flox}$ mice resemble the SLy1$^{KO}$ mice of that strain. To rule out any changes in the phenotype, these controls were also analyzed in a set of experiments. SLy1$^{WT}$ NCR-Cre$^{TG}$ p53$^{flox/flox}$ and SLy1$^{KO}$ NCR-Cre$^{TG}$ p53$^{flox/flox}$ mice additionally express the NK cell specific NCR-Cre recombinase, an enzyme that cleaves DNA at the *LoxP* sites. As in this mouse model, the *Tp53* gene is floxed on both alleles (p53$^{flox/flox}$), expression of the NCR-Cre recombinase leads to a deletion of exons 2-10 of the *Tp53* gene in

NK cells and creation of a null allele. **Figure 8** illustrates the NCR-Cre recombinase p53-loxP system, and **Table 8** gives an overview of the characteristics of each of the four different genotypes of strain 76 mice.

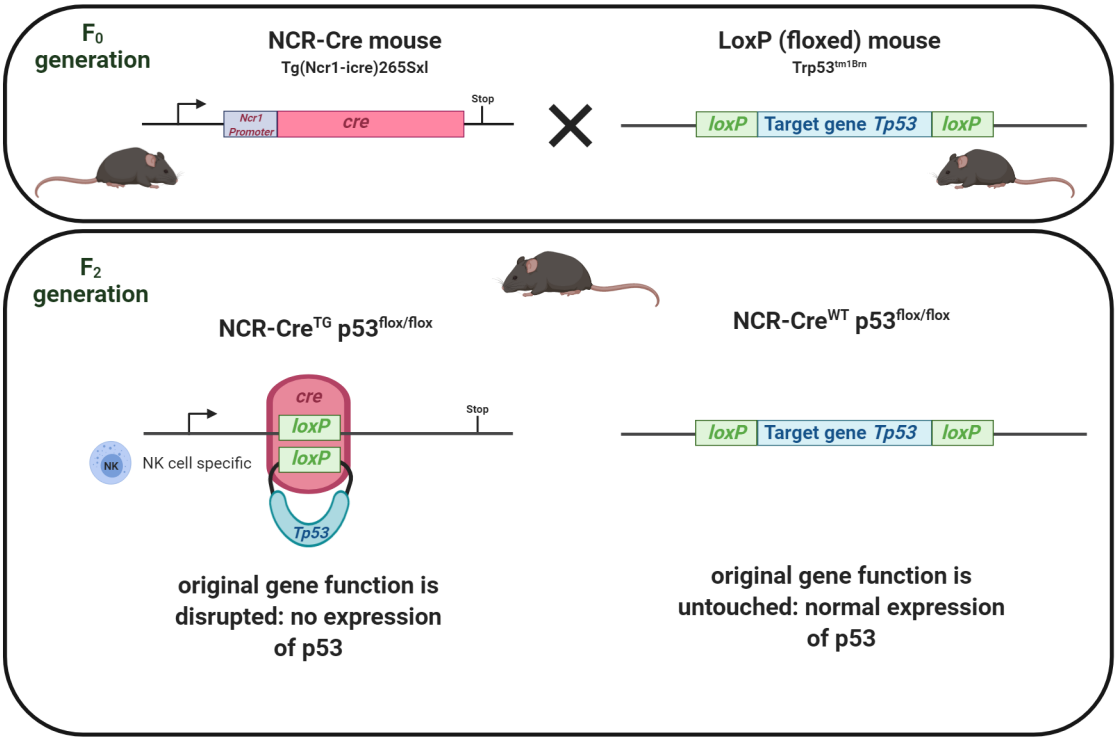


**Figure 8: NCR-Cre recombinase p53-loxP system**

In the $F_0$ generation, NCR-Cre mice that express the NK cell specific NCR-Cre recombinase are interbred with LoxP mice that have a floxed *Tp53* gene, In NCR-Cre$^{TG}$ p53$^{flox/flox}$ mice of the $F_2$ generation, the original gene function of p53 is disrupted and the gene is no more being expressed. By contrast, in NCR-Cre$^{WT}$ p53$^{flox/flox}$ mice the original gene function remains untouched and p53 is expressed normally. Figure created with BioRender.com.

All four genotypes of strain 76 carry a floxed *Tp53* gene (p53$^{flox/flox}$). Therefore, this feature will no more be explicitly mentioned in the following when referring to these mice, and instead naming will be carried out as listed in **Table 8**.

**Table 8: Genotypes of p53-floxed mice**

| Genotype (strain 76) | Characteristics | In the following referred to as |
|---|---|---|
| $SLy1^{WT}$ NCR-$Cre^{WT}$ $p53^{flox/flox}$ | analogue to $SLy1^{WT}$ of strain 3, but with a floxed *Tp53* gene | $SLy1^{WT}$ $NCR^{WT}$ |
| $SLy1^{KO}$ NCR-$Cre^{WT}$ $p53^{flox/flox}$ | analogue to $SLy1^{KO}$ of strain 3, but with a floxed *Tp53* gene | $SLy1^{KO}$ $NCR^{WT}$ |
| $SLy1^{WT}$ NCR-$Cre^{TG}$ $p53^{flox/flox}$ | $SLy1^{WT}$ and deleted expression of p53 in NK cells (because of NK cell specific expression of the Cre-Recombinase) | $SLy1^{WT}$ $NCR^{TG}$ |
| $SLy1^{KO}$ NCR-$Cre^{TG}$ $p53^{flox/flox}$ | $SLy1^{KO}$ and deleted expression of p53 in NK cells (because of NK cell specific expression of the Cre-Recombinase) | $SLy1^{KO}$ $NCR^{TG}$ |

Breeding of all mice that were used for this work was performed in the specific pathogen-free (SPF) animal facility of the Department of Pharmacology/ Toxicology of the Medical Faculty at the University of Tuebingen. A twelve-hour day and night rhythm was kept, and water as well as food were present at free disposal at all times. Inbreeding was performed with 8-10 weeks old animals. The offspring was separated from their parents at 3-4 weeks age. Marking of the animals for identification was performed by the use of ear punching.

### 2.7.2 Selection criteria

Mice were selected and pooled in groups according to their genotype, which was controlled by PCR. Experiments were performed with 9-25 weeks old mice. Age-matched wildtype animals were used as controls. All animal experiments were conducted according to the german animal care regulations and approved by the local government (AZ 23.05.2013 and AZ 26.04.2018).

### 2.7.3 Preparation of spleen and lung

Mice were sacrificed by cervical dislocation after isoflurane-induced anesthesia, and spleen and lung were prepared.
The spleen was carefully removed and homogenized using a 70 μm cell strainer. Spleen cells were centrifuged and resuspended in 3 ml of erythrocyte lysis buffer in order to get rid of the erythrocytes. Lysis was carried out for 3 minutes at room temperature and stopped with 5 ml of ice cold PBS. Again, cells were centrifuged and resuspended in 5 ml of PBS for cell counting. All centrifugation steps were carried out at 4 °C and 500 *g* for 5 minutes.
The lungs were also removed and cut with scissors into small pieces. Then, a lung digestion was performed. A digestion solution containing 1 ml Collagenase, 1 ml Dispase and 20 μl DNase was added and incubated at 37 °C for 60 minutes. The lungs digestion was then pressed through a 70 μm cell strainer. Cells were washed with 5 ml of PBS and centrifuged. Erythrocyte lysis was performed in the same manner as for the spleen. Lung cells were then collected in 1 ml of PBS for cell counting.

## 2.8 Molecular Biology

### 2.8.1 Genotyping of mice

Earmarks were taken from 3-4 weeks old animals and tissue biopsies were subsequently lysed with tissue lysis buffer. Lysis was carried out for at least 6 h at 55 °C. Therafter, lysates were heat-inactivated at 85 °C for 45 minutes and centrifuged for 5 minutes at 500 *g.* They were then stored at -20 °C. PCR was performed with specific primers targeting the respective gene construct. **Table 9 - Table 11** show the applied PCR protocols. PCR products were subsequently separated using the QIAxcel DNA analyzer.

**Table 9: SLy1 PCR run protocol and reaction mix**

| Temperature | Time | |
|---|---|---|
| 95°C | 3 min | |
| 95°C<br>64°C<br>72°C | 15 sec<br>30 sec<br>95 sec | 40 cycles |
| 72°C | 10 min | |

| Ingredient | Volume |
|---|---|
| $H_2O$ | 17.95 µl |
| 10x $NH_4$ Reaction Buffer | 2.50 µl |
| MgCl2 50mM | 1.25 µl |
| dNTPs 10mM | 0.50 µl |
| Primer 3 (fwd) 100 µM | 0.80 µl |
| Primer 4 (neo-rev) 100 µM | 0.40 µl |
| Primer 6 (rev-wt) 100 µM | 0.40 µl |
| Taq-Polymerase (5 units/ µl) | 0.20 µl |

**Table 10: p53 PCR run protocol and reaction mix**

| Temperature | Time | |
|---|---|---|
| 94°C | 3 min | |
| 94°C<br>60°C<br>72°C | 30 sec<br>30 sec<br>60 sec | 34 cycles |
| 72°C | 10 min | |

| Ingredient | Volume |
|---|---|
| $H_2O$ | 17.90 µl |
| 10x $NH_4$ Reaction Buffer | 2.50 µl |

| | |
|---|---|
| MgCl2 50mM | 1.00 µl |
| dNTPs 10mM | 0.50 µl |
| Primer p53flox (fwd) 10 µM | 1.00 µl |
| Primer p53flox (rev) 10 µM | 1.00 µl |
| Taq-Polymerase (5 units/ µl) | 0.10 µl |

**Table 11: NCR-Cre PCR run protocol and reaction mix**

| Temperature | Time | |
|---|---|---|
| 94°C | 5 min | |
| 94°C<br>57°C<br>72°C | 30 sec<br>40 sec<br>60 sec | 30 cycles |
| 72°C | 5 min | |

| Ingredient | Volume |
|---|---|
| $H_2O$ | 18.60 µl |
| 10x $NH_4$ Reaction Buffer | 2.50 µl |
| MgCl2 50mM | 0.75 µl |
| dNTPs 10mM | 0.50 µl |
| Primer NCR-Cre (fwd) 10 µM | 0.50 µl |
| Primer NCR-Cre (rev) 10 µM | 0.50 µl |
| Primer IPC (fwd) 5 µM | 0.25 µl |
| Primer IPC (rev) 5 µM | 0.25 µl |
| Taq-Polymerase (5 units/ µl) | 0.15 µl |

### 2.8.2 p53 signaling pathway array and quantitative real-time PCR

#### RNA isolation

Splenic NK cells were isolated *via* MACS (see page 35). Total cellular RNA was extracted using an RNA purification Kit (RNeasy Plus Mini Kit) for single cell suspensions, according to the manufacturer's instructions. Optical density at 260

nm and 280 nm was measured to assess RNA concentration and purity ($A_{260/280}$). Lambert-Beer equation was used for calculation.

**cDNA synthesis and pre-amplification**

Reverse transcription of RNA was performed with the RT$^2$ First Strand Kit for transcription of 1-100 ng RNA, according to the protocols provided. A pre-amplification was performed using the RT$^2$ PreAMP PCR Mastermix and the RT$^2$ PreAMP Pathway Primer Mix, according to the manufacturer's instructions. The preamplification reaction was then used for the p53 Signaling Pathway RT$^2$ Profiler PCR Array.

**p53 Signaling Pathway RT$^2$ Profiler PCR Array**

RT$^2$ Profiler PCR Arrays are tools for gene expression profiling which can be used for the analysis of distinct panels of genes *via* SYBR-green based real-time PCR. They each contain a list of the pathway-focused genes, five housekeeping genes and a panel of proprietary controls to monitor genomic DNA contamination as well as the first strand synthesis and real-time PCR efficiency (Doe, 2018).
The Mouse p53 Signaling Pathway RT$^2$ Profiler PCR Array analyzes the expression of 84 genes that play a role in the p53-mediated signal transduction. More precisely, these p53-related genes are involved in the processes of apoptosis, cell cycle, cell growth, proliferation, and differentiation, and DNA repair (Doe, 2018). **Appendix Table 1** (see page 97) displays a list of all genes analyzed by the assay.

The array was performed according to the manufacturer's instructions. The preamplification reaction was mixed with appropriate volumes of 2x RT$^2$ SYBR Green Mastermix and RNase-free water, and 25 µl of the newly formed PCR components mix were dispensed into each well of the RT Profiler PCR Array. After a one minute centrifugation at 1000 *g* for the removal of any air bubbles, the RT Profiler PCR Array was placed in the Roche LightCycler 480° and the run was started.

Afterwards, a table of the $C_T$ values was created. The table was then uploaded to “GeneGlobe”, the data analysis web portal from Qiagen. As part of the data anlaysis process, samples were assigned to controls ($SLy1^{WT}$) and test groups ($SLy1^{KO}$), and $C_T$ values were normalized based on a manual selection of reference genes. GeneGlobe calculates fold change/ regulation by the use of the delta delta $C_T$ method and afterwards, a data analysis report is provided (Doe, 2018).

### qPCR

SYBR Green assays were applied for qPCR reactions. Specific primers were used for each target gene to be analyzed (see **Table 5**). For each reaction, *β-actin* was used as a reference gene. An internal positive control sample was run side-by-side for each gene, and fold values were calculated for each sample. Primers were designed with the Universal ProbeLibrary Assay Design Centre from Roche and qPCR data was analyzed with the LightCycler 480° software.

### qPCR run protocol for SYBR Green assays

**Table 12: qPCR run protocol and reaction mix**

| Temperature | Time | |
|---|---|---|
| 98°C | 5 min | |
| 98°C | 10 sec | 45 cycles |
| 60°C | 10 sec | |
| 72°C | 10 sec | |
| 72°C | 5 min | |

| Ingredient | Volume |
|---|---|
| $H_2O$ | 1.7 µl |
| 2x SYBRMaster | 5.0 µl |
| fwd primer | 0.4 µl |
| rev primer | 0.4 µl |
| cDNA | 2.5 µl |

## 2.9 Cellular Biology

### 2.9.1 Isolation of NK cells *via* Magnetic Cell Sorting (MACS)

Isolated spleen cells were homogenized and depleted of erythrocytes. Cells were then washed with PBS, counted and NK cells were isolated using either the NK Cell Isolation Kit II or its successor, the NK Cell Isolation Kit, mouse, which were both purchased from Miltenyi Biotec. Both kits constitute an indirect magnetic labeling system for the isolation of untouched NK cells. The NK Cell Isolation Kit II can be used to isolate NK cells from suspensions of murine spleen, liver as well as lymph node cells, whereas the NK Cell Isolation Kit, mouse has the specific purpose to isolate NK cells from suspensions of murine spleen cells. Non-NK cells, such as T cells, dendritic cells, B cells, granulocytes, macrophages, and erythroid cells are indirectly labelled by using a cocktail of biotin-conjugated antibodies and anti-Biotin MicroBeads. Both kits were used according to the manufacturer's instructions, and the NK cell purity was afterwards measured by flow cytometric analysis. The isolated NK cells were then either used for RNA isolation as part of the p53 signaling pathway array and performance of qPCRs (see page 32), or they were incubated with LLC cells for the performance of a Killing Assay (see page 39).

### 2.9.2 Flow cytometric (FACS) analysis of NK cells

Fluorescence Activated Cell Sorting (FACS) was used as a standard method to 1) analyze NK cell numbers, viability and the expression of surface proteins, 2)

validate NK cell purity after isolation *via* MACS and 3) analyze results of the Killing Assay (see page 39). The applied device was the BD FACSCanto™ II cytometer, and all flow cytometry data were analyzed with FlowJo software.

**Compensation Controls**

Flow cytometry using BD FACSCanto™ II cytometer allows the simultaneous detection of fluorescence in eight different colors, also referred to as channels. Each color absorbs light within an individual range of wavelengths and accordingly emits like that. However, there is always a spill-over of emission into other channels causing false positive signals. After calibrating with single-colored samples, also referred to as compensation controls, the BD FACSDiva software automatically calculates a compensation that counterbalances false positive signals. For this purpose, BD™ CompBeads were applied according to the manufacturer's instructions.

**Surface staining protocol**

Following organ preparation, cells were routinely kept on ice in PBS. Previous to fluorescent staining, $1x10^6$ cell were resuspended in 50 µl of CD16/CD32 antibody dilution (1:50) and incubated for 15 minutes on ice in order to block unspecific binding to Fc-Receptors. For the analysis of NK cell abundance, the spleen and lung cells were stained with 50 µl of a 2x-concentrated master mix containing CD45.2-FITC (1:100), CD3-PacificBlue (1:200) and CD49b-APC (1:400) making it possible to distinguish $CD49b^+$ NK cells from other cell types in the FACS analysis. After 25 minutes of incubation in the dark, cells were washed with 1 ml PBS and centrifuged at 4 °C and 500 *g* for 5 minutes. Finally, $1x10^6$ cells were resuspended in 150 – 200 µl PBS and flow cytometry was performed. **Figure 9** shows the applied gating strategy for the NK cells.

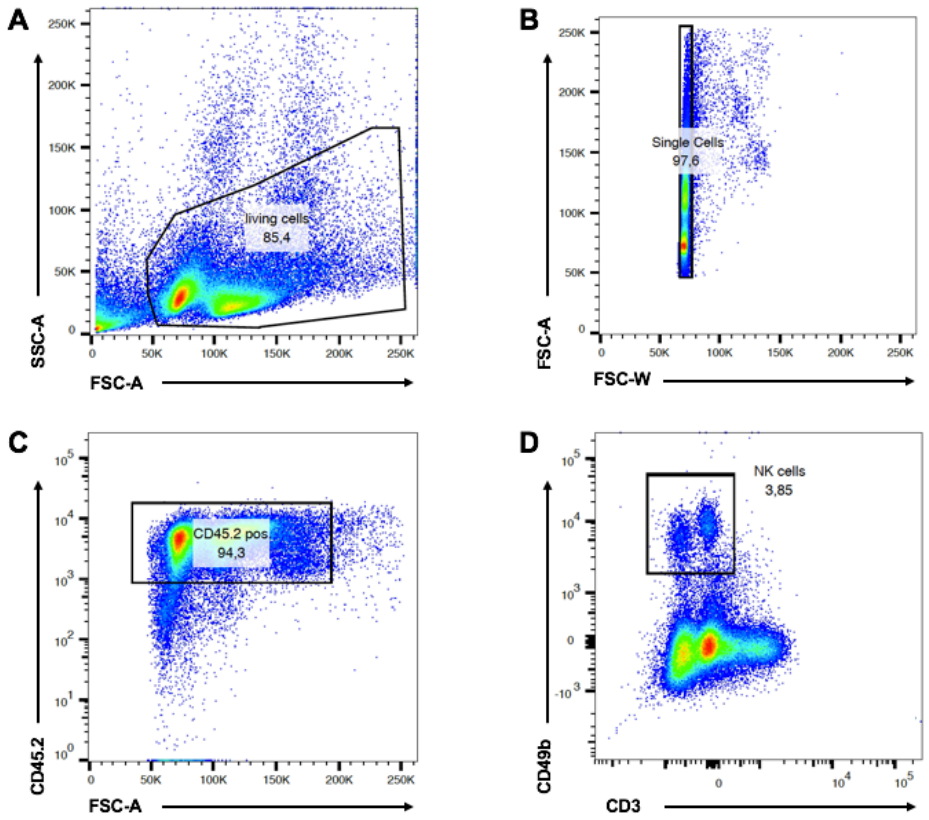


**Figure 9: Gating strategy: NK cells**

**A)** Spleen and lung cells were gated for living cells. **B)** Living cells were gated for single cells. **C)** Single cells were gated for CD45.2 positive hematopoietic cells. **D)** CD45.2 positive cells were gated for CD49b positive/ CD3 negative NK cells.

For the analysis of NK cell viability, cells were additionally stained with Annexin-V and 7AAD. Per sample, 100 µl of Annexin binding buffer, 0.5 µl of Annexin-V and 2.5 µl of 7AAD were applied. Then, cells were incubated for 15 to no more than 60 minutes, before 200 µl PBS were added in advance of cytometric analyses. Annexin-V detects early apopototic cells which contain phosphatidylserine in their outer membrane, whereas 7AAD binds to the DNA of late apoptotic and necrotic cells that have a disrupted cell membrane. Through the combination of both stainings it is possible to distinguish between living cells, early apoptotic cells and late apoptotic/ necrotic cells (**Figure 10**).

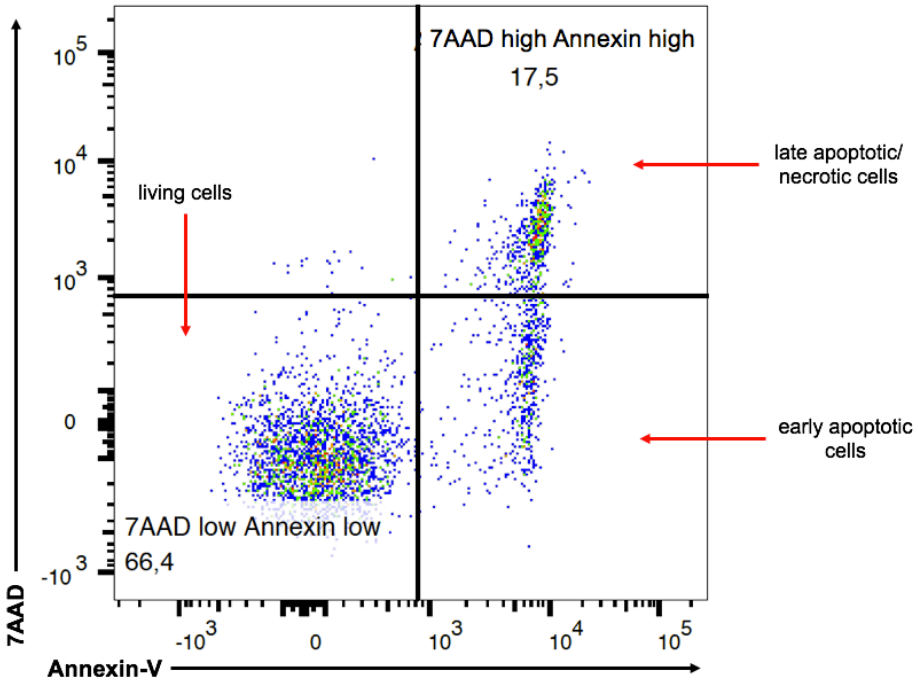


**Figure 10: Gating strategy: Viability of NK cells**

In order to assess NK cell viability, cells were additionally stained with Annexin-V and 7-AAD. Early apoptotic cells are characterized by a high expression of Annexin-V, but are 7AAD negative. In contrast, late apoptotic/ necrotic cells are characterized by a high expression of Annexin-V as well as 7AAD. Living cells are Annexin-V$^{low}$ and 7AAD$^{low}$.

Furthermore, the expression of activating and inhibitory receptors on the surface of NK cells was examined. Therefore, each sample was additionally stained with one of the PE-conjugates (1:200) listed in **Table 7** (see page 26), and the mean fluorescence intensity (gMFI) was measured *via* flow cytometry.

For the validation of NK cell purity, NK cells that were previously isolated *via* MACS were first stained with the CD16/CD32 antibody and then with the 2x concentrated master mix containing CD45.2-FITC (1:100), CD3-PacificBlue (1:200) and CD49b-APC (1:400) in the before described manner, and cells were afterwards measured *via* FACS. **Figure 11** shows the applied gating strategy.

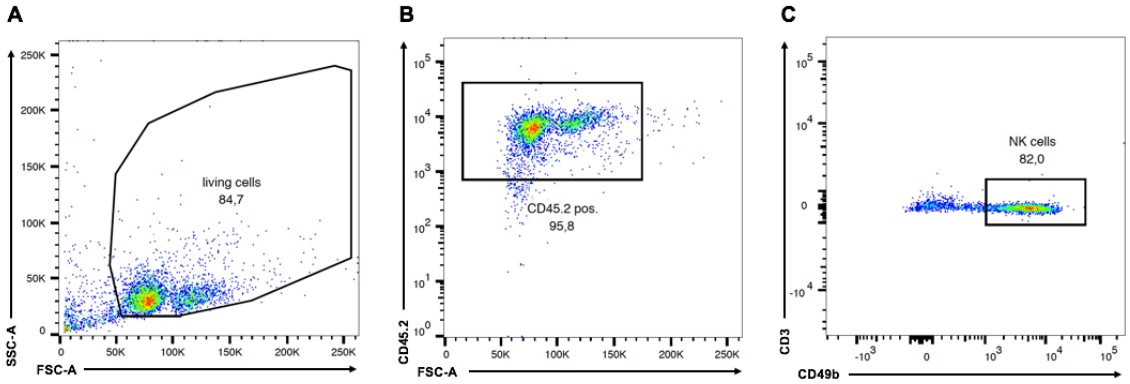


**Figure 11: Gating Strategy: Validation of NK cell purity**

After isolation of NK cells *via* MACS, their purity was validated *via* FACS. **A)** In a first step, gating for living cells was performed. **B)** living cells were gated for CD45.2 positive hematopoietic cells. **C)** CD45.2 positive cells were gated forCD49b positive CD3 negative NK cells. In this example, NK cell purity of 82 % was detected.

The use of flow cytometry for the analysis of the Killing Assays is described in chapter 2.9.4.

### 2.9.3 LLC Cell Culture

Lewis Lung Carcinoma (LLC) cells were purchased from ATCC and stored in liquid nitrogen. Cells were quickly thawed on ice, washed with pre-warmed culture medium and plated on T75 flasks for cultivation. LLC adherent cells were routinely split twice a week. To this end, medium was aspirated, cells were washed with 10 ml PBS and treated with 1 ml trypsin/ EDTA for 30 seconds. Approximately $1x10^6$ cells were resuspended in 20 ml fresh medium and plated on T75 flasks.

### 2.9.4 Killing Assay

In order to analyze the functional capability of splenic NK cells to attack and lyse tumor cells with regard to their expression of SLy1 and p53, Killing Assays were performed. Splenic NK cells were incubated with LLC cells for four hours, and afterwards viability of the tumor cells was analyzed *via* FACS.

**Preparation of LLC cells**

The day before the experiment, LLC cells were split in T75 flasks. On the day of the experiment, medium was removed and cells were washed with 5 ml PBS. 1 ml trypsin-EDTA (0.05 % / 0.02 %) were added and incubated for no longer than one minute. Then, 9 ml of fresh medium were added for resuspension of the cells. After centrifugation for 5 minutes with 300 *g* at room temperature, cells were counted and resuspended in medium to a concentration of $1x10^5$ cells/ ml. In order to achieve a single cell suspension, cells were pushed through a 70 μm nylon filter. Single cells were confirmed under the microscope. Cells were counted and resuspended in PBS to a concentration of $1x10^5$ cells/ ml.

**Preparation of NK cells**

Organ preparation of the spleen and NK cell isolation *via* MACS was conducted as described before (see page 35). Cells were counted and $5x10^4$ NK cells were used for flow cytometric validation of NK cell purity.

**Incubation of LLC cells and NK cells**

After preparation of LLC cells and NK cells, both cell types were jointly incubated on a U-bottom 96-well plate for four hours. For each mouse, triplicates were used (3 wells per mouse) if NK cell amounts were sufficient, and on each well $1x10^4$ LLC cells were incubated with $25x10^4$ NK cells in 200 μl medium at 37 °C and 5 % $CO_2$. After four hours, cells were looked at under the microscope and then harvested for further staining and flow cytometric analysis. **Figure 12** shows a potograph of the LLC cells and NK cells after the four-hour incubation period.

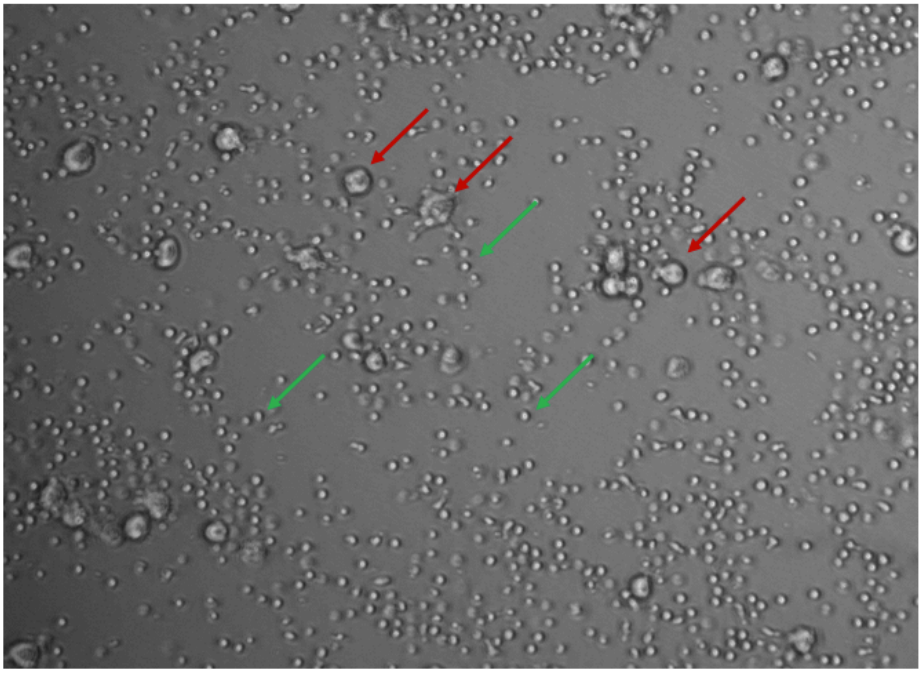

**Figure 12: Photograph of LLC cells and NK cells**

Photograph taken after the four-hour incubation period of LLC cells (exemplarily labelled with red arrows) and NK cells (exemplarily labelled with green arrows). Afterwards, cells were jointly harvested for further analyses.

### Analysis of LLC cell viability *via* FACS

For the flow cytometric analysis of LLC cell viability, LLC cells and NK cells were jointly harvested directly into FACS-tubes after four hours of incubation. After two washing processes with 1 ml and 2 ml PBS, apoptosis/necrosis-staining was performed. In order to do so, cells were stained with Annexin-V and 7AAD. Per sample, 100 µl of Annexin binding buffer, 0.5 µl of Annexin-V and 2.5 µl of 7AAD were applied. Then, cells were incubated for 10 minutes, before 100 µl Annexin binding buffer were added in advance of cytometric analyses.

The cytometric differentiation between LLC cells and NK cells was performed based on the different cell sizes and their granulation using FSC-A and SSC-A. In order to determine LLC cell viability, dead LLC cells were distinguished from living LLC cells by their higher 7AAD signal. **Figure 13** demonstrates the applied gating strategy.

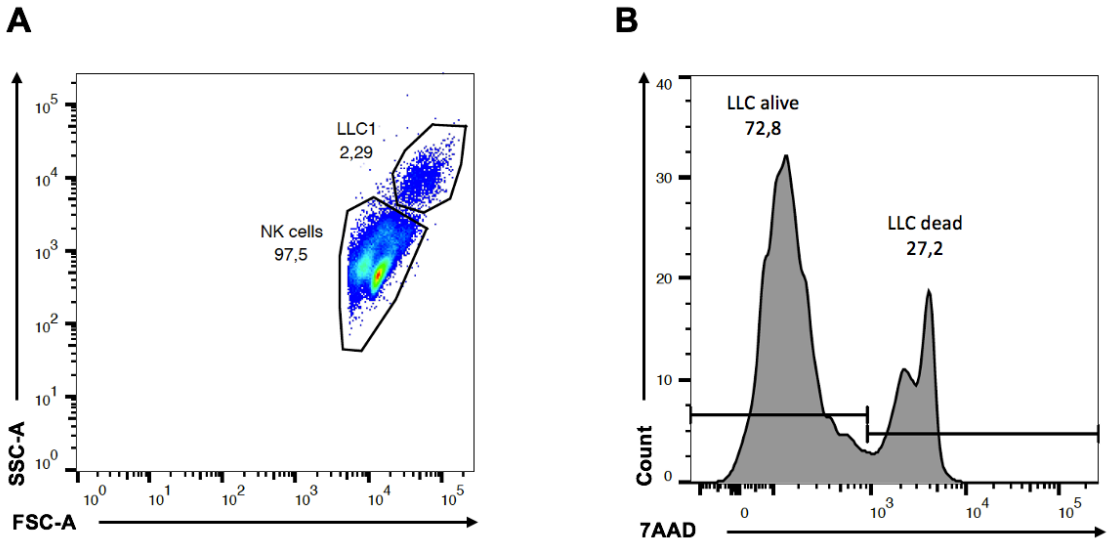


**Figure 13: Gating Strategy: Killing Assay**

LLC cells and NK cells were measured with FACS after 4 hours of incubation. **A)** Gating on LLC cells was performed. **B)** Dead LLC cells were detected by their high signal of 7AAD. By contrast, LLC cells that were still alive after the incubation with NK cells exhibit a lower fluorescence intensity.

### Controls

Three different controls were used to ensure correct analysis of the LLC cell viability.

1) LLC cells: alive
2) LLC cells: dead
3) LLC cells: incubated for four hours without NK cells

For the second control, LLC cells had to be killed and were therefore treated with the BD Transcription Factor Buffer Set according to the manufacturer's instructions. 1 ml Fix/Perm working solution was added to $1x10^6$ LLC cells and incubated at 2-8 °C in the dark for 40-50 minutes. Afterwards, cells were washed with 2 ml PBS for two times. All controls were then stained with Annexin V and 7AAD as described before and analyzed *via* FACS.

## 2.10 Statistical analysis

Statistical evaluation was performed as indicated in the corresponding figure legends. Statistical analyses were performed with GraphPad Prism software and the data analysis web portal “GeneGlobe”. Graphics were created with FlowJo, GraphPad Prism, BioRender.com and GeneGlobe softwares. Figures were composed with PowerPoint.

# 3 Results

## 3.1 Analysis of NK cells in SLy1$^{WT}$ NCR$^{WT}$ and SLy1$^{KO}$ NCR$^{WT}$ mice

In order to validate the results gained by Arefanian *et al.* concerning the function of SLy1 in NK cells, in a first step, analysis of SLy1$^{WT}$ NCR$^{WT}$ and SLy1$^{KO}$ NCR$^{WT}$ mice (strain 76) was performed. These mice resemble the SLy1$^{WT}$ and SLy1$^{KO}$ mice of strain 3, but additionally contain a floxed *Tp53* gene on both alleles. This feature makes them suitable for further analysis of the involvement of p53 in the function of SLy1 in NK cells (see chapter 3.2).
As part of the experiments with SLy1$^{WT}$ NCR$^{WT}$ and SLy1$^{KO}$ NCR$^{WT}$ mice, splenic as well as lung NK cells were analyzed with regard to their numbers, viability, expression of activating and inhibitory receptors and their functional capability to kill tumor cells.

### 3.1.1 Reduced relative and absolute numbers of splenic NK cells in SLy1$^{KO}$ NCR$^{WT}$ mice

In a first step, relative as well as absolute numbers of splenic NK cells in SLy1$^{WT}$ NCR$^{WT}$ and SLy1$^{KO}$ NCR$^{WT}$ mice were assessed.
Relative numbers of NK cells were measured using flow cytometry. Therefore, isolated spleen cells were stained with an antibody mastermix containing CD45.2-FITC, CD3-PacBlue and CD49b-APC and were then analyzed *via* FACS. The measurements showed a significantly reduced percentage of splenic NK cells in SLy1$^{KO}$ NCR$^{WT}$ mice (mean ± SEM: 3.400 ± 0.21 % NK cells) compared to SLy1$^{WT}$ NCR$^{WT}$ controls (mean ± SEM: 4.289 ± 0.28 % NK cells) (**Figure 14**).

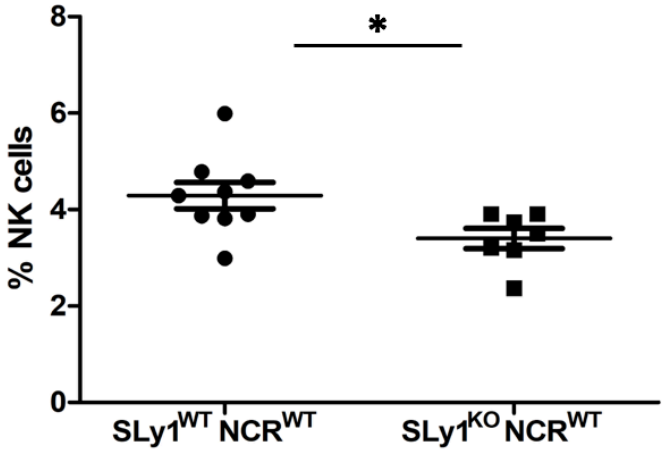


**Figure 14: Reduced relative numbers of splenic NK cells in SLy1$^{KO}$ NCR$^{WT}$ mice**

Relative quantification of splenic NK cells in SLy1$^{WT}$ NCR$^{WT}$ and SLy1$^{KO}$ NCR$^{WT}$ mice. Comparison performed by unpaired t-test. The graph shows mean ± SEM of more than three independent experiments. Star indicates statistical significance: * $p < 0.05$; SLy1$^{WT}$ NCR$^{WT}$: n = 9 mice; SLy1$^{KO}$ NCR$^{WT}$: n = 7 mice.

Absolute numbers of splenic NK cells in SLy1$^{WT}$ NCR$^{WT}$ and SLy1$^{KO}$ NCR$^{WT}$ mice were assessed by two manners: First, the relative amounts of splenic NK cells measured *via* FACS were used to calculate absolute NK cell numbers by using the following equation:

$$Absolute\ NK\ cell\ number =$$

$$\frac{percentage\ of\ NK\ cells\ from\ total\ splenic\ cell\ count\ \times\ total\ splenic\ cell\ count}{100}$$

The calculations showed significantly reduced absolute numbers of splenic NK cells in SLy1$^{KO}$ NCR$^{WT}$ mice (mean ± SEM: 1713000 ± 286200 NK cells) compared to SLy1$^{WT}$ NCR$^{WT}$ controls (mean ± SEM: 3171000 ± 358200 NK cells) (**Figure 15A**).

Secondly, splenic NK cells of SLy1$^{WT}$ NCR$^{WT}$ and SLy1$^{KO}$ NCR$^{WT}$ mice were isolated *via* MACS and cells were counted to measure absolute NK cell numbers. In accordance with the above described findings, these measurements also showed significantly reduced absolute numbers of splenic NK cells in SLy1$^{KO}$

NCR$^{WT}$ mice (mean ± SEM: 336700 ± 36070 NK cells) compared to SLy1$^{WT}$ NCR$^{WT}$ controls (mean ± SEM: 771100 ± 99900 NK cells) (**Figure 15B**).

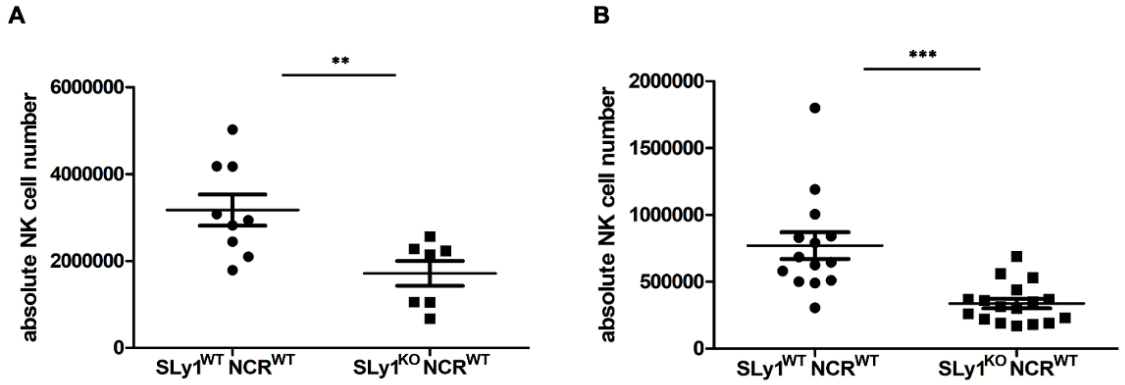


**Figure 15: Reduced absolute numbers of splenic NK cells in SLy1$^{KO}$ NCR$^{WT}$ mice**

**A)** Absolute quantification of splenic NK cells in SLy1$^{WT}$ NCR$^{WT}$ and SLy1$^{KO}$ NCR$^{WT}$ mice *via* mathematical calculation using FACS data. Comparison performed by unpaired t-test. The graph shows mean ± SEM of more than three independent experiments. Stars indicate statistical significance: ** $p < 0.01$; SLy1$^{WT}$ NCR$^{WT}$: n = 9 mice; SLy1$^{KO}$ NCR$^{WT}$: n = 7 mice. **B)** Absolute quantification of splenic NK cells in SLy1$^{WT}$ NCR$^{WT}$ and SLy1$^{KO}$ NCR$^{WT}$ mice after isolation *via* MACS. Comparison performed by unpaired t-test. The graph shows mean ± SEM of more than three independent experiments. Stars indicate statistical significance: *** $p < 0.001$; SLy1$^{WT}$ NCR$^{WT}$: n = 14 mice; SLy1$^{KO}$ NCR$^{WT}$: n = 17 mice.

### 3.1.2 Reduced relative numbers of lung NK cells in SLy1$^{KO}$ NCR$^{WT}$ mice

In addition to the analysis of splenic NK cells, experiments with lung NK cells were conducted. In a first step, relative amounts of lung NK cells in SLy1$^{WT}$ NCR$^{WT}$ and SLy1$^{KO}$ NCR$^{WT}$ mice were measured using flow cytometry. Isolated lung cells were stained with an antibody mastermix containing CD45.2-FITC, CD3-PacBlue and CD49b-APC and were then analyzed *via* FACS. The measurements showed a significantly reduced percentage of lung NK cells in SLy1$^{KO}$ NCR$^{WT}$ mice (mean ± SEM: 4.010 ± 0.18 % NK cells) compared to SLy1$^{WT}$ NCR$^{WT}$ controls (mean ± SEM: 6.855 ± 0.79 % NK cells) (**Figure 16**).

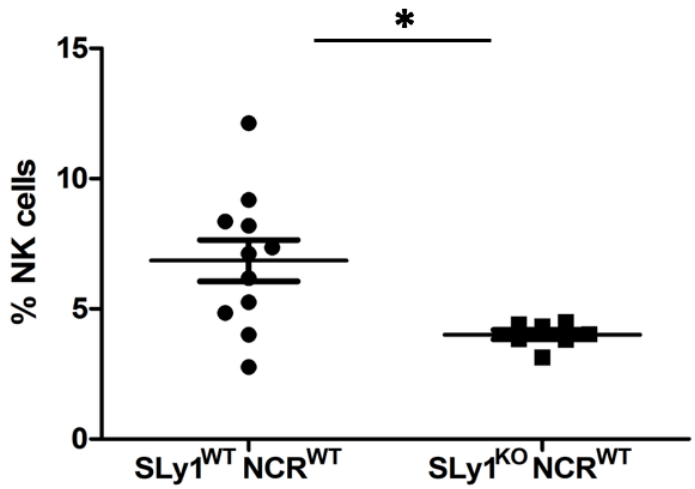


**Figure 16: Reduced relative numbers of lung NK cells in SLy1$^{KO}$ NCR$^{WT}$ mice**

Relative quantification of lung NK cells in SLy1$^{WT}$ NCR$^{WT}$ and SLy1$^{KO}$ NCR$^{WT}$ mice. Comparison performed by unpaired t-test. The graph shows mean ± SEM of more than three independent experiments. Star indicates statistical significance: * $p < 0.05$; SLy1$^{WT}$ NCR$^{WT}$: n = 11 mice; SLy1$^{KO}$ NCR$^{WT}$: n = 7 mice.

Secondly, absolute numbers of lung NK cells in SLy1$^{WT}$ NCR$^{WT}$ and SLy1$^{KO}$ NCR$^{WT}$ mice were assessed. Therefore, the relative amounts of lung NK cells measured *via* FACS were used to calculate absolute NK cell numbers by using the following equation:

$$Absolute\ NK\ cell\ number\ =$$

$$\frac{percentage\ of\ NK\ cells\ from\ total\ lung\ cell\ count\ \times\ total\ lung\ cell\ count}{100}$$

The calculations showed no statistically significant reduction of absolute numbers of lung NK cells in SLy1$^{KO}$ NCR$^{WT}$ mice (mean ± SEM: 161900 ± 18990 NK cells) compared to SLy1$^{WT}$ NCR$^{WT}$ controls (mean ± SEM: 268000 ± 47670 NK cells) due to the high scatter in the SLy1$^{WT}$ NCR$^{WT}$ controls (**Figure 17**).

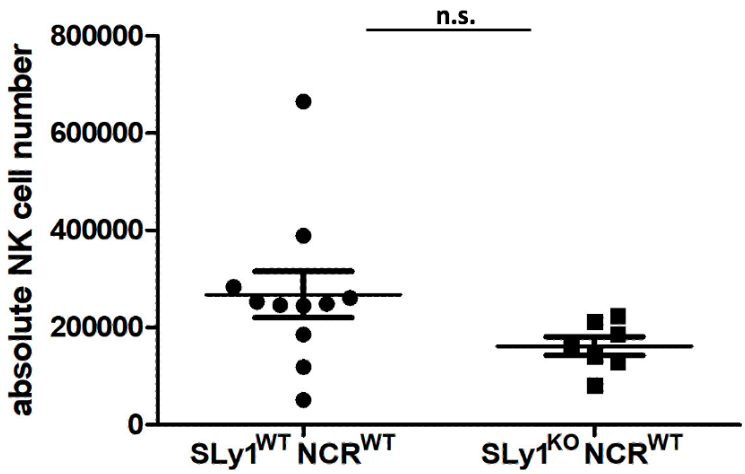


**Figure 17: No reduced absolute numbers of lung NK cells in SLy1$^{KO}$ NCR$^{WT}$ mice**

Absolute quantification of lung NK cells in SLy1$^{WT}$ NCR$^{WT}$ and SLy1$^{KO}$ NCR$^{WT}$ mice. Comparison performed by unpaired t-test. The graph shows mean ± SEM of more than three independent experiments; n.s. = statistically not significant; SLy1$^{WT}$ NCR$^{WT}$: n = 11 mice; SLy1$^{KO}$ NCR$^{WT}$: n = 7 mice.

### 3.1.3 Reduced viability of splenic NK cells in SLy1$^{KO}$ NCR$^{WT}$ mice

In a second step, the viability of splenic NK cells in SLy1$^{WT}$ NCR$^{WT}$ and SLy1$^{KO}$ NCR$^{WT}$ mice was measured using flow cytometry. Isolated spleen cells were stained with an antibody mastermix containing CD45.2-FITC, CD3-PacBlue and CD49b-APC as well as with Annexin-V and 7-AAD. Cells were then analyzed *via* FACS and the percentages of apoptotic NK cells (sum of early and late apoptotic cells) were determined. The measurement showed a significantly increased percentage of apoptotic NK cells in SLy1$^{KO}$ NCR$^{WT}$ mice (mean ± SEM: 30.13 ± 1.58 % apoptotic cells) compared to SLy1$^{WT}$ NCR$^{WT}$ controls (mean ± SEM: 23.97 ± 1.39 % apoptotic cells) (**Figure 18**).

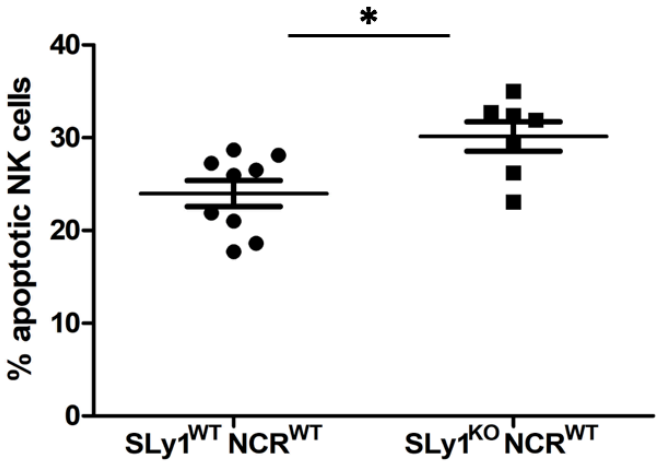


**Figure 18: Reduced viability of splenic NK cells in SLy1$^{KO}$ NCR$^{WT}$ mice**

Quantification of splenic apoptotic NK cells in SLy1$^{WT}$ NCR$^{WT}$ and SLy1$^{KO}$ NCR$^{WT}$ mice. Comparison performed by unpaired t-test. The graph shows mean ± SEM of more than three independent experiments. Star indicates statistical significance: * $p < 0.05$; SLy1$^{WT}$ NCR$^{WT}$: n = 9 mice; SLy1$^{KO}$ NCR$^{WT}$: n = 7 mice.

### 3.1.4 Reduced expression of activating receptors on splenic SLy1$^{KO}$ NCR$^{WT}$ NK cells

Furthermore, the expression of the activating receptors NKG2D, NK1.1 and NKp46 on splenic NK cells of SLy1$^{WT}$ NCR$^{WT}$ and SLy1$^{KO}$ NCR$^{WT}$ mice was measured using flow cytometry. Isolated spleen cells were stained with an antibody mastermix containing CD45.2-FITC, CD3-PacBlue, CD49b-APC and one of the following PE-conjugates: NKG2D-PE, NK1.1-PE and NKp46-PE. Cells were then analyzed *via* FACS. The measurements showed a significantly reduced expression of all three activating receptors on splenic SLy1$^{KO}$ NCR$^{WT}$ NK cells compared to SLy1$^{WT}$ NCR$^{WT}$ controls (**Figure 19**). Concerning the expression of NKG2D (**Figure 19A**), the mean gMFI ± SEM was detected as 316.0 ± 19.51 in SLy1$^{WT}$ NCR$^{WT}$ NK cells compared to 177.6 ± 33.32 in SLy1$^{KO}$ NCR$^{WT}$ NK cells. Regarding the expression of NK1.1 (**Figure 19B**) the mean gMFI ± SEM was detected as 748.8 ± 58.89 in SLy1$^{WT}$ NCR$^{WT}$ NK cells compared to 450.6 ± 49.83 in SLy1$^{KO}$ NCR$^{WT}$ NK cells. Concerning the expression of NKp46 (**Figure 19C**), the mean gMFI ± SEM was detected as 280.8 ± 21.02 in SLy1$^{WT}$ NCR$^{WT}$ NK cells compared to 184.1 ± 14.79 in SLy1$^{KO}$ NCR$^{WT}$ NK cells.

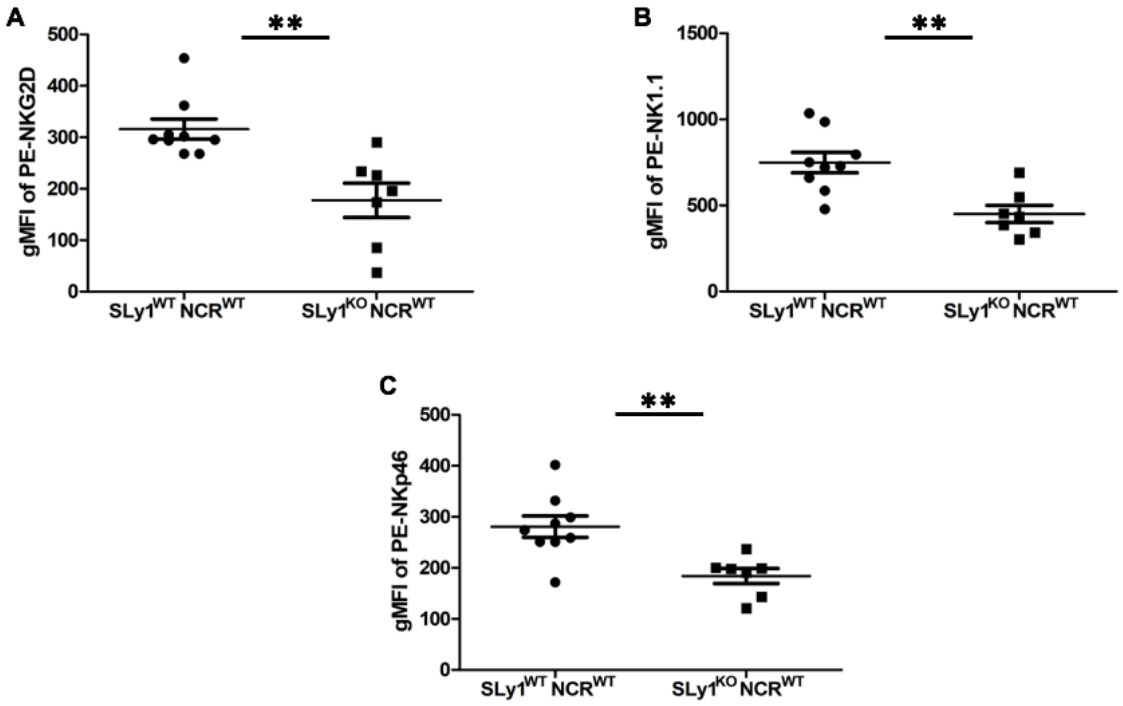


**Figure 19: Reduced expression of activating receptors on splenic SLy1$^{KO}$ NCR$^{WT}$ NK cells**

Relative expression of **A)** NKG2D, **B)** NK1.1 and **C)** NKp46 on SLy1$^{WT}$ NCR$^{WT}$ and SLy1$^{KO}$ NCR$^{WT}$ splenic NK cells. Comparison performed by unpaired t-test. The graphs show mean gMFI ± SEM of more than three independent experiments. Stars indicate statistical significance: ** $p < 0.01$; SLy1$^{WT}$ NCR$^{WT}$: n = 9 mice; SLy1$^{KO}$ NCR$^{WT}$: n = 7 mice.

### 3.1.5 Unaltered expression of activating receptors on lung SLy1$^{KO}$ NCR$^{WT}$ NK cells

Furthermore, the expression of the activating receptors NKG2D, NK1.1 and NKp46 on lung NK cells of SLy1$^{WT}$ NCR$^{WT}$ and SLy1$^{KO}$ NCR$^{WT}$ mice was measured using flow cytometry. Isolated lung cells were stained with an antibody mastermix containing CD45.2-FITC, CD3-PacBlue, CD49b-APC and one of the following PE-conjugates: NKG2D-PE, NK1.1-PE and NKp46-PE. Cells were then analyzed *via* FACS. The measurement showed no differences in the expression of any of the three activating receptors between lung SLy1$^{KO}$ NCR$^{WT}$ NK cells and SLy1$^{WT}$ NCR$^{WT}$ controls (**Figure 20**). Concerning the expression of NKG2D (**Figure 20A**), the mean gMFI ± SEM was detected as 54.07 ± 17.21 in SLy1$^{WT}$ NCR$^{WT}$ NK cells compared to 66.92 ± 15.22 in SLy1$^{KO}$ NCR$^{WT}$ NK cells. Regarding the expression of NK1.1 (**Figure 20B**), the mean gMFI ± SEM was detected as 496.5 ± 33.30 in SLy1$^{WT}$ NCR$^{WT}$ NK cells compared to 403.7 ± 47.21

in SLy1$^{KO}$ NCR$^{WT}$ NK cells. Concerning the expression of NKp46 (**Figure 20C**), the mean gMFI ± SEM was detected as 346.4 ± 19.35 in SLy1$^{WT}$ NCR$^{WT}$ NK cells compared to 317.0 ± 31.77 in SLy1$^{KO}$ NCR$^{WT}$ NK cells.

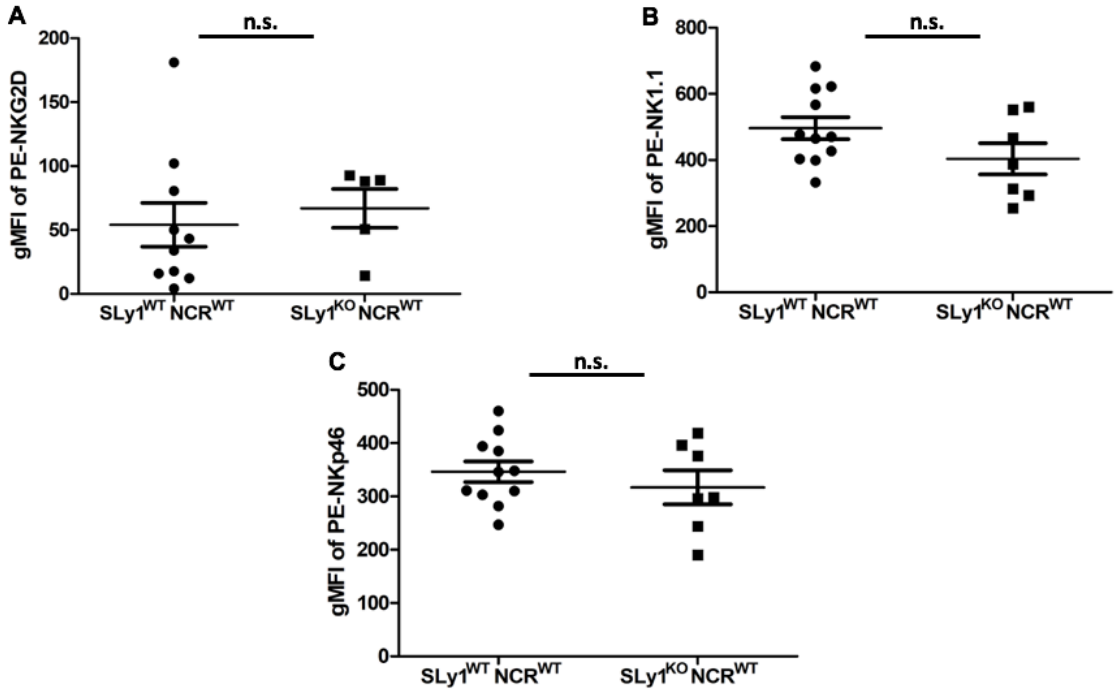


**Figure 20: Unaltered expression of activating receptors on lung SLy1$^{KO}$ NCR$^{WT}$ NK cells**

Relative expression of **A)** NKG2D, **B)** NK1.1 and **C)** NKp46 on SLy1$^{WT}$ NCR$^{WT}$ and SLy1$^{KO}$ NCR$^{WT}$ lung NK cells. Comparison performed by unpaired t-test. The graphs show mean gMFI ± SEM of more than three independent experiments; n.s. = statistically not significant; SLy1$^{WT}$ NCR$^{WT}$: n = 10-11 mice; SLy1$^{KO}$ NCR$^{WT}$: n = 5-7 mice.

### 3.1.6 Unaltered expression of inhibitory receptors on splenic SLy1$^{KO}$ NCR$^{WT}$ NK cells

Arefanian *et al.* analyzed the expression of activating receptors on SLy1$^{KO}$ NK cells compared to wildtype controls, but did not measure the expression of inhibitory receptors. In the present work, the expression of the inhibitory receptors KLRG-1 and Sca-1 on splenic NK cells of SLy1$^{WT}$ NCR$^{WT}$ and SLy1$^{KO}$ NCR$^{WT}$ mice was additionally measured using flow cytometry. Isolated spleen cells were stained with an antibody mastermix containing CD45.2-FITC, CD3-PacBlue, CD49b-APC and one of the following PE-conjugates: KLRG-1-PE and Sca-1-PE. Cells were then analyzed *via* FACS. The measurement showed no dysregulated

expression of any inhibitory receptor on splenic SLy1$^{KO}$ NCR$^{WT}$ NK cells (KLRG1: mean gMFI ± SEM: 260.6 ± 14.88; Sca-1: mean gMFI ± SEM: 275.9 ± 35.40) compared to SLy1$^{WT}$ NCR$^{WT}$ controls (KLRG1: mean gMFI ± SEM: 295.3 ± 24.65; Sca-1: mean gMFI ± SEM: 277.7 ± 31.11) (**Figure 21**).

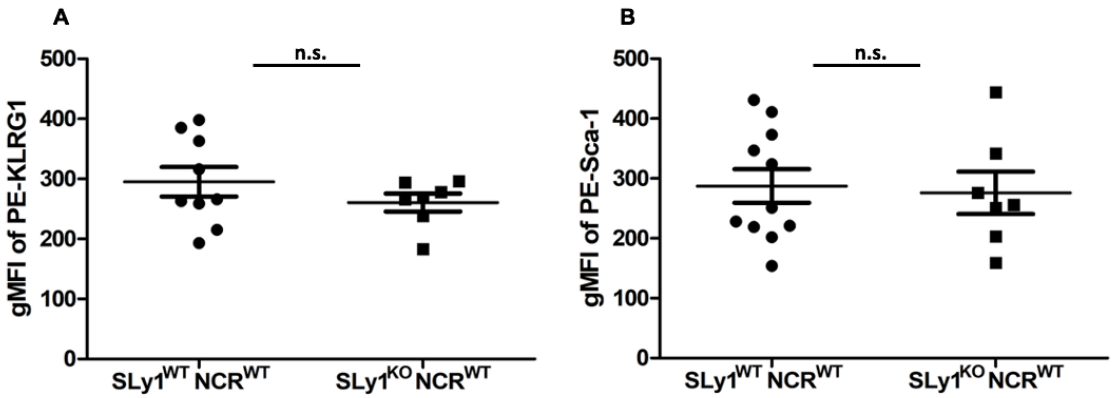


**Figure 21: Unaltered expression of inhibitory receptors on splenic SLy1$^{KO}$ NCR$^{WT}$ NK cells**

**A)** Relative expression of KLRG1 on SLy1$^{WT}$ NCR$^{WT}$ and SLy1$^{KO}$ NCR$^{WT}$ splenic NK cells. **B)** Relative expression of Sca-1 on SLy1$^{WT}$ NCR$^{WT}$ and SLy1$^{KO}$ NCR$^{WT}$ splenic NK cells. Comparison performed by unpaired t-test. The graphs show mean gMFI ± SEM of more than three independent experiments; n.s. = statistically not significant; SLy1$^{WT}$ NCR$^{WT}$: n = 9 mice; SLy1$^{KO}$ NCR$^{WT}$: n = 7 mice.

### 3.1.7 Functional impairment of splenic SLy1$^{KO}$ NCR$^{WT}$ NK cells

In a next step, the functional capability of splenic SLy1$^{KO}$ NCR$^{WT}$ NK cells to attack and kill tumor cells compared to SLy1$^{WT}$ NCR$^{WT}$ controls was assessed. Splenic SLy1$^{KO}$ NCR$^{WT}$ NK cells were isolated *via* MACS and incubated with LLC cells. After four hours, the viability of the tumor cells was analyzed *via* FACS. The measurements showed significantly reduced percentages of apoptotic LLC cells, as a surrogate parameter for the capability of NK cells to kill tumor cells, for the SLy1$^{KO}$ NCR$^{WT}$ NK cells (mean ± SEM: 10.25 ± 2.446 % apoptotic cells) compared to the SLy1$^{WT}$ NCR$^{WT}$ controls (mean ± SEM: 20.42 ± 2.195 % apoptotic cells) (**Figure 22**).

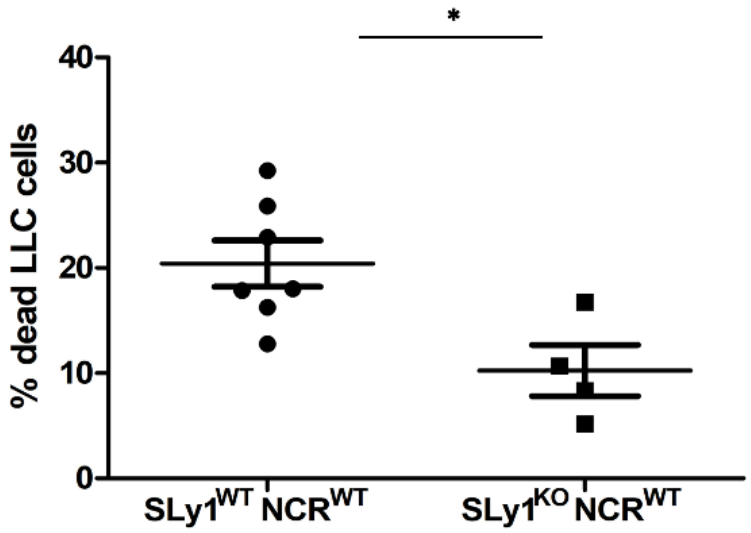


**Figure 22: Functional impairment of splenic SLy1$^{KO}$ NCR$^{WT}$ NK cells**

Quantification of dead LLC cells after 4 hours of incubation with SLy1$^{WT}$ NCR$^{WT}$ and SLy1$^{KO}$ NCR$^{WT}$ splenic NK cells. Comparison performed by unpaired t-test. The graph shows mean ± SEM of four independent experiments; Star indicates statistical significance: * $p < 0.05$; SLy1$^{WT}$ NCR$^{WT}$: n = 7 mice; SLy1$^{KO}$ NCR$^{WT}$: n = 4 mice.

## 3.2 Influence of p53 deletion on NK cells of SLy1$^{WT}$ NCR$^{TG}$ and SLy1$^{KO}$ NCR$^{TG}$ mice

Absence of the SLy1 protein causes a reduction of number, viability and functionality of splenic NK cells, as well as a decreased expression of certain activating receptors (see chapter 3.1). In 2016, Arefanian *et al.* postulated an involvement of p53-upregulation in this process, yet, the exact mechanism of the NK cell dysfunction remains unclear. In order to further proof Arefanian's theory, experiments with SLy1$^{WT}$ NCR$^{TG}$ and SLy1$^{KO}$ NCR$^{TG}$ mice were performed. These mice express the NK cell-specific NCR-Cre recombinase, an enzyme that cleaves DNA at specific LoxP sites. As in this mouse model, the *Tp53* gene is floxed on both alleles, p53 expression is completely disrupted in NK cells of NCR$^{TG}$ mice. If the dysregulation of SLy1-deficient NK cells is p53-dependent, as postulated by Arefanian *et al.*, deletion of the p53-protein should lead to restoration of the observed effects.

### 3.2.1 Deletion of p53 restores relative numbers of splenic NK cells in SLy1$^{KO}$ NCR$^{TG}$ mice

The relative amount of splenic NK cells in SLy1$^{KO}$ NCR$^{TG}$ mice compared to SLy1$^{WT}$ NCR$^{TG}$ controls was measured using flow cytometry. Isolated spleen cells were stained with an antibody mastermix containing CD45.2-FITC, CD3-PacBlue and CD49b-APC and were then analyzed *via* FACS. In contrast to the analysis of SLy1$^{WT}$ NCR$^{WT}$ and SLy1$^{KO}$ NCR$^{WT}$ NK cells (see page 44) there was no statistically significant difference detected between the percentages of splenic NK cells in SLy1$^{KO}$ NCR$^{TG}$ mice (mean ± SEM: 3.309 ± 0.16 % NK cells) and SLy1$^{WT}$ NCR$^{TG}$ controls (mean ± SEM: 3.284 ± 0.33 % NK cells) (**Figure 23**).

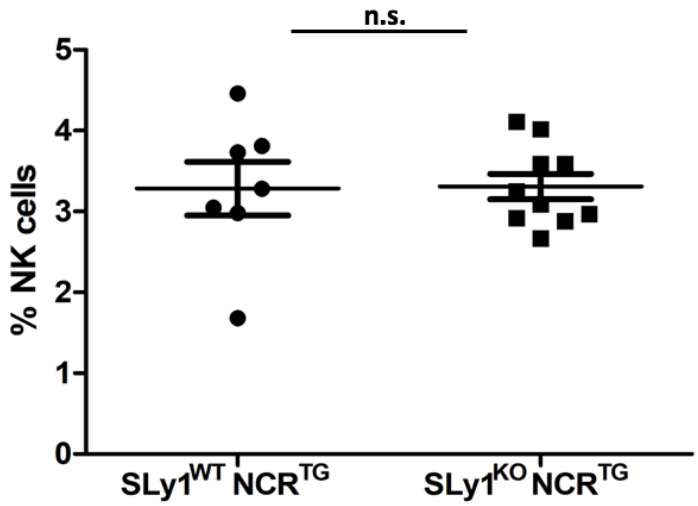


**Figure 23: Deletion of p53 restores relative numbers of splenic NK cells in SLy1$^{KO}$ NCR$^{TG}$ mice**

Relative quantification of splenic NK cells in SLy1$^{WT}$ NCR$^{TG}$ and SLy1$^{KO}$ NCR$^{TG}$ mice. Comparison performed by unpaired t-test. The graph shows mean ± SEM of more than three independent experiments; n.s. = statistically not significant; SLy1$^{WT}$ NCR$^{WT}$: n = 7 mice; SLy1$^{KO}$ NCR$^{WT}$: n = 10 mice.

### 3.2.2 Deletion of p53 restores relative numbers of lung NK cells in SLy1$^{KO}$ NCR$^{TG}$ mice

In addition to the analysis of splenic NK cells, experiments with lung NK cells were conducted. The relative amount of lung NK cells in SLy1$^{KO}$ NCR$^{TG}$ mice compared to SLy1$^{WT}$ NCR$^{TG}$ controls was measured using flow cytometry. Isolated lung cells were stained with an antibody mastermix containing CD45.2-

FITC, CD3-PacBlue and CD49b-APC and were then analyzed *via* FACS. In contrast to the analysis of SLy1$^{WT}$ NCR$^{WT}$ and SLy1$^{KO}$ NCR$^{WT}$ NK cells (see page 46), there was no statistically significant difference detected between the percentages of lung NK cells in SLy1$^{KO}$ NCR$^{TG}$ mice (mean ± SEM: 4.490 ± 0.42 % NK cells) and SLy1$^{WT}$ NCR$^{TG}$ controls (mean ± SEM: 5.001 ± 0.62 % NK cells) (**Figure 24**).

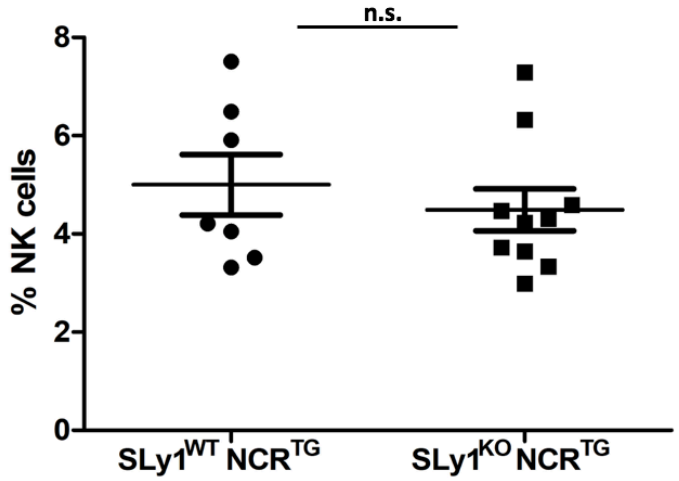


**Figure 24: Deletion of p53 restores relative numbers of lung NK cells in SLy1$^{KO}$ NCR$^{TG}$ mice**

Quantification of lung NK cells in SLy1$^{WT}$ NCR$^{TG}$ and SLy1$^{KO}$ NCR$^{TG}$ mice. Comparison performed by unpaired t-test. The graph shows mean ± SEM of more than three independent experiments; n.s. = statistically not significant; SLy1$^{WT}$ NCR$^{WT}$: n = 7 mice; SLy1$^{KO}$ NCR$^{WT}$: n = 10 mice.

### 3.2.3 Deletion of p53 does not restore absolute numbers of splenic NK cells in SLy1$^{KO}$ NCR$^{TG}$ mice

The absolute numbers of splenic NK cells in SLy1$^{KO}$ NCR$^{TG}$ mice compared to SLy1$^{WT}$ NCR$^{TG}$ controls were assessed by two manners, as previously described in chapter 3.1.1: First, the relative amounts of splenic NK cells measured *via* FACS were used to calculate absolute NK cell numbers by using the following equation:

$$Absolute\ NK\ cell\ number\ =$$

$$\frac{percentage\ of\ NK\ cells\ from\ total\ splenic\ cell\ count\ \times\ total\ splenic\ cell\ count}{100}$$

Secondly, splenic NK cells of SLy1$^{WT}$ NCR$^{TG}$ and SLy1$^{KO}$ NCR$^{TG}$ mice were isolated *via* MACS and cells were counted to measure absolute NK cell numbers. In contrast to the findings concerning the relative amounts of NK cells, deletion of p53 did not restore the absolute numbers of splenic NK cells in SLy1$^{KO}$ NCR$^{TG}$ mice (**Figure 25**). Both, the calculation of absolute NK cell numbers with FACS data (**Figure 25A**) as well as the measurement of absolute NK cell numbers after isolation *via* MACS (**Figure 25B**) showed significantly reduced absolute numbers of splenic NK cells in SLy1$^{KO}$ NCR$^{TG}$ mice (FACS: mean ± SEM: 1588000 ± 214400 NK cells; MACS: mean ± SEM: 304100 ± 25230 NK cells) compared to SLy1$^{WT}$ NCR$^{TG}$ controls (FACS: mean ± SEM: 2801000 ± 444000 NK cells; MACS: mean ± SEM: 706100 ± 41410 NK cells).

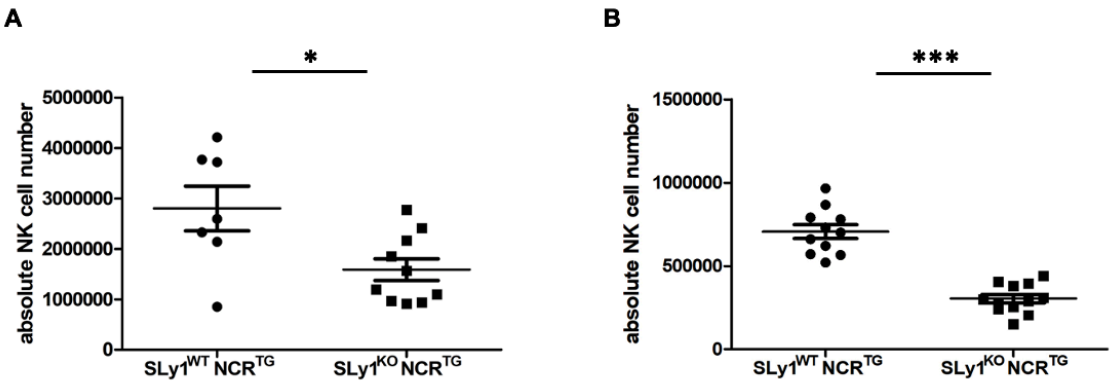


**Figure 25: Deletion of p53 does not restore absolute numbers of splenic NK cells in SLy1$^{KO}$ NCR$^{TG}$ mice**

(**A**) Absolute quantification of splenic NK cells in SLy1$^{WT}$ NCR$^{TG}$ and SLy1$^{KO}$ NCR$^{TG}$ mice *via* mathematical calculation using FACS data. Comparison performed by unpaired t-test. The graph shows mean ± SEM of more than three independent experiments. Star indicates statistical significance: * $p < 0.05$; SLy1$^{WT}$ NCR$^{TG}$: n = 7 mice; SLy1$^{KO}$ NCR$^{TG}$: n = 10 mice. (**B**) Absolute quantification of splenic NK cells in SLy1$^{WT}$ NCR$^{WT}$ and SLy1$^{KO}$ NCR$^{WT}$ mice after isolation *via* MACS. Comparison performed by unpaired t-test. The graph shows mean ± SEM of more than three independent experiments. Stars indicate statistical significance: * $p < 0.05$; *** $p < 0.001$; SLy1$^{WT}$ NCR$^{TG}$: n = 11 mice; SLy1$^{KO}$ NCR$^{TG}$: n = 12 mice.

### 3.2.4 Deletion of p53 restores viability of splenic NK cells in SLy1$^{KO}$ NCR$^{TG}$ mice

Furthermore, the viability of splenic NK cells in SLy1$^{KO}$ NCR$^{TG}$ mice compared to SLy1$^{WT}$ NCR$^{TG}$ controls was assessed. Isolated spleen cells were stained with

an antibody mastermix containing CD45.2-FITC, CD3-PacBlue and CD49b-APC as well as with Annexin-V and 7-AAD. Cells were then analyzed *via* FACS and the percentage of apoptotic NK cells was measured. In contrast to the analysis of SLy1$^{WT}$ NCR$^{WT}$ and SLy1$^{KO}$ NCR$^{WT}$ NK cells (see page 48), there was no statistically significant difference detected between the percentages of apoptotic NK cells in SLy1$^{KO}$ NCR$^{TG}$ mice (mean ± SEM: 26.50 ± 1.166 % apoptotic cells) and SLy1$^{WT}$ NCR$^{TG}$ controls (mean ± SEM: 27.47 ± 2.280 % apoptotic cells) (**Figure 26**).

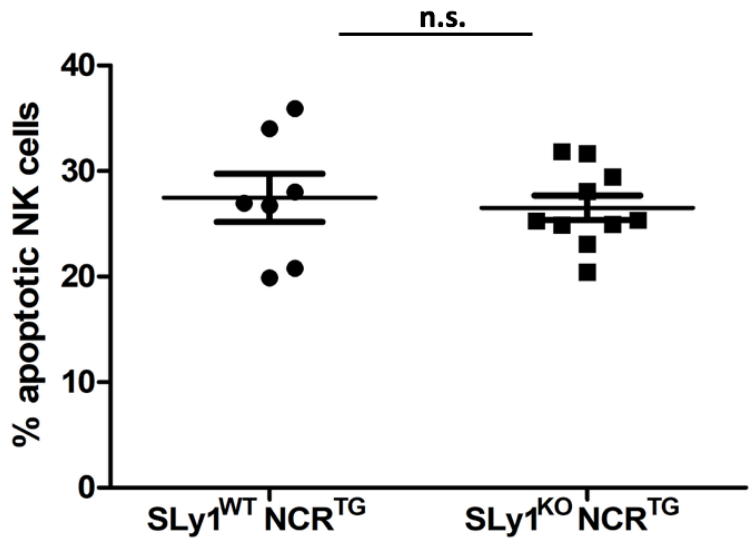


**Figure 26: Deletion of p53 restores viability of splenic NK cells in SLy1$^{KO}$ NCR$^{TG}$ mice**

Quantification of splenic apoptotic NK cells in SLy1$^{WT}$ NCR$^{TG}$ and SLy1$^{KO}$ NCR$^{TG}$ mice. Comparison performed by unpaired t-test. The graph shows mean ± SEM of more than three independent experiments; n.s. = statistically not significant; SLy1$^{WT}$ NCR$^{WT}$: n = 7 mice; SLy1$^{KO}$ NCR$^{WT}$: n = 10 mice.

### 3.2.5 Deletion of p53 restores expression of activating receptors on splenic NK cells in SLy1$^{KO}$ NCR$^{TG}$ mice

The expression of the activating receptors NKG2D, NK1.1 and NKp46 on splenic NK cells of SLy1$^{WT}$ NCR$^{TG}$ and SLy1$^{KO}$ NCR$^{TG}$ mice was measured using flow cytometry. Isolated spleen cells were stained with an antibody mastermix containing CD45.2-FITC, CD3-PacBlue, CD49b-APC and one of the following PE-conjugates: NKG2D-PE, NK1.1-PE and NKp46-PE. Cells were then analyzed *via* FACS. In contrast to the analysis of SLy1$^{WT}$ NCR$^{WT}$ and SLy1$^{KO}$ NCR$^{WT}$ NK

cells (see page 49), the measurement showed no statistically significant differences in the expression of any of the three activating receptors on splenic SLy1$^{KO}$ NCR$^{TG}$ NK cells compared to SLy1$^{WT}$ NCR$^{TG}$ controls (**Figure 27**). Concerning the expression of NKG2D (**Figure 27A**), the mean gMFI ± SEM was detected as 258.8 ± 34.36 in SLy1$^{WT}$ NCR$^{TG}$ NK cells compared to 222.6 ± 22.49 in SLy1$^{KO}$ NCR$^{TG}$ NK cells. Regarding the expression of NK1.1 (**Figure 27B**), the mean gMFI ± SEM was detected as 437.0 ± 44.66 in SLy1$^{WT}$ NCR$^{TG}$ NK cells compared to 383.0 ± 30.69 in SLy1$^{KO}$ NCR$^{TG}$ NK cells. Concerning the expression of NKp46 (**Figure 27C**), the mean gMFI ± SEM was detected as 200.6 ± 15.74 in SLy1$^{WT}$ NCR$^{TG}$ NK cells compared to 191.8 ± 15.50 in SLy1$^{KO}$ NCR$^{TG}$ NK cells.

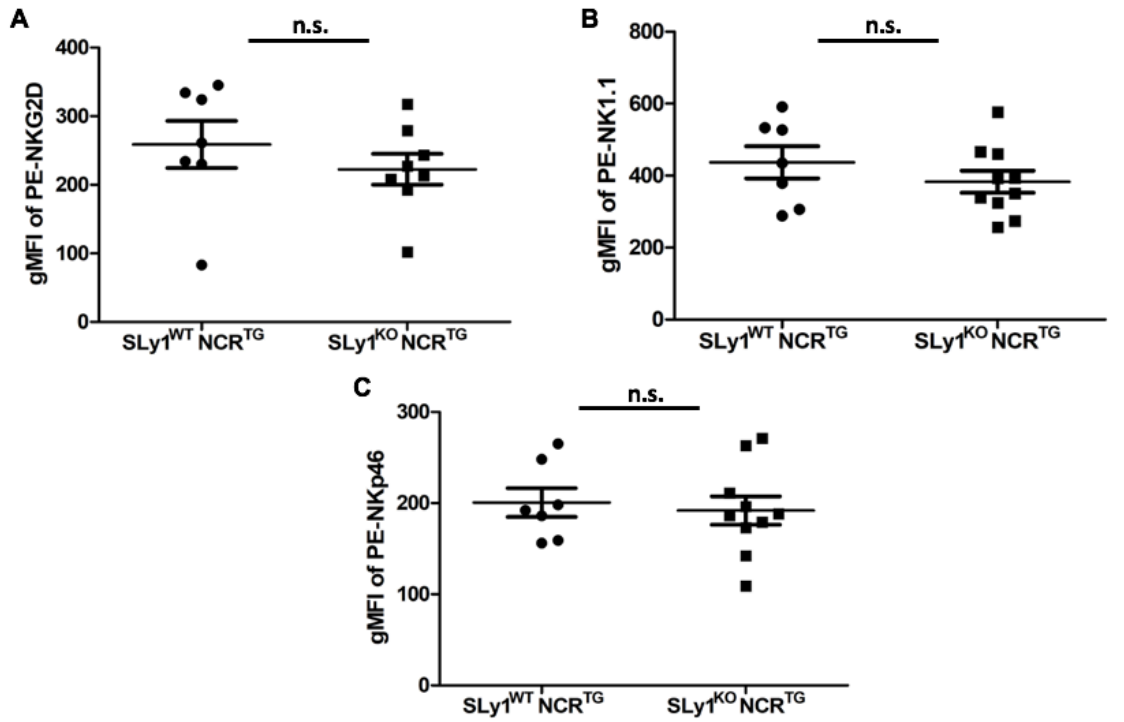


**Figure 27: Deletion of p53 restores expression of activating receptors on splenic NK cells in SLy1$^{KO}$ NCR$^{TG}$ mice**

Relative expression of **A)** NKG2D, **B)** NK1.1 and **C)** NKp46 on SLy1$^{WT}$ NCR$^{TG}$ and SLy1$^{KO}$ NCR$^{TG}$ splenic NK cells. Comparison performed by unpaired t-test. The graphs show mean gMFI ± SEM of more than three independent experiments; n.s. = statistically not significant; SLy1$^{WT}$ NCR$^{WT}$: n = 7 mice; SLy1$^{KO}$ NCR$^{WT}$: n = 8-10 mice.

### 3.2.6 Deletion of p53 restores functionality of splenic NK cells in SLy1$^{KO}$ NCR$^{TG}$ mice

The functional capability of splenic SLy1$^{KO}$ NCR$^{TG}$ NK cells to attack and kill tumor cells compared to SLy1$^{WT}$ NCR$^{TG}$ controls was assessed. Splenic SLy1$^{KO}$ NCR$^{TG}$ NK cells were isolated *via* MACS and incubated with LLC cells. After four hours, the viability of the tumor cells was analyzed *via* FACS. In contrast to the analysis of SLy1$^{WT}$ NCR$^{WT}$ and SLy1$^{KO}$ NCR$^{WT}$ NK cells (see page 52), there was no statistically significant difference detected between the percentages of apoptotic LLC cells in SLy1$^{KO}$ NCR$^{TG}$ mice (mean ± SEM: 17.71 ± 2.376 % dead LLC cells) and SLy1$^{WT}$ NCR$^{TG}$ controls (mean ± SEM: 19.94 ± 1.798 % dead LLC cells) (**Figure 28**).

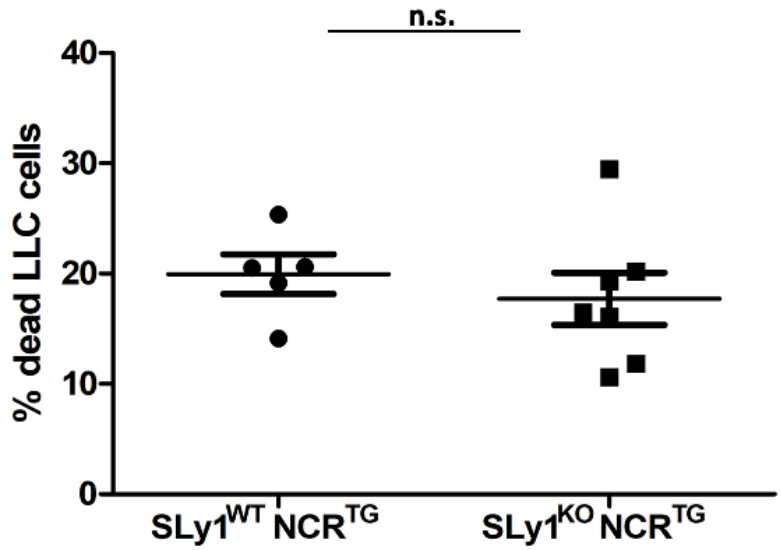


**Figure 28: Deletion of p53 restores functionality of splenic NK cells in SLy1$^{KO}$ NCR$^{TG}$ mice**

Quantification of dead LLC cells after 4 h incubation with SLy1$^{WT}$ NCR$^{TG}$ and SLy1$^{KO}$ NCR$^{TG}$ splenic NK cells. Comparison performed by unpaired t-test. The graph shows mean ± SEM of four independent experiments; n.s. = statistically not significant; SLy1$^{WT}$ NCR$^{TG}$: n = 5 mice; SLy1$^{KO}$ NCR$^{TG}$: n = 7 mice.

## 3.3 Analysis of the p53 signaling pathway in SLy1$^{WT}$ and SLy1$^{KO}$ splenic NK cells

The experiments with SLy1$^{KO}$ NCR$^{TG}$ mice (see chapter 3.2) showed that a deletion of p53 leads to restoration of the effects observed in SLy1$^{KO}$ NCR$^{WT}$ mice (see chapter 3.1) providing further evidence for the crucial role of p53 in the dysregulation of SLy1$^{KO}$ NK cells.
Therefore, the p53 signaling pathway was extensively analyzed in SLy1$^{KO}$ splenic NK cells compared to wildtype controls with the goal to potentially reveal other dysregulated genes in this pathway. For this analysis, splenic NK cells of SLy1$^{WT}$ and SLy1$^{KO}$ mice (strain 3) were used.

### 3.3.1 Identification of dysregulated genes in the p53 signaling pathway of splenic SLy1$^{KO}$ NK cells

In a first step, a p53 signaling pathway array that analyzes 84 genes involved in the p53 signaling pathway was conducted to screen for potentially dysregulated genes in SLy1$^{KO}$ splenic NK cells compared to wildtype controls. RNA from NK cells was isolated and transcribed into cDNA. After a pre-amplification, the RT$^2$ Profiler PCR Array was performed, and data was analyzed with the Qiagen GeneGlobe tool. Analysis with the tool provided a result report including the volcano plot shown in **Figure 29.**

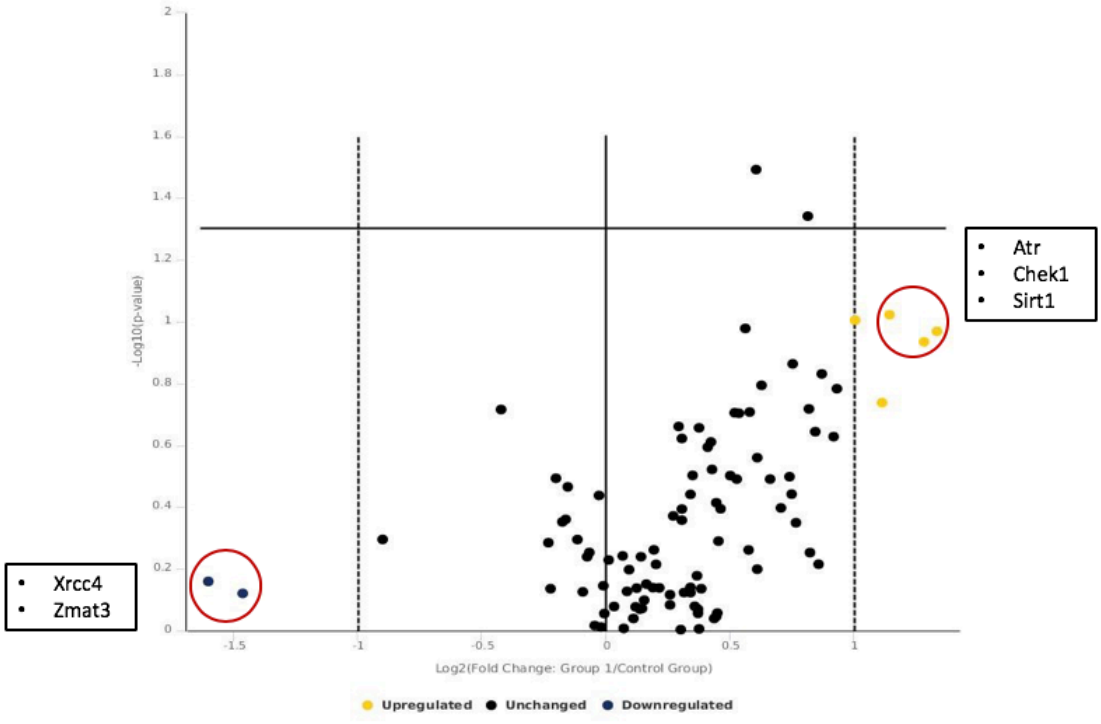


**Figure 29: Volcano plot displaying results of the p53 signaling pathway RT$^2$ Profiler PCR Array**

Analysis of the relative expression of 84 genes in the p53 signaling pathway in SLy1$^{KO}$ splenic NK cells compared to SLy1$^{WT}$ controls. The volcano plot displays statistical significance *versus* fold-change on the y- and x-axes, respectively. It combines a p-value statistical test with the fold regulation change enabling identification of genes with both large and small expression changes that are statistically significant. Genes detected as downregulated are indicated with blue dots, upregulated genes are represented by yellow dots. However, dysregulation was never statistically significant ($-Log_{10}$(p-value) < 1.3). Expression of the genes circled in red was further validated by qPCR (see pages 62-66); SLy1$^{WT}$: n = 8; SLy1$^{KO}$: n = 7.

The analysis of the p53 signaling pathway *via* RT$^2$ Profiler PCR Array in SLy1$^{KO}$ splenic NK cells compared to wildtype controls showed a dysregulation of seven genes.

*Xrcc4* and *Zmat3* were detected as downregulated, whereas *Atr*, *Chek1* and *Sirt1* were detected as upregulated in SLy1$^{KO}$ NK cells. However, for neither of these genes the dysregulation measured in the array was statistically significant ($p > 0.05$ for all values).

Two other genes, *Serpinb5* and *Nf1*, were also detected as upregulated by the array. However, the average threshold cycle of these genes was relatively high (>30), meaning that their relative expression levels were low, in both control and test samples, making the detected upregulations likely to be false positive and therefore were not followed up further.

**Table 13 and Table 14** demonstrate the genes detected as dysregulated and their respective fold changes.

**Table 13: Genes detected as downregulated by the p53 signal pathway RT$^2$ Profiler PCR Array**

| Gene Symbol | Fold Regulation |
|---|---|
| Xrcc4 | **-3.03** |
| Zmat3 | **-2.76** |

**Table 14: Genes detected as upregulated by the p53 signal pathway RT$^2$ Profiler PCR Array**

| Gene Symbol | Fold Regulation |
|---|---|
| Atr | **2.52** |
| Sirt1 | **2.43** |
| Serpinb5 | **2.21** |
| Chek1 | **2.17** |
| Nf1 | **2.00** |

The RT$^2$ Profiler PCR Array can be considered as a relatively fast and easy screening method to detect dysregulated genes in a specific signal pathway by analyzing a multitude of genes at the same time. Nevertheless, the array does not provide a precise analysis of each gene. In order to analyze the detected up- (*Atr*, *Chek1* and *Sirt1*) and downregulated genes (*Xrcc4* and *Zmat3*) in a more precise manner, qPCRs were performed for each gene comparing the expression in splenic SLy1$^{KO}$ and SLy1$^{WT}$ NK cells. Additionally, expression of the genes *Chek2* and *Atm*, which are closely related to *Chek1* and *Atr*, was also analyzed *via* qPCR, eventhough these genes were not detected as dysregulated by the array.

### 3.3.2 *Xrcc4*, *Zmat3* and *Sirt1* are not dysregulated in splenic SLy1$^{KO}$ NK cells

The mRNA expression of the genes *Xrcc4* and *Zmat3* was detected as downregulated in splenic SLy1$^{KO}$ NK cells compared to wildtype controls by the RT$^2$ Profiler PCR Array (see chapter 3.3.1). Nevertheless, this dysregulation was not statistically significant, and validation of the array results *via* qPCR did not show any significant downregulation of these mRNAs either (**Figure 30**). Concerning the relative expression of *Xrcc4* (**Figure 30A**), the mean ± SEM was

detected as 1.044 ± 0.10 in SLy1$^{WT}$ NK cells compared to 1.079 ± 0.09 in SLy1$^{KO}$ NK cells. Regarding the relative expression of *Zmat3* (**Figure 30B**), the mean ± SEM was detected as 0.7012 ± 0.06 in SLy1$^{WT}$ NK cells compared to 0.8353 ± 0.06 in SLy1$^{KO}$ NK cells.

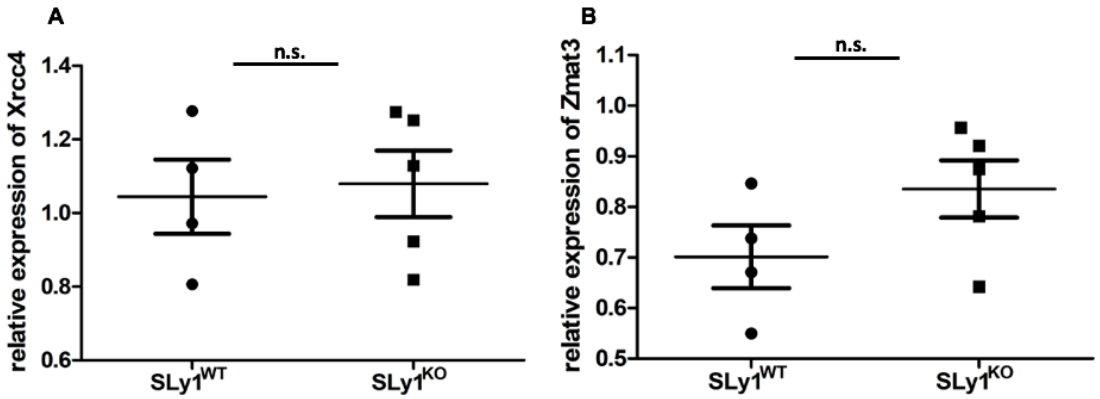


**Figure 30: Expression levels of *Xrcc4* and *Zmat3* are not altered in splenic SLy1$^{KO}$ NK cells**

**A)** Relative expression of *Xrcc4* in SLy1$^{WT}$ and SLy1$^{KO}$ splenic NK cells. **B)** Relative expression of *Zmat3* in SLy1$^{WT}$ and SLy1$^{KO}$ splenic NK cells. Comparison performed by unpaired t-test. The graphs show mean ± SEM; n.s. = statistically not significant; SLy1$^{WT}$: n = 4 mice; SLy1$^{KO}$: n = 5 mice.

Furthermore, dysregulation of the expression of the gene *Sirt1*, that was detected as upregulated in splenic SLy1$^{KO}$ NK cells by the RT$^2$ Profiler PCR Array (see chapter 3.3.1), was also not statistically significant when analyzed *via* qPCR (**Figure 31**). The relative expression (mean ± SEM) of *Sirt1* in SLy1$^{WT}$ NK cells was detected as 1.630 ± 0.23, compared to 2.149 ± 0.13 in SLy1$^{KO}$ NK cells. Nevertheless, results show a tendency towards an upregulation of *Sirt1* in SLy1$^{KO}$ NK cells.

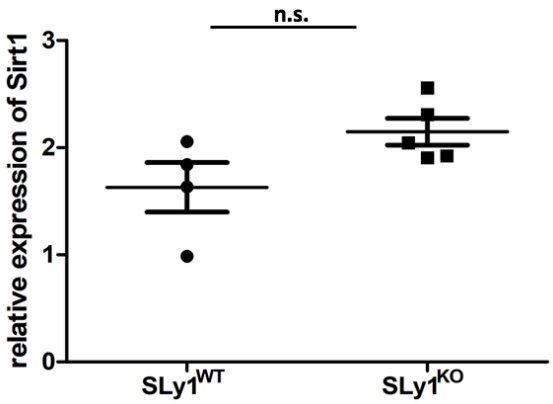


**Figure 31: *Sirt1* expression is not altered in splenic SLy1$^{KO}$ NK cells**

Relative expression of *Sirt1* in SLy1$^{WT}$ and SLy1$^{KO}$ splenic NK cells. Comparison performed by unpaired t-test. The graph shows mean ± SEM; n.s. = statistically not significant; SLy1$^{WT}$: n = 4 mice; SLy1$^{KO}$: n = 5 mice.

### 3.3.3 *Atr* and *Chek1* are upregulated in splenic SLy1$^{KO}$ NK cells

The mRNA expression of the genes *Atr* and *Chek1* was detected as upregulated in splenic SLy1$^{KO}$ NK cells compared to wildtype controls by the RT$^2$ Profiler PCR Array (see chapter 3.3.1). Nevertheless, in the array, this dysregulation was not statistically significant. Interestingly, validation of the array results *via* qPCR showed a statistically significant upregulation of the mRNA expression of *Atr* as well as *Chek1* in SLy1$^{KO}$ NK cells (**Figure 32**). Concerning the relative expression of *Atr* (**Figure 32A**), the mean ± SEM was detected as 2.459 ± 0.36 in SLy1$^{WT}$ NK cells compared to 5.085 ± 0.31 in SLy1$^{KO}$ NK cells. Regarding the relative expression of *Chek1* (**Figure 32B**), the mean ± SEM was detected as 1.877 ± 0.49 in SLy1$^{WT}$ NK cells compared to 3.733 ± 0.18 in SLy1$^{KO}$ NK cells.

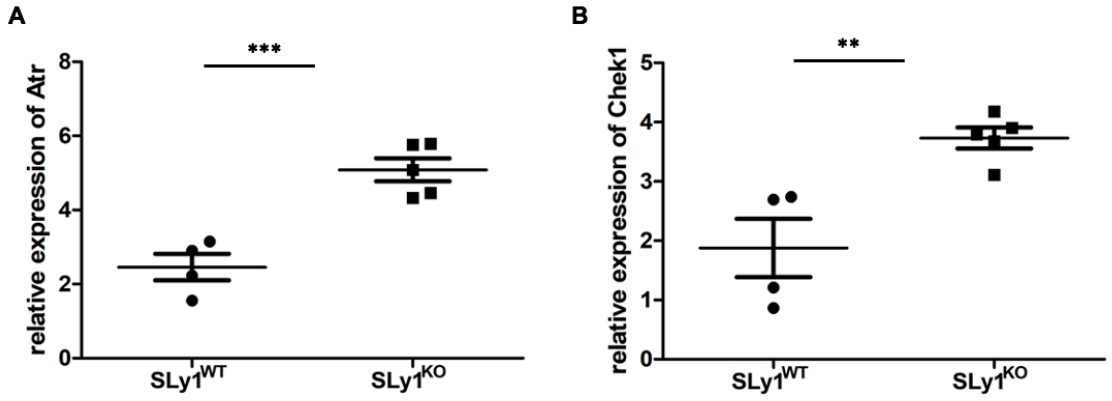


**Figure 32: *Atr* and *Chek1* are upregulated in splenic SLy1$^{KO}$ NK cells**

**A)** Relative expression of *Atr* in SLy1$^{WT}$ and SLy1$^{KO}$ splenic NK cells. **B)** Relative expression of *Chek1* in SLy1$^{WT}$ and SLy1$^{KO}$ splenic NK cells. Comparison performed by unpaired t-test. The graphs show mean ± SEM. Stars indicate statistical significance: ** $p < 0.01$; *** $p < 0.001$; SLy1$^{WT}$: n = 4 mice; SLy1$^{KO}$: n = 5 mice.

### 3.3.4 *Chek2*, but not *Atm*, is upregulated in splenic SLy1$^{KO}$ NK cells

mRNA expression of the genes *Chek2* and *Atm* in splenic SLy1$^{KO}$ NK cells compared to wildtype controls was not detected as dysregulated by the RT$^2$ Profiler PCR Array. Nevertheless, expression levels of the closely related genes *Chek1* and *Atr* are strongly upregulated in splenic SLy1$^{KO}$ NK cells (see page 64), suggesting a possible dysregulation of *Chek2* and *Atm* that was not detected by the array. In order to prove this hypothesis, expression of *Chek2* and *Atm* in splenic SLy1$^{KO}$ and SLy1$^{WT}$ NK cells was analyzed *via* qPCR (**Figure 33**).
Interestingly, the relative expression of *Chek2* in SLy1$^{KO}$ NK cells (mean ± SEM: 2.151 ± 0.09) was detected as significantly higher than in wildtype controls (mean ± SEM: 1.101 ± 0.28) (**Figure 33A**). By contrast, analysis of the relative expression of *Atm* showed no significant dysregulation in SLy1$^{KO}$ NK cells (mean ± SEM: 4.509 ± 0.52) compared to wildtype controls (mean ± SEM: 3.194 ± 0.80) (**Figure 33B**). Nevertheless, results show a tendency towards an upregulation of *Atm* in SLy1$^{KO}$ NK cells, but the values scatter too widely for statistical significance.

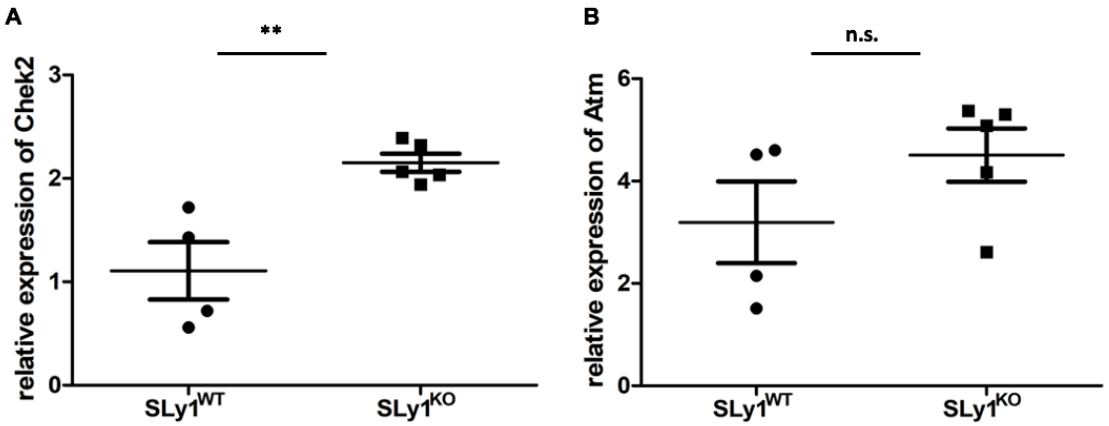


**Figure 33: *Chek2*, but not *Atm*, is upregulated in splenic SLy1$^{KO}$ NK cells**

**A)** Relative expression of *Chek2* in SLy1$^{WT}$ and SLy1$^{KO}$ splenic NK cells. **B)** Relative expression of *Atm* in SLy1$^{WT}$ and SLy1$^{KO}$ splenic NK cells. Comparison performed by unpaired t-test. The graphs show mean ± SEM. Stars indicate statistical significance: ** $p < 0.01$; n.s. = statistically not significant; SLy1$^{WT}$: n = 4 mice; SLy1$^{KO}$: n = 5 mice.

Taken together, the analysis of the p53 signaling pathway revealed an upregulation of the mRNA expression of *Chek1*, *Chek2*, *Atr* and, as a tendency, also *Atm* in SLy1$^{KO}$ splenic NK cells compared to WT controls. Interestingly, these genes are all part of the DNA damage response (DDR). The DDR signaling pathway as well as its dysregulation in SLy1-deficient NK cells will therefore be extensively discussed in chapter 4.2.2.

# 4 Discussion

## 4.1 Discussion of the methodology

Before interpreting the results of the present work, one needs to take into account the methods used for gaining the data and critically reflect upon these. This is outlined in the following sections.

### 4.1.1 Murine model organisms for immunological investigations

The human immune system is a complex integrative system with a variety of cellular as well as non-cellular components. Mice are easy to handle and relatively low-cost model animals, and their immune system resembles closely the human one. Hence, for immunologists, the mouse represents the experimental tool of choice to exemplarily study the human immune system. However, there are significant limitations of such models, which need to be considered before translating results from mice to humans. Some important differences and general specifications of the mouse models used in the present work are outlined in the following.

In the present work, $SLy1^{KO}$ mice were used to investigate the significance of SLy1-deficiency in NK cells. The KO mouse is a valid model to study the role of SLy1 in immune cells and has been used several times, for example as part of the investigation of the function of SLy1 in T cells (Schäll *et al.*, 2015). However, one needs to consider that there a some significant differences between mouse and human NK cells, also concerning their expression of surface markers (Vivier *et al.*, 2011). This could limit the transferability of the results from the animal studies to humans.
Furthermore, experiments with NK cells derived from a $NCR\text{-}Cre^{TG}$ $p53^{flox/flox}$ mouse model were performed in order to validate the crucial role of p53 in the SLy1-deficiency mediated dysregulation of NK cells. In this mouse model, p53 is

specifically deleted in NK cells, but otherwise normally expressed. This specific absence of p53 in NK cells was shown on protein level as part of research works from other members of our group and had therefore not to be reexamined in this project.
Generally, one also needs to take into account that the experiments of the present work were performed *in vitro* after organ removal and cell preparation, rather than *in vivo*. These *ex vivo* studies are very well suited for a rapid and precise analysis of distinct immune cell types, but cannot represent the complex interplay of the different components of the immune system *in vivo*.

### 4.1.2 Analysis of lung NK cells

Lung NK cells were analyzed concerning their numbers and surface expression of NKARs. In order to do so, lungs were removed from the mice and cut with scissors into small pieces. Then, a lung digestion and erythrocyte lysis was performed as described in chapter 2.7.3. Unfortunately, the analyses of the expression of NKARs on lung NK cells showed great fluctuations which limits the interpretability of the data. Therefore, in future follow-up studies, NK cells will be obtained from lungs after perfusing mice and harvesting the bronchoalveolar lavage (BAL) fluid before disruption of the lung. By applying this method, it will also be possible to investigate different subsets of lung NK cells separately (also see page 69).

### 4.1.3 Analysis of splenic NK cells

For the Killing Assay and qPCR analyses, splenic NK cells were purified *via* MACS and, if necessary, RNA was subsequently isolated from the cells. Both NK cell purity and RNA purity were checked in each of the experiments (see pages 32-33 and 38-39). However, because the NK cell numbers and thus the amounts of RNA obtained were very low, especially in $SLy1^{KO}$ mice, optimal purity of cells or RNAs could not always be achieved. For the performance of the qPCR analyses, those mice were used in which the combination of NK cell purity and

RNA purity was as optimal as possible. However, these aspects should be taken into account when interpreting the data obtained.

## 4.2 The function of SLy1 in NK cells

The function of SLy1 in T cells has already been well explored (Schäll *et al.*, 2015), and for B cells evidence shows a relevance of SLy1 especially in marginal-zone B cells (Beer *et al.*, 2005). Concerning the function of SLy1 in NK cells, it is known that the adaptor protein holds an important function for ribosomal stability (Arefanian *et al.*, 2016). Lack of SLy1 leads to decreased NK cell numbers, viability and functionality, as well as decreased expression of NKARs on the cell surface. In the present work, these effects of SLy1-deficiency in NK cells could be verified in the p53-floxed mouse model (strain 76). $SLy1^{KO}$ $NCR^{WT}$ mice showed significantly reduced amounts of absolute as well as relative splenic NK cell numbers compared to $SLy1^{WT}$ $NCR^{WT}$ littermates. Furthermore, their viability and functionality as well as the surface expression of NKARs were significantly reduced. However, these effects caused by the SLy1-deficiency were mostly seen in splenic NK cells. Analyses of lung NK cells, which were also performed as part of the present work, so far only showed a reduction of relative NK cell numbers in SLy1-deficient mice, but no significant changes in their expression of NKARs. This might on the hand be explained by methodological issues in the process of lung cell preparation (see chapter 4.1.2). On the other hand, another possible reason might be a different NKAR expression pattern of lung NK cells compared to splenic NK cells. More precisely, recent findings demonstrate the existance of distinct subsets of human lung NK cells with distinct expression patterns of surface markers (Marquardt *et al.*, 2017; Ardain, Marakalala and Leslie, 2020), which might also be present in mice. Therefore, further experiments regarding the function of SLy1 in lung NK cells should be performed in the future, which may investigate the different subsets of lung NK cells separately.

Our group postulated that lack of SLy1 decreases ribosomal stability in NK cells (Arefanian *et al.*, 2016), resulting in increased presence of free ribosomal protein

in the cytoplasm. This increased amount of free ribosomal protein, also referred to as "ribosomal stress", was shown to block the binding site of Mdm2 to p53, preventing ubiquitination of p53 and thus leading to accumulation of the transcription factor in the cell (Arefanian *et al.*, 2016). The present work now provides further evidence for the crucial role of p53 in the dysregulation of SLy1-deficient NK cells and, for the first time, gives a more detailed insight into the p53 signaling pathway in SLy1$^{KO}$ NK cells.

### 4.2.1 Validation of the crucial role of p53 in the dysregulation of SLy1$^{KO}$ NK cells

In the present work, by the use of the p53-floxed mouse model (strain 76), the critical role of p53 in the dysregulation of SLy1$^{KO}$ NK cells could be validated: Except for the reduced absolute numbers of NK cells, all effects (reduced relative NK cell numbers, viability, expression of NKARs and functionality) observed in splenic SLy1$^{KO}$ NK cells with p53 expression were restored by specific deletion of p53 in SLy1-deficient NK cells. However, expression of the NCR-Cre recombinase and therefore the functional deletion of the *Tp53* gene itself already seems to cause a decrease of the relative amount of splenic NK cells in SLy1$^{WT}$ NCR$^{TG}$ mice compared to SLy1$^{WT}$ NCR$^{WT}$ mice with an expressed *Tp53* gene (**Figure 34A**). By contrast, the absolute amounts of splenic SLy1$^{WT}$ NK cells were not affected by the expression of the NCR-Cre recombinase (**Figure 34B+C**). To further investigate this effect, in the future, one should analyze other splenic cell types, such as for example B cells, T cells and macrophages, in these mice to detect possible changes in their numbers.

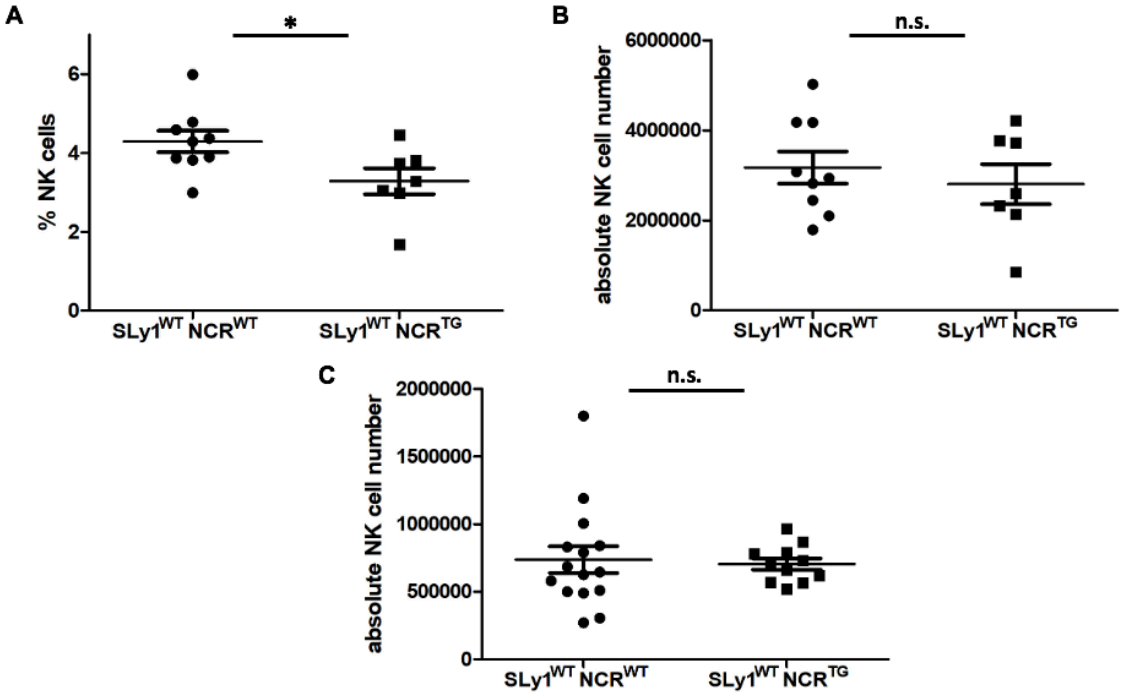


**Figure 34: Expression of the NCR-Cre recombinase causes decreased relative numbers of splenic NK cells in SLy1$^{WT}$ p53$^{flox/flox}$ mice**

**A)** Relative quantification of splenic NK cells in SLy1$^{WT}$ NCR$^{WT}$ and SLy1$^{WT}$ NCR$^{TG}$ mice. **B)** Absolute quantification of splenic NK cells in SLy1$^{WT}$ NCR$^{WT}$ and SLy1$^{WT}$ NCR$^{TG}$ mice *via* mathematical calculation using FACS data. **C)** Absolute quantification of splenic NK cells in SLy1$^{WT}$ NCR$^{WT}$ and SLy1$^{WT}$ NCR$^{TG}$ mice after isolation *via* MACS. Comparison performed by unpaired t-test. The graph shows mean ± SEM of more than three independent experiments; Star indicates statistical significance: * $p < 0.05$; n.s. = statistically not significant; SLy1$^{WT}$ NCR$^{WT}$: n = 9-15 mice; SLy1$^{KO}$ NCR$^{WT}$: n = 7-11 mice.

Nevertheless, most importantly, there were no significant differences detectable between relative NK cell numbers, their viability, functionality and expression of NKARs in SLy1$^{KO}$ NCR$^{TG}$ mice compared to SLy1$^{WT}$ NCR$^{TG}$ mice, demonstrating the critical role of p53 in the process.

However, with regard to the NK cell amounts, deletion of p53 led to a rescue of only the relative NK cell numbers in SLy1-deficient mice. Absolute NK cell numbers (both counted after MACSing and calculated based on FACS data) could not be restored in any of the experiments. To further address this fact, future studies will be conducted analyzing ribosomal stability as well as the p53 signaling pathway and the DNA damage response in the NCR-Cre$^{TG}$ p53$^{flox/flox}$ mouse model (strain 76).

Arefanian *et al.* postulated that the accumulation of p53 in SLy1-deficient NK cells is due to ribosomal stress with increased presence of free ribosomal protein that interferes with the binding of Mdm2 to p53 (Arefanian *et al.*, 2016). In future experiments it could therefore be investigated, whether increased free ribosomal protein is still present in SLy1$^{KO}$ NCR$^{TG}$ NK cells despite their p53 deletion. This should be the case, since the absence of the SLy1 protein should still cause ribosomal instability, but in this scenario the increased amounts of free ribosomal protein could no longer induce p53 accumulation.

### 4.2.2 Dysregulated DNA damage response in SLy1-deficient NK cells

Certainly, the question raises whether and to what extent other genes of the p53 signaling pathway, despite p53 itself, are also dysregulated in SLy1$^{KO}$ NK cells. Therefore, in the present work, the p53 signaling pathway was intensively analyzed in SLy1$^{KO}$ NK cells compared to SLy1$^{WT}$ NK cells. And indeed, these analyses revealed upregulation of the mRNA expression of *Atr*, *Atm*, *Chek1* and *Chek2* in splenic NK cells from SLy1-deficient mice. In contrast to *Atr*, *Chek1* and *Chek2*, the upregulation of *Atm* was indeed not statistically significant, but there was a clear trend towards an increased expression of the gene. Most interestingly, *Atr*, *Atm*, *Chek1* and *Chek2* are all part of the DNA damage response (DDR) signaling pathway.

The DNA damage response is an important signaling pathway within the cell ensuring that, in the presence of DNA damage, the cell is prevented from progressing through the cell cycle. The DNA damage initially induces the activation of the two protein kinases ATM and ATR, encoded by the genes *Atm* and *Atr* respectively. These protein kinases then bind to the damage site and phosphorylate various target proteins, including two other protein kinases, CHK1 and CHK2, encoded by the genes *Chek1* and *Chek2*. Together, these different kinases phosphorylate other target proteins leading to cell cycle arrest *via* p53, among others. CHK1 and CHK2 also block cell cycle progression *via* phosphorylation of Cdc25 phosphatases, thereby inhibiting their function. Cdc25

phosphatases are particularly important for activation of the complex of M cyclin and cyclin-dependent kinase 1 (CDK1) at the onset of mitosis, and their inhibition therefore prevents cell entry into mitosis. **Figure 35** illustrates the DDR signaling pathway.

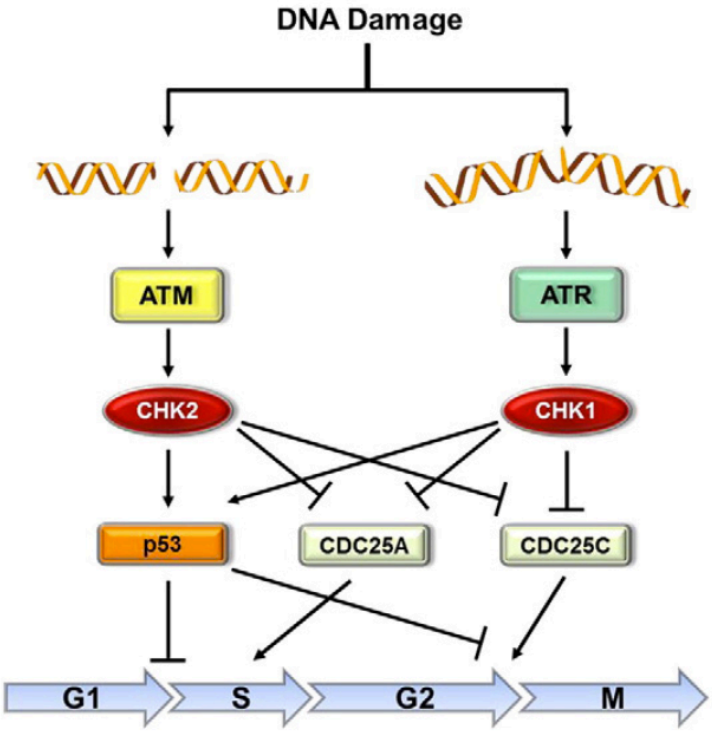


**Figure 35: The DNA damage response signaling pathway**

ATM is activated by DNA double strand breaks, while ATR is activated by single-stranded DNA. ATM and ATR phosphoryate CHK2 and CHK1, respectively. CHK2 and CHK1 phopshorylate and stabilize p53 which blocks cells at the G1/S and G2/M checkpoints. Additionally, CHK2 and CHK1 phosphorylate Cdc25 phosphatases which prevents activation of CDKs, thereby causing cell cycle arrest. Figure and legend from (McNeely, Beckmann and Bence Lin, 2014).

It should be noted, though, that SLy1 deficiency itself most likely does not induce DNA damage and thus does not initially trigger DDR. Possible mechanisms of activation of the DDR signaling pathway in SLy1-deficient NK cells will therefore be discussed in chapter 4.2.3.

Overall, however, the dysregulation of the DDR signaling pathway in SLy1-deficient NK cells has so far only been shown *via* qPCR at the mRNA level. In a next step, these results still need to be verified at the protein level *via* Western Blot. In the context of these studies, it would also be interesting to look at the

phosphorylation status of CHK1 and CHK2, as these proteins are phosphorylated by ATR and ATM, respectively.

### 4.2.3 DDR and ribosomal stress response

Looking at the p53 signaling pathway, it is striking that the genes *Atr*, *Atm*, *Chek1* and *Chek2* are all located upstream of p53. Assuming the "ribosomal protein - Mdm2 - p53" mechanism postulated by Arefanian *et al.*, one would rather expect that, instead of these upstream-located genes, genes located downstream of p53 are dysregulated in SLy1-deficient NK cells. So how can the activation of the DDR signaling pathway in SLy1$^{KO}$ NK cells be explained? Two options might be conceivable (**Figure 36**): First, there could be a synergistic effect of two independent mechanisms in SLy1$^{KO}$ NK cells, both acting on p53 (**Figure 36A**), with the first mechanism being the "ribosomal protein - Mdm2 - p53" axis. In this scenario, the second mechanism would be a direct activation of the DDR signaling pathway caused by the SLy1-deficiency, without any involvement of the increased free ribosomal proteins in this process. In this case, however, it would be unclear how exactly absence of the SLy1 protein could cause activation of *Atr* and *Atm*. Second, and more likely, it could be possible that the increased free ribosomal protein exhibits two functions, namely blocking the binding site for Mdm2 at p53 and at the same time leading to activation of the DDR signaling pathway (**Figure 36B**). Activation of the DDR by ribosomal stress or free ribosomal protein has already previously been described, for example for the ribosomal protein RPL6 (Yang *et al.*, 2019; Ma and Pederson, 2013), and would therefore also be conceivable in this scenario. Nevertheless, further studies are needed to fully investigate the underlying mechansims. These future experiments should also address the fact that free ribosomal protein must be localized in the nucleoplasm to inhibit ubiquitination of p53 by Mdm2 as well as to activate the DDR, as both processes occur in the nucleus. However, in their 2016 work, Arefanian *et al.* have so far only detected an increased amount of free ribosomal protein in the cytoplasm of SLy1-deficient NK cells.

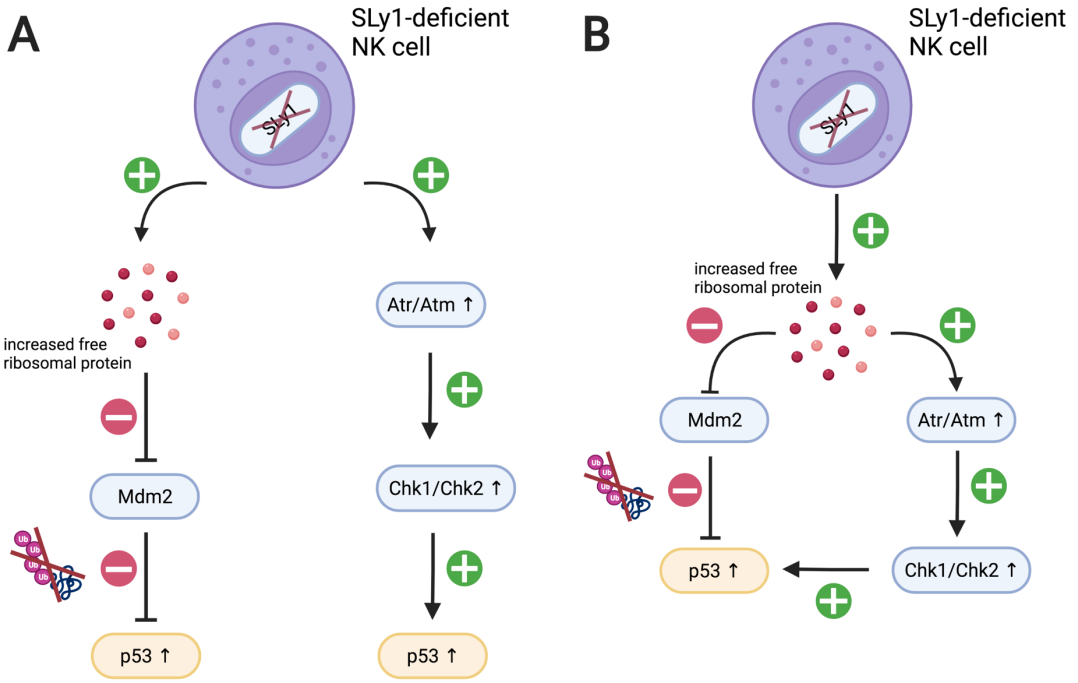


**Figure 36: Potential mechanisms of activation of the "ribosomal protein - Mdm2 - p53" axis and the DDR signaling pathway in SLy1$^{KO}$ NK cells**

Two possible mechanisms of activation of the “ribosomal protein – Mdm2 – p53” axis and the DDR signaling pathway in SLy1$^{KO}$ NK cells might be conceivable: **A)** Synergistic effect of two independent mechanisms, both acting on p53: on the one hand the "ribosomal protein - Mdm2 - p53" axis, and on the other hand direct activation of the DDR signal pathway caused by the SLy1-deficiency, without any involvement of the increased free ribosomal proteins in this process. **B)** Increased free ribosomal proteins may exhibit two functions: blocking the binding site for Mdm2 at p53, and at the same time activation of the DDR signaling pathway, both mechanisms converging on p53 activation. Figure created with BioRender.com.

## 4.3 Future perspectives: SLy1 in NK cells and its clinical relevance

It is clear that the present work was performed as part of a basic research project with the aim to contribute to our general understanding oft the human immune system. Nevertheless, the question raises to which extent the function of SLy1 in NK cells has a clinical relevance and might in the future even present a therapeutical target for patients suffering from immunoregulatory disorders or cancer.

### 4.3.1 SLy1 mutation causes a novel form of combined immunodeficiency

Interestingly, it was recently shown that certain SLy1 mutations in humans cause a novel form of X-linked combined immunodeficiency with immune dysregulation (Delmonte *et al.*, 2021). This is especially striking as it translates the findings concerning the function of SLy1 from basic research in mice to humans and puts emphasis on the clinical relevance of the human SLy1 protein. Through the use of Whole Exome Sequencing, Delmonte *et al.* could reveal three novel hemizygous loss-of-function SLy1 variants in four unrelated male patients. These patients suffered from a previously unexplained combined immunodeficiency and immune dysregulation manifesting as recurrent sinopulmonary, cutaneous and mucosal infections, as well as autoimmune cytopenias. The main focus of Delmonte's *et al.* experiments was the severe dysfunction of T cells caused by the SLy1-deficiency in the patients. Nevertheless, they could also show that NK cell development as well as functionality were affected by the SLy1 mutation: All patients suffered from severe NK cell lymphopenia and the remaining NK cells showed impaired IFN-$\gamma$ secretion upon stimulation. In the end, the authors therefore conclude that *"it is tempting to speculate that NK cells from SLy1-deficient patients have a survival defect, consistent with similar abnormalities observed in T cells"* (Delmonte *et al.*, 2021).

These findings put emphasis on the clinical relevance of the SLy1 adaptor protein and show that testing for pathogenic variants in this gene should in the future potentially be included in established genetic panels for combined immunodeficiencies, for example the predefined gene set "combined immunodeficiencies and other T-cell defects" (PID03) which currently includes 40 genes and is part of the panel for genetic immune disorders from the company CeGaT GmbH, located in Tuebingen, Germany (CeGaT, 2022).

Furthermore, as an outlook for future experiments, it would be highly interesting to further analyze the NK cells of patients suffering from SLy1 deficiency, with specific regard to potentially increased amounts of free ribosomal protein as well as dysregulation of the p53 signal pathway. If upregulation of the DDR signal pathway in the NK cells of these patients is confirmed, novel therapies, such as

the ATR inhibitor berzosertib, which is currently being tested in a phase II trial for the treatment of small-cell lung cancer (EMD Serono Research & Development Institute, 2021), might be used to improve patient outcome.

### 4.3.2 Potential relevance of the "tumorsuppressor-like" activity of SLy1 in NK cells

It is commonly known that a robust NK cell activity leads to better clearance of tumor cells or, as part of the endogenous immunosurveillance, can even prevent formation of tumors (Malmberg *et al.*, 2017). In recent years, the use of NK cells as part of anti-tumor therapy has therefore been part of intensive research as lately reviewed by Du *et al.* (Du *et al.*, 2021). Currently, the main focus lays on the application of adoptive NK cell transfer: NK cells are obtained from various sources, for example primary NK cells from peripheral blood or apheresis products (autologous or allogeneic), *in vitro* expanded, functionally enhanced and genetically modified, and are then being transferred back into the patient (Kundu, Gurney and O'Dwyer, 2021). However, major breakthroughs in the field of NK cell-based anti-tumor therapy have so far failed to materialize, in contrast to the success of checkpoint inhibitors, which primarily target T cell function. This is mainly due to a rapid exhaustion of NK cells in the human body after *in vitro* expansion as well as suppression of the NK cell activity by TGF-β in the tumor microenvironment (Viel *et al.*, 2016; Yang, Pang and Moses, 2010; Felices *et al.*, 2018).

SLy1 seems to have a protective effect on NK cell function, since the absence of the protein leads to decreased NK cell functionality, as shown by Arefanian *et al.* (Arefanian *et al.*, 2016) as well as in the present work. It would therefore be interesting to explore whether increased SLy1 expression in NK cells ($SLy1^{TG}$) leads to improved cell function. For example, this could provide additional benefit in the context of NK cell-based anti-tumor therapy, as NK cells expressing increased amounts of SLy1 could potentially lead to more robust NK cell function *in vivo*. Nevertheless, based on current knowledge, this is pure speculation and would need to be investigated in detail in future experiments.

# 5 Summary

## 5.1 English summary

The SH3 lymphocyte protein 1 (SLy1) is a multifunctional adaptor protein that is expressed exclusively in B cells, T cells and NK cells, and has a different specific function in each of the cell types. Through the present work, further insights were gained regarding the function of SLy1 in NK cells.

Previously, it was shown by our group that SLy1 contributes to ribosomal stability in this type of lymphocytes. In $SLy1^{KO}$ mice, which lack SLy1 expression, there is a decrease in NK cell number, decreased expression of NK cell activation receptors, and decreased viability and functionality of NK cells (Arefanian *et al.*, 2016). Arefanian *et al.* postulated that these effects are due to an increased presence of free ribosomal proteins in $SLy1^{KO}$ NK cells, which block the binding site of Mdm2 to p53, leading to accumulation of p53 and activation of the signaling pathway.

In the present work, experiments were performed using an $NCR^{TG}$ $p53^{flox/flox}$ mouse model that exhibits deletion of p53 specifically in NK cells. This mouse model was validated by verifying the findings of Arefanian *et al.* regarding decreased NK cell numbers, decreased expression of NK cell activation receptors, and decreased viability and functionality of NK cells in SLy1 deficiency. In addition, and most importantly, in the present work the essential role of p53 in $SLy1^{KO}$ NK cell dysregulation was further confirmed using this mouse model: Upon specific deletion of p53 in NK cells, both relative NK cell numbers and activation receptor expression, as well as $SLy1^{KO}$ NK cell viability and functionality, were restored. These results strongly support the hypothesis of a p53-mediated dysregulation of NK cells in SLy1-deficiency.

In a second step, the present work demonstrated that in SLy1-deficient NK cells the DNA damage response (DDR) is additionally dysregulated. More specifically, the DDR genes *Atr*, *Atm*, *Chek1* and *Chek2* are upregulated. In order to find out how exactly the absence of SLy1 leads to DDR activation in NK cells, further experiments will need to be performed. However, one possible mechanism would

be the activation of the DDR by the increased free ribosomal protein, also referred to as ribosomal stress.

In conclusion, the present work provides further proof of the essential function of the adaptor protein SLy1 for robust NK cell functionality. We therefore characterize SLy1 in NK cells as a "tumor suppressor-like" protein that may for example have future clinical relevance in the context of NK cell-based tumor therapies.

## 5.2 German summary (deutsche Zusammenfassung)

Das SH3-Lymphozytenprotein 1 (SLy1) ist ein multifunktionales Adaptorprotein, welches ausschließlich in B Zellen, T Zellen und NK Zellen exprimiert wird und in jedem der Zelltypen eine andere spezifische Funktion ausübt. Durch die vorliegende Arbeit konnten weitere Erkenntnisse über die Funktion von SLy1 in NK Zellen gewonnen werden.

Zuvor hatte unsere Gruppe gezeigt, dass SLy1 zur ribosomalen Stabilität in dieser Art von Lymphozyten beiträgt. In $SLy1^{KO}$-Mäusen, denen die SLy1-Expression fehlt, kommt es zu einem Rückgang der NK-Zellzahl, einer verminderten Expression von NK-Zellaktivierungsrezeptoren und einer verminderten Viabilität und Funktionalität der NK-Zellen (Arefanian *et al.*, 2016). Arefanian *et al.* postulierten, dass diese Effekte auf das vermehrte Vorhandensein von freien ribosomalen Proteinen in $SLy1^{KO}$ NK Zellen zurückzuführen sind, die die Bindungsstelle von Mdm2 an p53 blockieren, was zur Akkumulation von p53 und zur Aktivierung des p53 Signalwegs führt.

In der vorliegenden Arbeit wurden Experimente mit einem $NCR^{TG}$ $p53^{flox/flox}$ Mausmodell durchgeführt, das eine Deletion von p53 spezifisch in NK-Zellen aufweist. Dieses Mausmodell wurde validiert, indem die Ergebnisse von Arefanian *et al.* bezüglich der verringerten Anzahl von NK-Zellen, der verringerten Expression von NK-Zellaktivierungsrezeptoren und der verringerten Viabilität und Funktionalität von NK Zellen bei SLy1-Defizienz verifiziert wurden. Darüber hinaus wurde in der vorliegenden Arbeit die wesentliche Rolle von p53 bei der Dysregulation von $SLy1^{KO}$ NK Zellen anhand dieses Mausmodells weiter bestätigt: Nach spezifischer Deletion von p53 in NK Zellen wurden sowohl die relative NK-Zellzahl und die Expression der Aktivierungsrezeptoren als auch die Viabilität und Funktionalität der $SLy1^{KO}$ NK Zellen wiederhergestellt. Diese Ergebnisse stützen nachdrücklich die Hypothese einer p53-vermittelten Dysregulation von NK Zellen bei SLy1-Defizienz.

In einem zweiten Schritt konnte in der vorliegenden Arbeit gezeigt werden, dass in SLy1-defizienten NK Zellen zusätzlich die „DNA Damage Response“ (DDR) dysreguliert ist. Genauer gesagt, sind die DDR-Gene *Atr*, *Atm*, *Chek1* und *Chek2* hochreguliert. Um herauszufinden, wie genau das Fehlen von SLy1 zur DDR-

Aktivierung in NK-Zellen führt, müssen in Zukunft weitere Experimente durchgeführt werden. Ein möglicher Mechanismus wäre jedoch die Aktivierung der DDR durch das erhöhte freie ribosomale Protein, das auch als ribosomaler Stress bezeichnet wird.

Abschließend lässt sich zusammenfassen, dass durch die vorliegende Arbeit die essentielle Funktion des Adaptorproteins SLy1 für eine robuste NK-Zellfunktionalität bekräftigt werden konnte. Wir charakterisieren SLy1 in NK Zellen daher als ein "Tumorsuppressor-ähnliches" Protein, welches in Zukunft eventuell eine klinische Relevanz beispielsweise im Rahmen NK-zellbasierter Tumortherapien haben könnte.

# 6 Bibliography

Abel, A. M., Yang, C., Thakar, M. S. and Malarkannan, S. (2018) 'Natural Killer Cells: Development, Maturation, and Clinical Utilization', *Front Immunol,* 9, pp. 1869.

Akesson, C., Uvebrant, K., Oderup, C., Lynch, K., Harris, R. A., Lernmark, A., Agardh, C. D. and Cilio, C. M. (2010) 'Altered natural killer (NK) cell frequency and phenotype in latent autoimmune diabetes in adults (LADA) prior to insulin deficiency', *Clin Exp Immunol,* 161(1), pp. 48-56.

Alvarez, M., Simonetta, F., Baker, J., Pierini, A., Wenokur, A. S., Morrison, A. R., Murphy, W. J. and Negrin, R. S. (2019) 'Regulation of murine NK cell exhaustion through the activation of the DNA damage repair pathway', *JCI Insight,* 5.

Andre, P., Denis, C., Soulas, C., Bourbon-Caillet, C., Lopez, J., Arnoux, T., Blery, M., Bonnafous, C., Gauthier, L., Morel, A., Rossi, B., Remark, R., Breso, V., Bonnet, E., Habif, G., Guia, S., Lalanne, A. I., Hoffmann, C., Lantz, O., Fayette, J., Boyer-Chammard, A., Zerbib, R., Dodion, P., Ghadially, H., Jure-Kunkel, M., Morel, Y., Herbst, R., Narni-Mancinelli, E., Cohen, R. B. and Vivier, E. (2018) 'Anti-NKG2A mAb Is a Checkpoint Inhibitor that Promotes Anti-tumor Immunity by Unleashing Both T and NK Cells', *Cell,* 175(7), pp. 1731-1743 e13.

Angelo, L. S., Banerjee, P. P., Monaco-Shawver, L., Rosen, J. B., Makedonas, G., Forbes, L. R., Mace, E. M. and Orange, J. S. (2015) 'Practical NK cell phenotyping and variability in healthy adults', *Immunol Res,* 62(3), pp. 341-56.

Arase, H., Suenaga, T., Arase, N., Kimura, Y., Ito, K., Shiina, R., Ohno, H. and Saito, T. (2001) 'Negative regulation of expression and function of Fc gamma RIII by CD3 zeta in murine NK cells', *J Immunol,* 166(1), pp. 21-5.

Ardain, A., Marakalala, M. J. and Leslie, A. (2020) 'Tissue-resident innate immunity in the lung', *Immunology,* 159(3), pp. 245-256.

Arefanian, S., Schäll, D., Chang, S., Ghasemi, R., Higashikubo, R., Zheleznyak, A., Guo, Y., Yu, J., Asgharian, H., Li, W., Gelman, A. E., Kreisel, D., French, A. R., Zaher, H., Plougastel-Douglas, B., Maggi, L., Yokoyama, W., Beer-Hammer, S. and Krupnick, A. S. (2016) 'Deficiency of the adaptor protein SLy1 results in a natural killer cell ribosomopathy affecting tumor clearance', *Oncoimmunology,* 5(12), pp. e1238543.

Astoul, E., Laurence, A. D., Totty, N., Beer, S., Alexander, D. R. and Cantrell, D. A. (2003) 'Approaches to define antigen receptor-induced serine kinase signal transduction pathways', *J Biol Chem,* 278(11), pp. 9267-75.

Atkinson, E. A., Barry, M., Darmon, A. J., Shostak, I., Turner, P. C., Moyer, R. W. and Bleackley, R. C. (1998) 'Cytotoxic T lymphocyte-assisted suicide. Caspase 3 activation is primarily the result of the direct action of granzyme B', *J Biol Chem,* 273(33), pp. 21261-6.

Augugliaro, R., Parolini, S., Castriconi, R., Marcenaro, E., Cantoni, C., Nanni, M., Moretta, L., Moretta, A. and Bottino, C. (2003) 'Selective cross-talk among natural cytotoxicity receptors in human natural killer cells', *Eur J Immunol,* 33(5), pp. 1235-41.

Aylon, Y. and Oren, M. (2016) 'The Paradox of p53: What, How, and Why?', *Cold Spring Harb Perspect Med,* 6(10).

Baker, S. J., Fearon, E. R., Nigro, J. M., Hamilton, S. R., Preisinger, A. C., Jessup, J. M., vanTuinen, P., Ledbetter, D. H., Barker, D. F., Nakamura, Y., White, R. and Vogelstein, B. (1989) 'Chromosome 17 deletions and p53 gene mutations in colorectal carcinomas', *Science,* 244(4901), pp. 217-21.

Barak, Y., Juven, T., Haffner, R. and Oren, M. (1993) 'mdm2 expression is induced by wild type p53 activity', *EMBO J,* 12(2), pp. 461-8.

Barry, M., Heibein, J. A., Pinkoski, M. J., Lee, S. F., Moyer, R. W., Green, D. R. and Bleackley, R. C. (2000) 'Granzyme B short-circuits the need for caspase 8 activity during granule-mediated cytotoxic T-lymphocyte killing by directly cleaving Bid', *Mol Cell Biol,* 20(11), pp. 3781-94.

Beer, S., Scheikl, T., Reis, B., Huser, N., Pfeffer, K. and Holzmann, B. (2005) 'Impaired immune responses and prolonged allograft survival in Sly1 mutant mice', *Mol Cell Biol,* 25(21), pp. 9646-60.

Beer, S., Simins, A. B., Schuster, A. and Holzmann, B. (2001) 'Molecular cloning and characterization of a novel SH3 protein (SLY) preferentially expressed in lymphoid cells', *Biochim Biophys Acta,* 1520(1), pp. 89-93.

Bhat, R. and Watzl, C. (2007) 'Serial killing of tumor cells by human natural killer cells--enhancement by therapeutic antibodies', *PLoS One,* 2(3), pp. e326.

Biron, C. A., Nguyen, K. B., Pien, G. C., Cousens, L. P. and Salazar-Mather, T. P. (1999) 'Natural killer cells in antiviral defense: function and regulation by innate cytokines', *Annu Rev Immunol,* 17, pp. 189-220.

Blanchard, D. K., Michelini-Norris, M. B. and Djeu, J. Y. (1991) 'Production of granulocyte-macrophage colony-stimulating factor by large granular lymphocytes stimulated with Candida albicans: role in activation of human neutrophil function', *Blood,* 77(10), pp. 2259-65.

Boisvert, F. M., van Koningsbruggen, S., Navascues, J. and Lamond, A. I. (2007) 'The multifunctional nucleolus', *Nat Rev Mol Cell Biol,* 8(7), pp. 574-85.

Carrega, P. and Ferlazzo, G. (2012) 'Natural killer cell distribution and trafficking in human tissues', *Front Immunol,* 3, pp. 347.

CeGaT (2022) *Panel for Immune disorders*. Available at: https://www.cegat.com/diagnostics/diagnostic-panels/immune-disorders/ (Accessed: 30.01.2022.

Chen, D., Zhang, Z., Li, M., Wang, W., Li, Y., Rayburn, E. R., Hill, D. L., Wang, H. and Zhang, R. (2007a) 'Ribosomal protein S7 as a novel modulator of p53-MDM2 interaction: binding to MDM2, stabilization of p53 protein, and activation of p53 function', *Oncogene,* 26(35), pp. 5029-37.

Chen, X., Trivedi, P. P., Ge, B., Krzewski, K. and Strominger, J. L. (2007b) 'Many NK cell receptors activate ERK2 and JNK1 to trigger microtubule organizing center and granule polarization and cytotoxicity', *Proc Natl Acad Sci U S A,* 104(15), pp. 6329-34.

Chiossone, L., Chaix, J., Fuseri, N., Roth, C., Vivier, E. and Walzer, T. (2009) 'Maturation of mouse NK cells is a 4-stage developmental program', *Blood,* 113(22), pp. 5488-96.

Claudio, J. O., Zhu, Y. X., Benn, S. J., Shukla, A. H., McGlade, C. J., Falcioni, N. and Stewart, A. K. (2001) 'HACS1 encodes a novel SH3-SAM adaptor protein differentially expressed in normal and malignant hematopoietic cells', *Oncogene,* 20(38), pp. 5373-7.

Coffey, A. J., Brooksbank, R. A., Brandau, O., Oohashi, T., Howell, G. R., Bye, J. M., Cahn, A. P., Durham, J., Heath, P., Wray, P., Pavitt, R., Wilkinson, J., Leversha, M., Huckle, E., Shaw-Smith, C. J., Dunham, A., Rhodes, S., Schuster, V., Porta, G., Yin, L., Serafini, P., Sylla, B., Zollo, M., Franco, B., Bolino, A., Seri, M., Lanyi, A., Davis, J. R., Webster, D., Harris, A., Lenoir, G., de St Basile, G., Jones, A., Behloradsky, B. H., Achatz, H., Murken, J., Fassler, R., Sumegi, J., Romeo, G., Vaudin, M., Ross, M. T., Meindl, A. and Bentley, D. R. (1998) 'Host response to EBV infection in X-linked lymphoproliferative disease results from mutations in an SH2-domain encoding gene', *Nat Genet,* 20(2), pp. 129-35.

Cohen, R. B. and Fayette, J. 2020. Assessment of Efficacy and Safety of Monalizumab Plus Cetuximab Compared to Placebo Plus Cetuximab in Recurrent or Metastatic Head and Neck Cancer.

Cook, K. D., Waggoner, S. N. and Whitmire, J. K. (2014) 'NK cells and their ability to modulate T cells during virus infections', *Crit Rev Immunol,* 34(5), pp. 359-88.

Crinier, A., Narni-Mancinelli, E., Ugolini, S. and Vivier, E. (2020) 'SnapShot: Natural Killer Cells', *Cell,* 180(6), pp. 1280-1280 e1.

Cudkowicz, G. and Stimpfling, J. H. (1964) 'Hybrid Resistance to Parental Marrow Grafts: Association with the K Region of H-2', *Science,* 144(3624), pp. 1339-40.

Dai, M. S. and Lu, H. (2004) 'Inhibition of MDM2-mediated p53 ubiquitination and degradation by ribosomal protein L5', *J Biol Chem,* 279(43), pp. 44475-82.

Dai, M. S., Shi, D., Jin, Y., Sun, X. X., Zhang, Y., Grossman, S. R. and Lu, H. (2006) 'Regulation of the MDM2-p53 pathway by ribosomal protein L11 involves a post-ubiquitination mechanism', *J Biol Chem,* 281(34), pp. 24304-13.

Dalbeth, N. and Callan, M. F. (2002) 'A subset of natural killer cells is greatly expanded within inflamed joints', *Arthritis Rheum,* 46(7), pp. 1763-72.

de Matos, C. T., Berg, L., Michaelsson, J., Fellander-Tsai, L., Karre, K. and Soderstrom, K. (2007) 'Activating and inhibitory receptors on synovial fluid natural killer cells of arthritis patients: role of CD94/NKG2A in control of cytokine secretion', *Immunology,* 122(2), pp. 291-301.

Degli-Esposti, M. (1999) 'To die or not to die--the quest of the TRAIL receptors', *J Leukoc Biol,* 65(5), pp. 535-42.

Deisenroth, C., Franklin, D. A. and Zhang, Y. (2016) 'The Evolution of the Ribosomal Protein-MDM2-p53 Pathway', *Cold Spring Harb Perspect Med,* 6(12).

Delmonte, O. M., Bergerson, J. R. E., Kawai, T., Kuehn, H. S., McDermott, D. H., Cortese, I., Zimmermann, M. T., Dobbs, A. K., Bosticardo, M., Fink, D., Majumdar, S., Palterer, B., Pala, F., Dsouza, N. R., Pouzolles, M., Taylor, N., Calvo, K. R., Daley, S. R., Velez, D., Agharahimi, A., Myint-Hpu, K., Dropulic, L. K., Lyons, J. J., Holland, S. M., Freeman, A. F., Ghosh, R., Similuk, M. B., Niemela, J. E., Stoddard, J., Kuhns, D. B., Urrutia, R., Rosenzweig, S. D., Walkiewicz, M. A., Murphy, P. M. and Notarangelo, L. D. (2021) 'SASH3 variants cause a novel form of X-linked combined immunodeficiency with immune dysregulation', *Blood,* 138(12), pp. 1019-1033.

Doe, J. 2018. RT² Profiler PCR Array Gene Expression Analysis Report. QIAGEN.

Dolgin, E. (2017) 'The most popular genes in the human genome', *Nature,* 551(7681), pp. 427-431.

Du, N., Guo, F., Wang, Y. and Cui, J. (2021) 'NK Cell Therapy: A Rising Star in Cancer Treatment', *Cancers (Basel),* 13(16).

Eckelhart, E., Warsch, W., Zebedin, E., Simma, O., Stoiber, D., Kolbe, T., Rulicke, T., Mueller, M., Casanova, E. and Sexl, V. (2011) 'A novel Ncr1-Cre mouse reveals the essential role of STAT5 for NK-cell survival and development', *Blood,* 117(5), pp. 1565-73.

EMD Serono Research & Development Institute, I. (2021) 'Berzosertib + Topotecan in Relapsed Platinum-Resistant Small-Cell Lung Cancer (DDRiver SCLC 250)', *ClinicalTrials.gov*. Available at: https://ClinicalTrials.gov/show/NCT04768296 (Accessed 30.01.2022).

Fauriat, C., Long, E. O., Ljunggren, H. G. and Bryceson, Y. T. (2010) 'Regulation of human NK-cell cytokine and chemokine production by target cell recognition', *Blood,* 115(11), pp. 2167-76.

Felices, M., Lenvik, A. J., McElmurry, R., Chu, S., Hinderlie, P., Bendzick, L., Geller, M. A., Tolar, J., Blazar, B. R. and Miller, J. S. (2018) 'Continuous treatment with IL-15 exhausts human NK cells via a metabolic defect', *JCI Insight,* 3(3).

Felices, M., Lenvik, T. R., Davis, Z. B., Miller, J. S. and Vallera, D. A. (2016) 'Generation of BiKEs and TriKEs to Improve NK Cell-Mediated Targeting of Tumor Cells', *Methods Mol Biol,* 1441, pp. 333-46.

Fernandez, N. C., Treiner, E., Vance, R. E., Jamieson, A. M., Lemieux, S. and Raulet, D. H. (2005) 'A subset of natural killer cells achieves self-tolerance without expressing inhibitory receptors specific for self-MHC molecules', *Blood,* 105(11), pp. 4416-23.

Freeman, B. E., Raue, H. P., Hill, A. B. and Slifka, M. K. (2015) 'Cytokine-Mediated Activation of NK Cells during Viral Infection', *J Virol,* 89(15), pp. 7922-31.

Freud, A. G., Mundy-Bosse, B. L., Yu, J. and Caligiuri, M. A. (2017) 'The Broad Spectrum of Human Natural Killer Cell Diversity', *Immunity,* 47(5), pp. 820-833.

Gleason, M. K., Verneris, M. R., Todhunter, D. A., Zhang, B., McCullar, V., Zhou, S. X., Panoskaltsis-Mortari, A., Weiner, L. M., Vallera, D. A. and Miller, J. S. (2012) 'Bispecific and trispecific killer cell engagers directly activate human NK cells through CD16 signaling and induce cytotoxicity and cytokine production', *Mol Cancer Ther,* 11(12), pp. 2674-84.

Green, M. R., Kennell, A. S., Larche, M. J., Seifert, M. H., Isenberg, D. A. and Salaman, M. R. (2005) 'Natural killer cell activity in families of patients with systemic lupus erythematosus: demonstration of a killing defect in patients', *Clin Exp Immunol,* 141(1), pp. 165-73.

Hafner, A., Bulyk, M. L., Jambhekar, A. and Lahav, G. (2019) 'The multiple mechanisms that regulate p53 activity and cell fate', *Nat Rev Mol Cell Biol,* 20(4), pp. 199-210.

Hager, K. M. and Gu, W. (2014) 'Understanding the non-canonical pathways involved in p53-mediated tumor suppression', *Carcinogenesis,* 35(4), pp. 740-6.

Haupt, Y., Maya, R., Kazaz, A. and Oren, M. (1997) 'Mdm2 promotes the rapid degradation of p53', *Nature,* 387(6630), pp. 296-9.

Herberman, R. B., Nunn, M. E., Holden, H. T. and Lavrin, D. H. (1975) 'Natural cytotoxic reactivity of mouse lymphoid cells against syngeneic and allogeneic tumors. II. Characterization of effector cells', *Int J Cancer,* 16(2), pp. 230-9.

Hodgins, J. J., Khan, S. T., Park, M. M., Auer, R. C. and Ardolino, M. (2019) 'Killers 2.0: NK cell therapies at the forefront of cancer control', *J Clin Invest,* 129(9), pp. 3499-3510.

Hollstein, M., Sidransky, D., Vogelstein, B. and Harris, C. C. (1991) 'p53 mutations in human cancers', *Science,* 253(5015), pp. 49-53.

Honda, R., Tanaka, H. and Yasuda, H. (1997) 'Oncoprotein MDM2 is a ubiquitin ligase E3 for tumor suppressor p53', *FEBS Lett,* 420(1), pp. 25-7.

Horikawa, M., Hasegawa, M., Komura, K., Hayakawa, I., Yanaba, K., Matsushita, T., Takehara, K. and Sato, S. (2005) 'Abnormal natural killer cell function in systemic sclerosis: altered cytokine production and defective killing activity', *J Invest Dermatol,* 125(4), pp. 731-7.

James, A. M., Hsu, H. T., Dongre, P., Uzel, G., Mace, E. M., Banerjee, P. P. and Orange, J. S. (2013) 'Rapid activation receptor- or IL-2-induced lytic granule convergence in human natural killer cells requires Src, but not downstream signaling', *Blood,* 121(14), pp. 2627-37.

Jaufmann, J., Franke, F. C., Sperlich, A., Blumendeller, C., Kloos, I., Schneider, B., Sasaki, D., Janssen, K. P. and Beer-Hammer, S. (2021) 'The emerging and diverse roles of the SLy/SASH1-protein family in health and disease-Overview of three multifunctional proteins', *FASEB J,* 35(4), pp. e21470.

Jewett, A., Man, Y. G. and Tseng, H. C. (2013) 'Dual functions of natural killer cells in selection and differentiation of stem cells; role in regulation of inflammation and regeneration of tissues', *J Cancer,* 4(1), pp. 12-24.

Jin, A., Itahana, K., O'Keefe, K. and Zhang, Y. (2004) 'Inhibition of HDM2 and activation of p53 by ribosomal protein L23', *Mol Cell Biol,* 24(17), pp. 7669-80.

Kandoth, C., McLellan, M. D., Vandin, F., Ye, K., Niu, B., Lu, C., Xie, M., Zhang, Q., McMichael, J. F., Wyczalkowski, M. A., Leiserson, M. D. M., Miller, C. A., Welch, J. S., Walter, M. J., Wendl, M. C., Ley, T. J., Wilson, R. K., Raphael, B. J. and Ding, L. (2013) 'Mutational landscape and significance across 12 major cancer types', *Nature,* 502(7471), pp. 333-339.

Kang, R., Kroemer, G. and Tang, D. (2019) 'The tumor suppressor protein p53 and the ferroptosis network', *Free Radic Biol Med,* 133, pp. 162-168.

Karre, K., Ljunggren, H. G., Piontek, G. and Kiessling, R. (1986) 'Selective rejection of H-2-deficient lymphoma variants suggests alternative immune defence strategy', *Nature,* 319(6055), pp. 675-8.

Khosravi-Far, R. and Esposti, M. D. (2004) 'Death receptor signals to mitochondria', *Cancer Biol Ther,* 3(11), pp. 1051-7.

Kiessling, R., Klein, E., Pross, H. and Wigzell, H. (1975) '"Natural" killer cells in the mouse. II. Cytotoxic cells with specificity for mouse Moloney leukemia cells. Characteristics of the killer cell', *Eur J Immunol,* 5(2), pp. 117-21.

Kiessling, R., Klein, E. and Wigzell, H. (1975) '"Natural" killer cells in the mouse. I. Cytotoxic cells with specificity for mouse Moloney leukemia cells. Specificity and distribution according to genotype', *Eur J Immunol,* 5(2), pp. 112-7.

Kiniwa, T., Enomoto, Y., Terazawa, N., Omi, A., Miyata, N., Ishiwata, K. and Miyajima, A. (2016) 'NK cells activated by Interleukin-4 in cooperation with Interleukin-15 exhibit distinctive characteristics', *Proc Natl Acad Sci U S A,* 113(36), pp. 10139-44.

Klose, C., Berchtold, S., Schmidt, M., Beil, J., Smirnow, I., Venturelli, S., Burkard, M., Handgretinger, R. and Lauer, U. M. (2019) 'Biological treatment of pediatric sarcomas by combined virotherapy and NK cell therapy', *BMC Cancer,* 19(1), pp. 1172.

Kruiswijk, F., Labuschagne, C. F. and Vousden, K. H. (2015) 'p53 in survival, death and metabolic health: a lifeguard with a licence to kill', *Nat Rev Mol Cell Biol,* 16(7), pp. 393-405.

Krzewski, K. and Strominger, J. L. (2008) 'The killer's kiss: the many functions of NK cell immunological synapses', *Curr Opin Cell Biol,* 20(5), pp. 597-605.

Kubbutat, M. H., Jones, S. N. and Vousden, K. H. (1997) 'Regulation of p53 stability by Mdm2', *Nature,* 387(6630), pp. 299-303.

Kumar, P., Thakar, M. S., Ouyang, W. and Malarkannan, S. (2013) 'IL-22 from conventional NK cells is epithelial regenerative and inflammation protective during influenza infection', *Mucosal Immunol,* 6(1), pp. 69-82.

Kundu, S., Gurney, M. and O'Dwyer, M. (2021) 'Generating natural killer cells for adoptive transfer: expanding horizons', *Cytotherapy,* 23(7), pp. 559-566.

Kwon, H. J., Choi, G. E., Ryu, S., Kwon, S. J., Kim, S. C., Booth, C., Nichols, K. E. and Kim, H. S. (2016) 'Stepwise phosphorylation of p65 promotes NF-kappaB activation and NK cell responses during target cell recognition', *Nat Commun,* 7, pp. 11686.

Lane, D. P. and Crawford, L. V. (1979) 'T antigen is bound to a host protein in SV40-transformed cells', *Nature,* 278(5701), pp. 261-3.

Langers, I., Renoux, V. M., Thiry, M., Delvenne, P. and Jacobs, N. (2012) 'Natural killer cells: role in local tumor growth and metastasis', *Biologics,* 6, pp. 73-82.

Lanier, L. L. (2008) 'Up on the tightrope: natural killer cell activation and inhibition', *Nat Immunol,* 9(5), pp. 495-502.

Lawrence, M. S., Stojanov, P., Mermel, C. H., Robinson, J. T., Garraway, L. A., Golub, T. R., Meyerson, M., Gabriel, S. B., Lander, E. S. and Getz, G. (2014) 'Discovery and saturation analysis of cancer genes across 21 tumour types', *Nature,* 505(7484), pp. 495-501.

Lee, J. C., Lee, K. M., Kim, D. W. and Heo, D. S. (2004) 'Elevated TGF-beta1 secretion and down-modulation of NKG2D underlies impaired NK cytotoxicity in cancer patients', *J Immunol,* 172(12), pp. 7335-40.

Lindstrom, M. S. (2009) 'Emerging functions of ribosomal proteins in gene-specific transcription and translation', *Biochem Biophys Res Commun,* 379(2), pp. 167-70.

Linzer, D. I. and Levine, A. J. (1979) 'Characterization of a 54K dalton cellular SV40 tumor antigen present in SV40-transformed cells and uninfected embryonal carcinoma cells', *Cell,* 17(1), pp. 43-52.

Liu, Y., Tavana, O. and Gu, W. (2019) 'p53 modifications: exquisite decorations of the powerful guardian', *J Mol Cell Biol,* 11(7), pp. 564-577.

Ljunggren, H. G. and Karre, K. (1990) 'In search of the 'missing self': MHC molecules and NK cell recognition', *Immunol Today,* 11(7), pp. 237-44.

Lohrum, M. A., Ludwig, R. L., Kubbutat, M. H., Hanlon, M. and Vousden, K. H. (2003) 'Regulation of HDM2 activity by the ribosomal protein L11', *Cancer Cell,* 3(6), pp. 577-87.

Lopez-Soto, A., Huergo-Zapico, L., Acebes-Huerta, A., Villa-Alvarez, M. and Gonzalez, S. (2015) 'NKG2D signaling in cancer immunosurveillance', *Int J Cancer,* 136(8), pp. 1741-50.

Ma, H. and Pederson, T. (2013) 'The nucleolus stress response is coupled to an ATR-Chk1-mediated G2 arrest', *Mol Biol Cell,* 24(9), pp. 1334-42.

Mace, E. M., Dongre, P., Hsu, H. T., Sinha, P., James, A. M., Mann, S. S., Forbes, L. R., Watkin, L. B. and Orange, J. S. (2014) 'Cell biological steps and checkpoints in accessing NK cell cytotoxicity', *Immunol Cell Biol,* 92(3), pp. 245-55.

Mace, E. M. and Orange, J. S. (2019) 'Emerging insights into human health and NK cell biology from the study of NK cell deficiencies', *Immunol Rev,* 287(1), pp. 202-225.

Mahapatra, S., Mace, E. M., Minard, C. G., Forbes, L. R., Vargas-Hernandez, A., Duryea, T. K., Makedonas, G., Banerjee, P. P., Shearer, W. T. and Orange, J. S. (2017) 'High-resolution phenotyping identifies NK cell subsets that distinguish healthy children from adults', *PLoS One,* 12(8), pp. e0181134.

Malmberg, K. J., Carlsten, M., Bjorklund, A., Sohlberg, E., Bryceson, Y. T. and Ljunggren, H. G. (2017) 'Natural killer cell-mediated immunosurveillance of human cancer', *Semin Immunol,* 31, pp. 20-29.

Marquardt, N., Kekalainen, E., Chen, P., Kvedaraite, E., Wilson, J. N., Ivarsson, M. A., Mjosberg, J., Berglin, L., Safholm, J., Manson, M. L., Adner, M., Al-Ameri, M., Bergman, P., Orre, A. C., Svensson, M., Dahlen, B., Dahlen, S. E., Ljunggren, H. G. and Michaelsson, J. (2017) 'Human lung natural killer cells are predominantly comprised of highly differentiated hypofunctional CD69(-)CD56(dim) cells', *J Allergy Clin Immunol,* 139(4), pp. 1321-1330 e4.

May, R. M., Okumura, M., Hsu, C. J., Bassiri, H., Yang, E., Rak, G., Mace, E. M., Philip, N. H., Zhang, W., Baumgart, T., Orange, J. S., Nichols, K. E. and Kambayashi, T. (2013) 'Murine natural killer immunoreceptors use distinct proximal signaling complexes to direct cell function', *Blood,* 121(16), pp. 3135-46.

McNeely, S., Beckmann, R. and Bence Lin, A. K. (2014) 'CHEK again: revisiting the development of CHK1 inhibitors for cancer therapy', *Pharmacol Ther,* 142(1), pp. 1-10.

Mentlik, A. N., Sanborn, K. B., Holzbaur, E. L. and Orange, J. S. (2010) 'Rapid lytic granule convergence to the MTOC in natural killer cells is dependent on dynein but not cytolytic commitment', *Mol Biol Cell,* 21(13), pp. 2241-56.

Mombaerts, P., Iacomini, J., Johnson, R. S., Herrup, K., Tonegawa, S. and Papaioannou, V. E. (1992) 'RAG-1-deficient mice have no mature B and T lymphocytes', *Cell,* 68(5), pp. 869-77.

Murphy, K. and Weaver, C. (2016) *Janeway's immunobiology.* 9th edition. edn. New York, NY: Garland Science/Taylor & Francis Group, LLC.

Nagata, S. and Golstein, P. (1995) 'The Fas death factor', *Science,* 267(5203), pp. 1449-56.

Negishi, K., Waldeck, N., Chandy, G., Buckingham, B., Kershnar, A., Fisher, L., Gupta, S. and Charles, M. A. (1986) 'Natural killer cell and islet killer cell activities in type 1 (insulin-dependent) diabetes', *Diabetologia,* 29(6), pp. 352-7.

Orange, J. S. (2013) 'Natural killer cell deficiency', *J Allergy Clin Immunol,* 132(3), pp. 515-525.

Osinska, I., Popko, K. and Demkow, U. (2014) 'Perforin: an important player in immune response', *Cent Eur J Immunol,* 39(1), pp. 109-15.

Parham, P. (2006) 'Taking license with natural killer cell maturation and repertoire development', *Immunol Rev,* 214, pp. 155-60.

Park, Y. W., Kee, S. J., Cho, Y. N., Lee, E. H., Lee, H. Y., Kim, E. M., Shin, M. H., Park, J. J., Kim, T. J., Lee, S. S., Yoo, D. H. and Kang, H. S. (2009) 'Impaired differentiation

and cytotoxicity of natural killer cells in systemic lupus erythematosus', *Arthritis Rheum,* 60(6), pp. 1753-63.

Perricone, R., Perricone, C., De Carolis, C. and Shoenfeld, Y. (2008) 'NK cells in autoimmunity: a two-edg'd weapon of the immune system', *Autoimmun Rev,* 7(5), pp. 384-90.

Peterson, E. J., Clements, J. L., Fang, N. and Koretzky, G. A. (1998) 'Adaptor proteins in lymphocyte antigen-receptor signaling', *Curr Opin Immunol,* 10(3), pp. 337-44.

Pinkoski, M. J., Waterhouse, N. J., Heibein, J. A., Wolf, B. B., Kuwana, T., Goldstein, J. C., Newmeyer, D. D., Bleackley, R. C. and Green, D. R. (2001) 'Granzyme B-mediated apoptosis proceeds predominantly through a Bcl-2-inhibitable mitochondrial pathway', *J Biol Chem,* 276(15), pp. 12060-7.

Rajasekaran, K., Kumar, P., Schuldt, K. M., Peterson, E. J., Vanhaesebroeck, B., Dixit, V., Thakar, M. S. and Malarkannan, S. (2013) 'Signaling by Fyn-ADAP via the Carma1-Bcl-10-MAP3K7 signalosome exclusively regulates inflammatory cytokine production in NK cells', *Nat Immunol,* 14(11), pp. 1127-36.

Rajasekaran, K., Riese, M. J., Rao, S., Wang, L., Thakar, M. S., Sentman, C. L. and Malarkannan, S. (2016) 'Signaling in Effector Lymphocytes: Insights toward Safer Immunotherapy', *Front Immunol,* 7, pp. 176.

Ramesh, N., Morio, T., Fuleihan, R., Worm, M., Horner, A., Tsitsikov, E., Castigli, E. and Geha, R. S. (1995) 'CD40-CD40 ligand (CD40L) interactions and X-linked hyperIgM syndrome (HIGMX-1)', *Clin Immunol Immunopathol,* 76(3 Pt 2), pp. S208-13.

Reefman, E., Kay, J. G., Wood, S. M., Offenhauser, C., Brown, D. L., Roy, S., Stanley, A. C., Low, P. C., Manderson, A. P. and Stow, J. L. (2010) 'Cytokine secretion is distinct from secretion of cytotoxic granules in NK cells', *J Immunol,* 184(9), pp. 4852-62.

Reis, B., Pfeffer, K. and Beer-Hammer, S. (2009) 'The orphan adapter protein SLY1 as a novel anti-apoptotic protein required for thymocyte development', *BMC Immunol,* 10, pp. 38.

Rosen, D. B., Araki, M., Hamerman, J. A., Chen, T., Yamamura, T. and Lanier, L. L. (2004) 'A Structural basis for the association of DAP12 with mouse, but not human, NKG2D', *J Immunol,* 173(4), pp. 2470-8.

Rosenau, W. and Moon, H. D. (1961) 'Lysis of homologous cells by sensitized lymphocytes in tissue culture', *J Natl Cancer Inst,* 27, pp. 471-83.

Rubbi, C. P. and Milner, J. (2003) 'Disruption of the nucleolus mediates stabilization of p53 in response to DNA damage and other stresses', *EMBO J,* 22(22), pp. 6068-77.

Schäll, D., Schmitt, F., Reis, B., Brandt, S. and Beer-Hammer, S. (2015) 'SLy1 regulates T-cell proliferation during Listeria monocytogenes infection in a Foxo1-dependent manner', *Eur J Immunol,* 45(11), pp. 3087-97.

Scoville, S. D., Freud, A. G. and Caligiuri, M. A. (2017) 'Modeling Human Natural Killer Cell Development in the Era of Innate Lymphoid Cells', *Front Immunol,* 8, pp. 360.

Shaw, A. S. and Filbert, E. L. (2009) 'Scaffold proteins and immune-cell signalling', *Nat Rev Immunol,* 9(1), pp. 47-56.

Shieh, S. Y., Ikeda, M., Taya, Y. and Prives, C. (1997) 'DNA damage-induced phosphorylation of p53 alleviates inhibition by MDM2', *Cell,* 91(3), pp. 325-34.

Shinkai, Y., Rathbun, G., Lam, K. P., Oltz, E. M., Stewart, V., Mendelsohn, M., Charron, J., Datta, M., Young, F., Stall, A. M. and et al. (1992) 'RAG-2-deficient mice lack mature lymphocytes owing to inability to initiate V(D)J rearrangement', *Cell,* 68(5), pp. 855-67.

Smith, H. J. (1966) 'Antigenicity of carcinogen-induced and spontaneous tumours in inbred mice', *Br J Cancer,* 20(4), pp. 831-7.

Smith, K. M., Wu, J., Bakker, A. B., Phillips, J. H. and Lanier, L. L. (1998) 'Ly-49D and Ly-49H associate with mouse DAP12 and form activating receptors', *J Immunol,* 161(1), pp. 7-10.

Smyth, M. J., Cretney, E., Kelly, J. M., Westwood, J. A., Street, S. E., Yagita, H., Takeda, K., van Dommelen, S. L., Degli-Esposti, M. A. and Hayakawa, Y. (2005) 'Activation of NK cell cytotoxicity', *Mol Immunol,* 42(4), pp. 501-10.

Spear, P., Wu, M. R., Sentman, M. L. and Sentman, C. L. (2013) 'NKG2D ligands as therapeutic targets', *Cancer Immun,* 13, pp. 8.

Spits, H., Artis, D., Colonna, M., Diefenbach, A., Di Santo, J. P., Eberl, G., Koyasu, S., Locksley, R. M., McKenzie, A. N., Mebius, R. E., Powrie, F. and Vivier, E. (2013) 'Innate lymphoid cells--a proposal for uniform nomenclature', *Nat Rev Immunol,* 13(2), pp. 145-9.

Stabile, H., Fionda, C., Gismondi, A. and Santoni, A. (2017) 'Role of Distinct Natural Killer Cell Subsets in Anticancer Response', *Front Immunol,* 8, pp. 293.

Stinchcombe, J. C., Majorovits, E., Bossi, G., Fuller, S. and Griffiths, G. M. (2006) 'Centrosome polarization delivers secretory granules to the immunological synapse', *Nature,* 443(7110), pp. 462-5.

Sun, J. C. (2015) 'Transcriptional Control of NK Cells. In: Vivier, E., Di Santo J., Moretta A. (eds) Natural Killer Cells.', *Curr Top Microbiol Immunol,* 395, pp. 1-36.

Sun, J. C., Beilke, J. N. and Lanier, L. L. (2009) 'Adaptive immune features of natural killer cells', *Nature,* 457(7229), pp. 557-61.

Tang, X., Yang, L., Li, Z., Nalin, A. P., Dai, H., Xu, T., Yin, J., You, F., Zhu, M., Shen, W., Chen, G., Zhu, X., Wu, D. and Yu, J. (2018) 'First-in-man clinical trial of CAR NK-92 cells: safety test of CD33-CAR NK-92 cells in patients with relapsed and refractory acute myeloid leukemia', *Am J Cancer Res,* 8(6), pp. 1083-1089.

Trinchieri, G. (1989) 'Biology of natural killer cells', *Adv Immunol,* 47, pp. 187-376.

Tschochner, H. and Hurt, E. (2003) 'Pre-ribosomes on the road from the nucleolus to the cytoplasm', *Trends Cell Biol,* 13(5), pp. 255-63.

Uchida, T., Nakao, A., Nakano, N., Kuramasu, A., Saito, H., Okumura, K., Ra, C. and Ogawa, H. (2001) 'Identification of Nash1, a novel protein containing a nuclear localization signal, a sterile alpha motif, and an SH3 domain preferentially expressed in mast cells', *Biochem Biophys Res Commun,* 288(1), pp. 137-41.

Valiante, N. M., Uhrberg, M., Shilling, H. G., Lienert-Weidenbach, K., Arnett, K. L., D'Andrea, A., Phillips, J. H., Lanier, L. L. and Parham, P. (1997) 'Functionally and structurally distinct NK cell receptor repertoires in the peripheral blood of two human donors', *Immunity,* 7(6), pp. 739-51.

Vallera, D. A., Felices, M., McElmurry, R., McCullar, V., Zhou, X., Schmohl, J. U., Zhang, B., Lenvik, A. J., Panoskaltsis-Mortari, A., Verneris, M. R., Tolar, J., Cooley, S., Weisdorf, D. J., Blazar, B. R. and Miller, J. S. (2016) 'IL15 Trispecific Killer Engagers (TriKE) Make Natural Killer Cells Specific to CD33+ Targets While Also Inducing Persistence, In Vivo Expansion, and Enhanced Function', *Clin Cancer Res,* 22(14), pp. 3440-50.

van den Bosch, G., Preijers, F., Vreugdenhil, A., Hendriks, J., Maas, F. and De Witte, T. (1995) 'Granulocyte-macrophage colony-stimulating factor (GM-CSF) counteracts the inhibiting effect of monocytes on natural killer (NK) cells', *Clin Exp Immunol,* 101(3), pp. 515-20.

van Hall, T., Andre, P., Horowitz, A., Ruan, D. F., Borst, L., Zerbib, R., Narni-Mancinelli, E., van der Burg, S. H. and Vivier, E. (2019) 'Monalizumab: inhibiting the novel immune checkpoint NKG2A', *J Immunother Cancer,* 7(1), pp. 263.

Viel, S., Marcais, A., Guimaraes, F. S., Loftus, R., Rabilloud, J., Grau, M., Degouve, S., Djebali, S., Sanlaville, A., Charrier, E., Bienvenu, J., Marie, J. C., Caux, C., Marvel, J., Town, L., Huntington, N. D., Bartholin, L., Finlay, D., Smyth, M. J. and Walzer, T. (2016) 'TGF-beta inhibits the activation and functions of NK cells by repressing the mTOR pathway', *Sci Signal,* 9(415), pp. ra19.

Vitale, M., Della Chiesa, M., Carlomagno, S., Romagnani, C., Thiel, A., Moretta, L. and Moretta, A. (2004) 'The small subset of CD56brightCD16- natural killer cells is selectively responsible for both cell proliferation and interferon-gamma production upon interaction with dendritic cells', *Eur J Immunol,* 34(6), pp. 1715-22.

Vivier, E., Artis, D., Colonna, M., Diefenbach, A., Di Santo, J. P., Eberl, G., Koyasu, S., Locksley, R. M., McKenzie, A. N. J., Mebius, R. E., Powrie, F. and Spits, H. (2018) 'Innate Lymphoid Cells: 10 Years On', *Cell,* 174(5), pp. 1054-1066.

Vivier, E., Raulet, D. H., Moretta, A., Caligiuri, M. A., Zitvogel, L., Lanier, L. L., Yokoyama, W. M. and Ugolini, S. (2011) 'Innate or adaptive immunity? The example of natural killer cells', *Science,* 331(6013), pp. 44-9.

Vivier, E. and Ugolini, S. (2009) 'Regulatory natural killer cells: new players in the IL-10 anti-inflammatory response', *Cell Host Microbe,* 6(6), pp. 493-5.

Walzer, T., Dalod, M., Robbins, S. H., Zitvogel, L. and Vivier, E. (2005) 'Natural-killer cells and dendritic cells: "l'union fait la force"', *Blood,* 106(7), pp. 2252-8.

Yang, C., Zang, W., Ji, Y., Li, T., Yang, Y. and Zheng, X. (2019) 'Ribosomal protein L6 (RPL6) is recruited to DNA damage sites in a poly(ADP-ribose) polymerase-dependent manner and regulates the DNA damage response', *J Biol Chem,* 294(8), pp. 2827-2838.

Yang, L., Pang, Y. and Moses, H. L. (2010) 'TGF-beta and immune cells: an important regulatory axis in the tumor microenvironment and progression', *Trends Immunol,* 31(6), pp. 220-7.

Zeller, C., Hinzmann, B., Seitz, S., Prokoph, H., Burkhard-Goettges, E., Fischer, J., Jandrig, B., Schwarz, L. E., Rosenthal, A. and Scherneck, S. (2003) 'SASH1: a candidate tumor suppressor gene on chromosome 6q24.3 is downregulated in breast cancer', *Oncogene,* 22(19), pp. 2972-83.

Zhang, Y. and Huang, B. (2017) 'The Development and Diversity of ILCs, NK Cells and Their Relevance in Health and Diseases', *Adv Exp Med Biol,* 1024, pp. 225-244.

Zhang, Y., Wolf, G. W., Bhat, K., Jin, A., Allio, T., Burkhart, W. A. and Xiong, Y. (2003) 'Ribosomal protein L11 negatively regulates oncoprotein MDM2 and mediates a p53-dependent ribosomal-stress checkpoint pathway', *Mol Cell Biol,* 23(23), pp. 8902-12.

Zhu, Y. X., Benn, S., Li, Z. H., Wei, E., Masih-Khan, E., Trieu, Y., Bali, M., McGlade, C. J., Claudio, J. O. and Stewart, A. K. (2004) 'The SH3-SAM adaptor HACS1 is up-regulated in B cell activation signaling cascades', *J Exp Med,* 200(6), pp. 737-47.

# 7 Declaration (Erklärung zum Eigenanteil)

**Erklärung zum Eigenanteil der Dissertationsschrift**

Die Arbeit wurde am Department für Experimentelle und Klinische Pharmakologie und Pharmakogenomik, Abteilung Pharmakologie, Experimentelle Therapie und Toxikologie unter Betreuung von Prof. Dr. rer. nat. Sandra Beer-Hammer durchgeführt.

Sämtliche Versuche wurden nach Einarbeitung durch Labormitglieder (insbesondere Claudia Müller) von mir mit Unterstützung durch Claudia Müller durchgeführt.

Die statistische Auswertung erfolgte nach Anleitung des Instituts durch mich.

Ich versichere, das Manuskript selbstständig verfasst zu haben und keine weiteren als die von mir angegebenen Quellen verwendet zu haben.

Tübingen, den 15.03.2022

_____

(Carolin Blumendeller)

# 8 Publications and Acknowledgements

## 8.1 Publications

The following publication is directly related to the present work:

Jaufmann J, Franke FC, Sperlich A, **Blumendeller C**, Kloos I, Schneider B, Sasaki D, Janssen KP, Beer-Hammer S.
„The emerging and diverse roles of the SLy/SASH1-protein family in health and disease-Overview of three multifunctional proteins.“
FASEB J. 2021 Apr;35(4):e21470. doi: 10.1096/fj.202002495R. PMID: 33710696.

*Further publications which are not directly related to the present work are listed in the Curriculum Vitae.*

## 8.2 Acknowledgements

I would like to express my sincere thanks to all those who have contributed to the successful completion of this work.

First and foremost, I would like to express my special thanks to Prof. Dr. Sandra Beer-Hammer for providing me with the interesting topic and for the continuous, both professionally and personally wonderful support for many years now. Without Prof. Beer-Hammer's outstanding supervision and enormous flexibility, it would not have been possible for me to complete this dissertation. A big thank you for that!

I would also like to thank Prof. Dr. Dr. Bernd Nürnberg for giving me the opportunity to conduct the research at the institute.

Furthermore, I would like to thank all staff members of the for their helpfulness and friendly cooperation.
I am especially grateful to Claudia Müller, who has always supported me enthusiastically and provided me with great suggestions as well as kind words since my time as a HiWi at the Institute and throughout the entire time of my doctoral studies. Also, I would like to thank Victoria Eiperle and Isabel Kloos for the great teamwork and the many wonderful days in the lab.

A special thanks goes to the “Interdisziplinäres Promotionskolleg Medizin”, which provided not only financial support for the work, but was also a great help in the completion of the doctorate through various training courses and offers.

Last but not least, I would like to thank my family and my wonderful friends in Tübingen, who have always supported me with encouraging words throughout the entire time.

# 9 Appendix

### Appendix Table 1: List of genes analyzed in the RT2 Profiler PCR Array

| Position | RefSeq Number | Symbol | Description |
|---|---|---|---|
| A01 | NM_009684 | Apaf1 | Apoptotic peptidase activating factor 1 |
| A02 | NM_009687 | Apex1 | Apurinic/apyrimidinic endonuclease 1 |
| A03 | NM_007499 | Atm | Ataxia telangiectasia mutated homolog (human) |
| A04 | NM_019864 | Atr | Ataxia telangiectasia and rad3 related |
| A05 | NM_009736 | Bag1 | Bcl2-associated athanogene 1 |
| A06 | NM_007527 | Bax | Bcl2-associated X protein |
| A07 | NM_133234 | Bbc3 | BCL2 binding component 3 |
| A08 | NM_009741 | Bcl2 | B-cell leukemia/lymphoma 2 |
| A09 | NM_007544 | Bid | BH3 interacting domain death agonist |
| A10 | NM_009689 | Birc5 | Baculoviral IAP repeat-containing 5 |
| A11 | NM_009760 | Bnip3 | BCL2/adenovirus E1B interacting protein 3 |
| A12 | NM_009764 | Brca1 | Breast cancer 1 |
| B01 | NM_009765 | Brca2 | Breast cancer 2 |
| B02 | NM_007570 | Btg2 | B-cell translocation gene 2, anti-proliferative |
| B03 | NM_007610 | Casp2 | Caspase 2 |
| B04 | NM_015733 | Casp9 | Caspase 9 |
| B05 | NM_172301 | Ccnb1 | Cyclin B1 |
| B06 | NM_007633 | Ccne1 | Cyclin E1 |
| B07 | NM_009831 | Ccng1 | Cyclin G1 |
| B08 | NM_023243 | Ccnh | Cyclin H |
| B09 | NM_007658 | Cdc25a | Cell division cycle 25 homolog A (S. pombe) |
| B10 | NM_009860 | Cdc25c | Cell division cycle 25 homolog C (S. pombe) |
| B11 | NM_007659 | Cdk1 | Cyclin-dependent kinase 1 |
| B12 | NM_009870 | Cdk4 | Cyclin-dependent kinase 4 |
| C01 | NM_007669 | Cdkn1a | Cyclin-dependent kinase inhibitor 1A (P21) |
| C02 | NM_009877 | Cdkn2a | Cyclin-dependent kinase inhibitor 2A |
| C03 | NM_007691 | Chek1 | Checkpoint kinase 1 homolog (S. pombe) |
| C04 | NM_016681 | Chek2 | CHK2 checkpoint homolog (S. pombe) |
| C05 | NM_009950 | Cradd | CASP2 and RIPK1 domain containing adaptor with death domain |
| C06 | NM_001081335 | Cul9 | Cullin 9 |
| C07 | NM_029653 | Dapk1 | Death associated protein kinase 1 |
| C08 | NM_010066 | Dnmt1 | DNA methyltransferase (cytosine-5) 1 |
| C09 | NM_007891 | E2f1 | E2F transcription factor 1 |
| C10 | NM_010093 | E2f3 | E2F transcription factor 3 |
| C11 | NM_007912 | Egfr | Epidermal growth factor receptor |
| C12 | NM_007913 | Egr1 | Early growth response 1 |
| D01 | NM_177821 | Ep300 | E1A binding protein p300 |
| D02 | NM_007948 | Ercc1 | Excision repair cross-complementing rodent repair deficiency, complementation group 1 |
| D03 | NM_007956 | Esr1 | Estrogen receptor 1 (alpha) |
| D04 | NM_010175 | Fadd | Fas (TNFRSF6)-associated via death domain |
| D05 | NM_007987 | Fas | Fas (TNF receptor superfamily member 6) |
| D06 | NM_010177 | Fasl | Fas ligand (TNF superfamily, member 6) |
| D07 | NM_019740 | Foxo3 | Forkhead box O3 |
| D08 | NM_007836 | Gadd45a | Growth arrest and DNA-damage-inducible 45 alpha |
| D09 | NM_010431 | Hif1a | Hypoxia inducible factor 1, alpha subunit |
| D10 | NM_031168 | Il6 | Interleukin 6 |
| D11 | NM_010591 | Jun | Jun oncogene |
| D12 | NM_021284 | Kras | V-Ki-ras2 Kirsten rat sarcoma viral oncogene homolog |
| E01 | NM_176953 | Lig4 | Ligase IV, DNA, ATP-dependent |
| E02 | NM_008562 | Mcl1 | Myeloid cell leukemia sequence 1 |
| E03 | NM_010786 | Mdm2 | Transformed mouse 3T3 cell double minute 2 |

| | | | |
|---|---|---|---|
| E04 | NM_008575 | Mdm4 | Transformed mouse 3T3 cell double minute 4 |
| E05 | NM_026810 | Mlh1 | MutL homolog 1 (E. coli) |
| E06 | NM_008628 | Msh2 | MutS homolog 2 (E. coli) |
| E07 | NM_010849 | Myc | Myelocytomatosis oncogene |
| E08 | NM_010866 | Myod1 | Myogenic differentiation 1 |
| E09 | NM_010897 | Nf1 | Neurofibromatosis 1 |
| E10 | NM_008689 | Nfkb1 | Nuclear factor of kappa light polypeptide gene enhancer in B-cells 1, p105 |
| E11 | NM_011045 | Pcna | Proliferating cell nuclear antigen |
| E12 | NM_021451 | Pmaip1 | Phorbol-12-myristate-13-acetate-induced protein 1 |
| F01 | NM_016910 | Ppm1d | Protein phosphatase 1D magnesium-dependent, delta isoform |
| F02 | NM_145150 | Prc1 | Protein regulator of cytokinesis 1 |
| F03 | NM_011101 | Prkca | Protein kinase C, alpha |
| F04 | NM_008960 | Pten | Phosphatase and tensin homolog |
| F05 | NM_013917 | Pttg1 | Pituitary tumor-transforming gene 1 |
| F06 | NM_009029 | Rb1 | Retinoblastoma 1 |
| F07 | NM_009045 | Rela | V-rel reticuloendotheliosis viral oncogene homolog A (avian) |
| F08 | NM_023396 | Rprm | Reprimo, TP53 dependent G2 arrest mediator candidate |
| F09 | NM_009257 | Serpinb5 | Serine (or cysteine) peptidase inhibitor, clade B, member 5 |
| F10 | NM_144907 | Sesn2 | Sestrin 2 |
| F11 | NM_018754 | Sfn | Stratifin |
| F12 | NM_019812 | Sirt1 | Sirtuin 1 (silent mating type information regulation 2, homolog) 1 (S. cerevisiae) |
| G01 | NM_009283 | Stat1 | Signal transducer and activator of transcription 1 |
| G02 | NM_013693 | Tnf | Tumor necrosis factor |
| G03 | NM_020275 | Tnfrsf10b | Tumor necrosis factor receptor superfamily, member 10b |
| G04 | NM_009421 | Traf1 | Tnf receptor-associated factor 1 |
| G05 | NM_011640 | Trp53 | Transformation related protein 53 |
| G06 | NM_173378 | Trp53bp2 | Transformation related protein 53 binding protein 2 |
| G07 | NM_011641 | Trp63 | Transformation related protein 63 |
| G08 | NM_011642 | Trp73 | Transformation related protein 73 |
| G09 | NM_144783 | Wt1 | Wilms tumor 1 homolog |
| G10 | NM_028012 | Xrcc4 | X-ray repair complementing defective repair in Chinese hamster cells 4 |
| G11 | NM_009533 | Xrcc5 | X-ray repair complementing defective repair in Chinese hamster cells 5 |
| G12 | NM_009517 | Zmat3 | Zinc finger matrin type 3 |
| H01 | NM_007393 | Actb | Actin, beta |
| H02 | NM_009735 | B2m | Beta-2 microglobulin |
| H03 | NM_008084 | Gapdh | Glyceraldehyde-3-phosphate dehydrogenase |
| H04 | NM_010368 | Gusb | Glucuronidase, beta |
| H05 | NM_008302 | Hsp90ab1 | Heat shock protein 90 alpha (cytosolic), class B member 1 |
| H06 | SA_00106 | MGDC | Mouse Genomic DNA Contamination |
| H07 | SA_00104 | RTC | Reverse Transcription Control |
| H08 | SA_00104 | RTC | Reverse Transcription Control |
| H09 | SA_00104 | RTC | Reverse Transcription Control |
| H10 | SA_00103 | PPC | Positive PCR Control |
| H11 | SA_00103 | PPC | Positive PCR Control |
| H12 | SA_00103 | PPC | Positive PCR Control |

## Curriculum Vitae (Lebenslauf)

Aus Datenschutzgründen wurde der Lebenslauf aus der elektronischen Version der Dissertation entfernt.